AD-A066 923 NAVAL RESEARCH LAB WASHINGTON D C F/G 20/9
COLLECTIVE RADIO-EMISSION FROM PLASMAS.(U)
FEB 79 K PAPADOPOULOS, H P FREUND
UNCLASSIFIED NRL-MR-3922 SBIE-AD-E000 277 NL

1 OF 2
AD
AD A066923

SECURITY CLASSIFICATION OF THIS PAGE *(When Data Entered)*

REPORT DOCUMENTATION PAGE		READ INSTRUCTIONS BEFORE COMPLETING FORM
1. REPORT NUMBER NRL Memorandum Report 3922	2. GOVT ACCESSION NO.	3. RECIPIENT'S CATALOG NUMBER
4. TITLE *(and Subtitle)* COLLECTIVE RADIO-EMISSION FROM PLASMAS		5. TYPE OF REPORT & PERIOD COVERED Interim report on a continuing NRL problem. 6. PERFORMING ORG. REPORT NUMBER
7. AUTHOR(s) K. Papadopoulos and H. P. Freund*		8. CONTRACT OR GRANT NUMBER(s) Proj. No. RR0242
9. PERFORMING ORGANIZATION NAME AND ADDRESS Naval Research Laboratory Washington, DC 20375		10. PROGRAM ELEMENT, PROJECT, TASK AREA & WORK UNIT NUMBERS NRL Problem A03-16B
11. CONTROLLING OFFICE NAME AND ADDRESS Office of Naval Research Arlington, Virginia 22217		12. REPORT DATE February 7, 1979 13. NUMBER OF PAGES 109
14. MONITORING AGENCY NAME & ADDRESS*(if different from Controlling Office)*		15. SECURITY CLASS. *(of this report)* UNCLASSIFIED 15a. DECLASSIFICATION/DOWNGRADING SCHEDULE

16. DISTRIBUTION STATEMENT *(of this Report)*

Approved for public release; distribution unlimited.

17. DISTRIBUTION STATEMENT *(of the abstract entered in Block 20, if different from Report)*

18. SUPPLEMENTARY NOTES

*National Research Council/Naval Research Laboratory Research Associate

19. KEY WORDS *(Continue on reverse side if necessary and identify by block number)*

Cerenkov emission	Synchrotron radiation	Bremsstrahlung radiation
Radio-emission	Plasma lasers	Stimulated scattering
Microwave emission	Free electron lasers	Type III solar bursts
Induced radiation	Maser amplification	
Spontaneous emission	Linear instabilities	

20. ABSTRACT *(Continue on reverse side if necessary and identify by block number)*

Collective radiation processes operating in laboratory and space plasmas are reviewed with an emphasis towards astrophysical applications. Particular stress is placed on the physics involved in the various processes rather than in the detailed derivation of the formulas. Radiation processes from stable non-thermal, weakly turbulent and strongly turbulent magnetized and unmagnetized plasmas are discussed. The general theoretical ideas involved in amplification processes such as stimulated scattering are presented along with their application to free electron and plasma lasers.

(Continues)

DD FORM 1 JAN 73 1473 EDITION OF 1 NOV 65 IS OBSOLETE
S/N 0102-014-6601

SECURITY CLASSIFICATION OF THIS PAGE *(When Data Entered)*

20. Abstract (Continued)

Direct radio-emission of electromagnetic waves by linear instabilities driven by beams or velocity anisotropies are shown to be of relevance in space applications. Finally, as an example of the computational state of the art pertaining to plasma radiation, a study of the type III solar radio bursts is presented.

CONTENTS

I. Introduction

The main problem of astrophysics is the analysis of the emission spectra of astrophysical objects. To a major extent, the early evolution of this discipline was connected with progress in atomic physics, without which the interpretation of the optical spectra and, often, of the radio spectra would have been impossible. More recently, the opening of new observational "windows", involving radio waves, x-rays and gamma rays has revolutionized the discipline by revealing the existence of a wide range of new and exciting phenomena. Due to the importance of plasma physics in the understanding of many of these phenomena, the discipline of plasma astrophysics has emerged. It is becoming increasingly clear that the development of modern astrophysics relies to a large extent on our understanding of plasma physics. Experience with laboratory plasmas, which can be probed directly, provides valuable insight into general problems of plasma physics and allows theories to be compared with observations. Without the constraints imposed by plasma physics, the theories of astrophysical phenomena would be much more speculative. There is every reason to expect that certain problems of plasma physics will find more ready application in astrophysical plasmas than in the laboratory. A case in point is the study of collective radiation mechanisms, which is the topic of the present review.

Observations have shown that astrophysical objects contain very intense radiation sources, which cannot always be interpreted in terms of the well-known bremsstrahlung and synchrotron mechanisms. However, a rather extensive list of collective radiation processes has been

Note: Manuscript submitted December 8, 1978.

discussed in the plasma physics literature in the last decade or so, many of which may be applicable to the study of astrophysical plasmas. A problem arises because many astrophysicists are unfamiliar with theoretical plasma physics, while many plasma physicists are unfamiliar with the observations. In view of this, the present review is an attempt to develop the physical principles of several relevant radiation mechanisms and to present convenient simplified formulas for the description of collective e-m radiation mechanisms, which is one of the most important topics of plasma physics for the astrophysicist. The emphasis is on the physical description and the presentation of convenient formulae, rather than in elaborate derivations. However, an extensive list of references is provided of the source literature for the interested reader. While most of the material has already been published, many results appear for the first time.

In analyzing the emission spectra there are two important considerations. First, the generation of the e-m radiation at the source and, second, the propagation between the source and the observer. We emphasize here the generation mechanisms, since the propagation effects can be treated by the well-known methods of geometric optics or numerical ray tracing.

The plan of this work is as follows. In Chapter II, we provide a brief description of the properties of electromagnetic waves in plasmas. Spontaneous emission, as well as radiation from non-thermal and turbulent field-free plasmas, is discussed in Chapter III, including strongly

turbulent emission mechanisms. In Chapter IV, we consider spontaneous and turbulent emission processes in a uniformly magnetized plasma. Stimulated scattering processes and the corresponding implications for free electron and plasma lasers are treated in Chapter V. In Chapter VI, we present a discussion of linear electromagnetic instabilities from plasmas having an aniostropic distribution in velocity space. The physics of type III solar bursts is discussed in Chapter VII for illustrative purposes. A summary and concluding remarks are given in Chapter VIII. A summary of the emission mechanisms, cataloged according to frequency, is given in the Appendix.

II. Linear characteristics of high frequency e-m waves:

A summary of the linear characteristics of high frequency e-m waves propagating in a plasma can be seen from figs. 1-7. The simplest situation corresponds to an isotropic plasma in the absence of a magnetic field. In this case the high frequency transverse and longitudinal oscillations are completely decoupled and their respective dispersion relations are (fig. 1)

$$\omega^2 = \omega_e^2 + k^2c^2 \tag{1}$$

$$\omega^2 = \omega_e^2 \left(1 + 3\, k^2\lambda_D{}^2\right) \tag{2}$$

The important aspect of the above dispersion relation is that the phase velocity of the transverse waves is greater than the speed of light, thereby excluding the possibility of Landau damping or Cerenkov excitation in the absence of finite boundaries or of an ambient magnetic field. Notice also a cut-off in propagation (i.e., $k \to 0$) when the e-m wave frequency ω becomes equal to the plasma frequency ($\omega \approx \omega_e$) indicating that the wave energy will be reflected at that point. The group velocity of the transverse waves is given by $\underline{V}_g = \frac{\partial \omega}{\partial \underline{k}} = \frac{c^2}{V_p}$ and as expected is smaller than c.

The presence of a magnetic field modifies substantially the above simple picture and introduces new physical phenomena. Some representative results can be illustrated in the limiting case of propagation perpendicular to the ambient magnetic field ($\underline{k} \perp \underline{B}_o$). In this case, the electrostatic and electromagnetic components are approximately decoupled, and two situations can be distinguished (fig. 2a). In the first one,

the wave electric field is parallel to the magnetic field (ordinary or O mode), while in the second it is perpendicular (extraordinary or Xmode). For the O mode, since $\underline{E}_1 || \underline{B}_o$ there is no $\underline{E}_1 x \underline{B}_o$ coupling, and the dispersion relation is the same as in the absence of a magnetic field (i.e. $\omega^2 = \omega_e^2 + k^2c^2$). The presence of $\underline{E}_1 \times \underline{B}_o$ drifts in the X-mode produces a charge separation in the x direction (fig. 2b) so that the mode becomes partly longitudinal, and its polarization elliptical rather than linear. The dispersion relation for the X-mode is given by

$$\eta^2 \equiv \frac{k^2c^2}{\omega^2} \equiv \frac{c^2}{V_p^2} = 1 - \frac{\omega_e^2}{\omega^2} \frac{\omega^2 - \omega_e^2}{\omega^2 - \Omega_u^2} \tag{3}$$

where $\Omega_u^2 = \omega_e^2 + \Omega_e^2$ is the upper hybrid frequency. The cutoffs of the X-mode are given by

$$\omega_{R,L} = \tfrac{1}{2} \left[(\Omega_e^2 + 4\omega_e^2)^{\frac{1}{2}} \pm \Omega_e \right], \tag{4}$$

while an additional feature is the presence of a resonance (i.e., $k \to \infty$) for $\omega \to \Omega_u$ at which the wave energy is absorbed (note that at the resonance frequency the transverse wave energy becomes longitudinal). The modes of propagation for $\underline{k} \cdot \underline{B}_o = 0$ are shown in fig. 3. There are two branches of X-mode propagation corresponding to the two roots of equ. (3), which are usually called the slow extraordinary mode (SX) and the fast extraordinary mode (FX). An interesting property of the SX-mode is a region where $V_p < c$, so that Landau damping

as well as Cerenkov excitation becomes possible for this mode. The implications of this fact will be examined later.

An interesting diagram connected with the propagation of the O and X modes is shown in fig. 4, where we plot $\frac{1}{\eta^2}$ vs. ω. The interpretation of this diagram, depends on whether the signal ω is generated inside or outside the relevant plasma region and on how it is changing with space. For example if we take Ω_e = const. and consider a fixed frequency radiated into the plasma from the outside, the wave encounters higher density and $\omega_L, \omega_e, \Omega_u$ and ω_R increase so that we move towards the right of the diagram. This is equivalent to keeping the density constant and increasing the frequency. Taking this point of view we find that for $\omega \gg \omega_e$ (or low density) $V_p \to c$. At $\omega = \omega_R$ we get a cutoff, so that the wave is reflected. There is no propagation between ω_R and Ω_u (forbidden band) unless tunneling can occur, which typically requires the gradient scale-length L to be smaller than the incoming wave-length λ. At $\omega = \Omega_u$, $V_p \to 0$ and a window of propagation occurs between ω_L and Ω_u within which $V_p > c$ for $\omega < \omega_e$, $V_p < c$ for $\omega > \omega_e$, and $V_p = c$ for $\omega = \omega_e$. There is no propagation for $\omega < \omega_L$. A similar diagram (fig. 4b) for the O-mode shows one cutoff and no resonance.

Before closing the discussion of propagation for $\theta = \pi/2$, we should notice that for $\omega_e \gg \Omega_e$, a commonly encountered situation in space plasmas, the propagation characteristics reduce to the O-mode since $\omega_L, \omega_R, \Omega_u \to \omega_e$.

Another limiting case of e-m wave propagation in a plasma corresponds to propagation parallel to $\underline{B}_o$ ($\underline{k} \| \underline{B}_o$). For high frequencies the ion motion can be neglected and one recovers the helicon or whistler mode,

which satisfies the dispersion equation

$$\omega^2 = k^2c^2 + \frac{\omega_e^2}{1 + \frac{\Omega_e}{\omega}} \qquad (5)$$

There are two different waves propagating along $\underline{B}_o$ (fig. 5) with circular polarization: the right (R) and the left (L) hand polarized waves. The cutoffs and resonances of these modes can be seen from fig. 6. As expected only the R-waves have resonance ($k \to \infty$) at $\omega = \Omega_e$, since the electric field of the R-mode rotates in the same direction as the electrons. (If we included ions the L-wave would show a resonance at $\omega = \Omega_i$). The cutoffs are the same as for the X-mode. The L-wave has a stop-band for $\omega < \omega_L$ and behaves as an O-mode with ω_e replaced by ω_L. The R-wave has a stop band between ω_R and Ω_e, For propagation with $\omega < \Omega_e$, we note that $V_p < c$. This corresponds to the whistler mode. For this mode V_p and V_g decreases with ω for $\omega > \frac{\Omega_e}{2}$ and increase for $\omega < \frac{\Omega_e}{2}$. A final remark on the whistler propagation concerns finite electron thermal velocity effects, which produce a substantial electron cyclotron damping effect in the vicinity of the resonance. Fig. 7 shows that cyclotron damping produces a gap in propagation for $|\Omega_e| - kV_e < \omega < |\Omega_e| + kV_e$. In the same fashion as we will see later temperature aniostropies or loss cone distributions can excite whistler instabilities.

III. Bremsstrahlung radiation from non-thermal and turbulent plasmas

In this chapter we present first an elementary computation of the collisional bremsstrahlung radiation in a field free plasma. A more detailed account of the spectral emission formulas including collective bremsstrahlung follows for both non-thermal and weakly turbulent plasmas. The chapter concludes with a discussion of the radiation from strongly turbulent plasmas.

1. Elementary physical considerations:

The physical reason for bremsstrahlung in a magnetic field free plasma, is the acceleration of free electrons by ions. An estimate of the total emission can be computed on the basis of simple physical arguments (Dawson,1968).

An electron with acceleration α radiates at a rate given by the Larmor formula

$$P = \frac{2}{3}\frac{e^2\alpha^2}{c^3} \tag{1}$$

The electron acceleration α by an ion of charge Z is given by

$$\alpha = \frac{Ze^2}{mr^2} \tag{2}$$

where r is the distance between electrons and ions.

Therefore the total power radiated can be found from eqs. (1) and (2) by multiplying by the electron and ion densities ($n_e = Zn_i = n$) and integrating over the volume. This gives

$$P_t = \frac{2Z^2e^2n^2}{3c^3m^2}\int_{r_o}^{\infty}\frac{4\pi r}{r^2}\,dr = \frac{8\pi}{3}\,\frac{Z^2e^2n^2}{m^2c^3r_o} \tag{3}$$

with r_o defined as the distance of closest approach where the classical approximation breaks down. Taking $r_o = \frac{\hbar}{mV_e} = \frac{\hbar}{m}\left(\frac{m}{T_e}\right)^{\frac{1}{2}}$ we find

$$P_t = \frac{16\pi^2 Z^2 e^6 n^2}{3mc^3 h}\left[\frac{T_e}{m}\right]^{\frac{1}{2}} \tag{4}$$

which is correct to within a few percent of the one calculated by quantum mechanical theory.

It is important to note that the radiation due to electron encounters gives a contribution smaller than (4) by $\left(\frac{V_e}{c}\right)^2$. The reason is that the accelerations of interacting electrons are equal but opposite so that to first order their radiation fields cancel each other, and appear first to quadrupole order $\left(\text{i.e.,}\frac{V_e^4}{c^4}\right)$.

It is interesting to examine the conditions under which a plasma radiates as a blackbody. Neglecting reabsorption a sphere of plasma with radius R, radiates a power

$$W = \tfrac{4}{3}\pi R^3 P_t = 6 \times 10^{-27}\, Z^2 n^2 T_e^{\frac{1}{2}} R^3 \ \frac{\text{ergs}}{\text{sec}} \tag{5}$$

where T is in ^{o}K. To find the minimum radius R_o of the plasma required in order to radiate like a blackbody, we equate equ. (5) with the blackbody radiation W_B from a plasma surface $4\pi R_o^2$. This gives

$$W_B = 4\pi\sigma T_e^4 R_o^2 = W(R_o) \tag{6}$$

where σ is the Stefan-Boltzmann constant. Using eqs. (6) and (7) we find that

$$R_o = \frac{1.2 \times 10^{17} T_e^{\frac{1}{2}}}{Z^2 n^2} \text{ km} \qquad (7)$$

Notice that for $T_e = 10^5\ ^oK$, $n = 10^{10}$ plasma, $R_o = 3 \times 10^{15}$ km . We can thus conclude that practically most thermal plasmas will radiate much lower levels than a blackbody, i.e. they will be optically thin. Whether an astrophysical plasma is optically thin or not should be the first consideration in examining its total emission power.

However the fact that the plasma is, in general, optically thin as whole can often be deceptive, since it can be optically thick for some frequencies and optically thin for others.

To determine this, we must find the absorption coefficient as a function of the frequency. Knowing the absorption coefficient $\mu(\omega)$ for a plasma of temperature T, we can find the emissivity by requiring that the absorption of blackbody radiation with temperature T at frequency ω be balanced by the plasma emission. A calculation of the electromagnetic fields from a stable plasma can be found by the application of the fluctuation dissipation theorem. The formulae give the spectral densities of the electromagnetic fields and are valid even for a non-equilibrium plasma.

2. Radiation from sources imbedded in a stable plasma:

There are many ways one can calculate the emission formulas from a stable plasma. The simplest and physically most transparent is the use of the dressed test particle method. The important physical concept involved is that a stable plasma even not in thermal equilibrium can be viewed as an ensemble of uncorrelated "dressed" test particles.

The collisional effects appear for $k\lambda_D > 1$, while the collective shielding dominates for $k\lambda_D < 1$. The work of Dawson and Nakayama (1966) actually showed that the concept of the dressed test particles can be generalized to all orders in the plasma expansion parameter ($g \approx \frac{1}{n\lambda_D^3}$).

The radiation from a plasma to any order can be computed in two steps. The first step is very general and gives the formula for the radiation emitted by arbitrary sources embedded in a plasma. The second is the determination of the sources to the appropriate order (Birmingham et al., 1965, 1966).

The energy emitted by a current source $\underline{j}_s(r,t)$, can be found by computing the work done by the current on its self-consistent electric field $\underline{E}$, i.e.

$$P_s = -\lim_{T\to\infty} \frac{1}{T}\int_{-T/2}^{T/2} dt \int d\underline{r}\ \underline{E}(\underline{r},t) \cdot \underline{j}_s(\underline{r},t) ,$$

or by Parseval's theorem

$$P_s = -\frac{1}{(2\pi)^4} \lim_{T\to\infty}\frac{1}{T}\iint \underline{E}(\underline{k},\omega) \cdot \underline{j}_s^*(\underline{k},\omega)\, d\underline{k}d\omega .$$

The emission per unit frequency will be

$$P_s(\omega) = \tfrac{1}{2} \frac{1}{(2\pi)^4} \mathrm{Re}\int d\underline{k}\ \underline{E}(\underline{k},\omega) \cdot \underline{j}_s^*(\underline{k},\omega). \qquad (8)$$

On the basis of the test particle theory, and for an isotropic plasma,

$$\underline{k} \cdot \underline{E}(\underline{k},\omega) = -4\pi i \frac{\underline{k} \cdot \underline{j}_s(\underline{k},\omega)}{\omega \epsilon_L(\underline{k},\omega)} , \qquad (9)$$

and

$$\underline{k} \times \underline{E}(\underline{k},\omega) = - \frac{4\pi \underline{k} \times \underline{j}_s(\underline{k},\omega)}{\omega \epsilon_T(\underline{k},\omega)} \tag{10}$$

From eqs. (8-10) we find

$$P_s(\omega) = \frac{1}{4\pi^3 \omega} \operatorname{Im} \int \frac{d\underline{k}}{k^2} \left\{ \frac{|\underline{k} \cdot \underline{j}_s(\underline{k},\omega)|^2}{\epsilon_L(\underline{k},\omega)} \right.$$

$$\left. + \frac{|k \times \underline{j}_s(\underline{k},\omega)|^2}{\epsilon_T(\underline{k},\omega)} \right\} . \tag{11}$$

An additional quantity which can be computed on the basis of superposition of uncorrelated test currents, as given by eqs. (9) and (10), is the spectral density tensor of the electric field, i.e.

$$\left\langle \underline{E}\, \underline{E}^* | \underline{k},\omega \right\rangle_s = \frac{16\pi^2}{\omega^2 k^2} \left[\frac{|\underline{k} \cdot \underline{j}_s(\underline{k},\omega)|^2}{|\epsilon_L(\underline{k},\omega)|^2} \right.$$

$$\left. + \frac{|\underline{k} \times \underline{j}_s(\underline{k},\omega)|^2}{|\epsilon_T(\underline{k},\omega)|^2} \right] . \tag{12}$$

3. Cerenkov emission from stable non-thermal plasmas:

The longitudinal and transverse power emission spectra can be computed from eq. (11) by first specifying $\underline{j}_s(\underline{k},\omega)$ and then summing over all available test charges. To first order the current sources are due to bare particles moving in their unperturbed trajectories

(i.e. $\underline{r}(t) = \underline{r}_o + \underline{v}_o t$). Therefore

$$\underline{j}_s(\underline{k},\omega) = 2\pi q \underline{v}_o \delta(\omega - \underline{k}\cdot\underline{v}_o) . \tag{13}$$

From eqs. (12) and (13) and integrating

$$\left\langle \underline{E}\,\underline{E}^* \middle| \underline{k},\omega \right\rangle_s = \frac{16\pi n e^2}{k^2} \int d\underline{v}\, f_e(\underline{v}) \delta(\omega - \underline{k}\cdot\underline{v}) \left[\frac{\underline{k}\,\underline{k}}{k^2} \frac{1}{|\epsilon_L(\underline{k},\omega)|^2} \right.$$

$$\left. + \tfrac{1}{2} \frac{|\underline{k} \times \underline{v}|^2}{\omega^2} \left(\underline{\underline{I}} - \frac{\underline{k}\underline{k}}{k^2} \right) \frac{1}{|\epsilon_T(\underline{k},\omega)|^2} \right] . \tag{14a}$$

This result is correct for stable plasmas in an equilibrium or non-equilibrium state. For an equilibrium plasma (i.e., f_e Maxwellian), we recover the result usually derived on the basis of the fluctuation dissipation theorem (Rostoker, 1961; Montgomery and Tidman, 1964)

$$\left\langle \underline{E}\,\underline{E}^* \middle| \underline{k},\omega \right\rangle_s = 8\pi \frac{T}{\omega} \left\{ \frac{\underline{k}\underline{k}}{k^2} \frac{\mathrm{Im}\epsilon_L(\underline{k},\omega)}{|\epsilon_L(\underline{k},\omega)|^2} \right.$$

$$\left. + \left(\underline{\underline{I}} - \frac{\underline{k}\,\underline{k}}{k^2} \right) \frac{\mathrm{Im}\epsilon_T(\underline{k},\omega)}{|\epsilon_T(\underline{k},\omega|^2} \right\} . \tag{14b}$$

At this stage, we should stop and examine the physics involved in the above radiation formulas. In computing the bremsstrahlung radiation in section 1, we considered the acceleration due to the electron-ion encounters. Since, in the present source model, the test charges were

moving in straight trajectories, no radiation will be exptected in a vacuum. However, the presence of the plasma can modify this, as seen from eq. (14). In the absence of collisions $\mathrm{Im}\,\epsilon_T(\underline{k},\omega)$ vanishes (to the order of validity of the Vlasov equation), and no e-m radiation will be emitted from particles moving in straight orbits. Since $\mathrm{Im}\epsilon_L(\underline{k},\omega)$ is different from zero, electrostatic radiation can be emitted. The electrostatic radiation emitted is Cerenkov radiation, i.e. radiation due to particles moving with velocities larger than the phase velocity of the waves. In a plasma with $\underline{B}_o = 0$ only the electrostatic modes have $V_p < c$ and can therefore produce Cerenkov radiation. As we will see later, the situation is different for the S-X mode if $\underline{B}_o \neq 0$.

In fig. 8 we plot the function $S(\underline{k},\omega) = \mathrm{Tr} < \underline{E}\,\underline{E}^* | \underline{k},\omega >_s$ as a function of ω for a fixed wave number $k < k_D$ and for a thermal equilibrium plasma. The spectral density has two plateaus at $0 < \omega < 0\,(kV_i)$ and $\omega \leq 0(kV_e)$ corresponding to waves with phase velocities of the order of V_i, V_e. In addition there is a sharp resonance at $\omega \approx \omega_e$ with width $\gamma_L\left(\frac{\omega_e}{k}\right)$ (i.e., the Landau decrement for e-s waves with $V_p \approx \frac{\omega_e}{k}$). It is important to notice that this resonance becomes broader and has <u>more area</u> under it for a non equilibrium plasma having non-Maxwellian tails (fig. 8). This effect is due to the fact that the suprathermal electrons emit enhanced Cerenkov radiation. The steady state level can be found by balancing the Cerenkov emission of the waves with their reabsorption due to Landau damping (Tidman and Dupree, 1965).

The energy density of the e-s waves near ω_e, can be computed by

integrating eq. (14a) over the resonance ω_e and is given by

$$\frac{<E^2>}{8\pi} = \frac{8ne^2}{\omega_e} \int_0^{k_D} dkk \frac{F_e(\frac{\omega_e}{k})}{|F_e'(\frac{\omega_e}{k})|}, \tag{15}$$

where $F_e(u)$ is the usual reduced distribution function

$$F_e(u) = \int d\underline{v}\ \delta\left(u - \frac{\underline{k}\cdot\underline{v}}{k}\right) f_e(\underline{v}).$$

Eq. (15) is basically a statement of Kirchoff's law; specifically, that emission is balanced by absorption in equilibrium (notice that the linear damping decrement $\gamma_L(k) \sim F_e'(\omega_e/k)$).

An estimate of the value of the enhanced wave level over the one expected in thermal equilibrium ($<E^2>_{TE}$) can be found for the model distribution (fig. 8)

$$f_e(v) = \frac{\beta}{(2\pi)^{\frac{3}{2}} V_e^3}\left[\exp\left(-\frac{v^2}{2V_e^2}\right) + (1-\beta)\frac{V_e^3}{V_E^3}\exp\left(-\frac{v^2}{2V_E^2}\right)\right] \tag{16}$$

with $1 \gg |1-\beta| \gg 0$, V_E^2. The case $\beta = 1$ reproduces the results for thermal equilibrium. From eqs. (15) and (16) we find

$$\frac{<E^2>}{<E^2>_{TE}} = \frac{V_E^2/V_e^2}{\ln[V_E/V_e(1-\beta)]} \tag{17}$$

For example, if $V_E = 20\ V_e$, and $\beta = .9$ we find an enhancement of 10^2. In order of magnitude the presence of suprathermal electrons of temperature T_E, enhances the steady state level of the electrostatic plasma waves at ω_e, by a factor $\frac{T_E}{T_e}$.

The emission of electromagnetic waves in this case involves higher order interactions. One can obviously see that the presence of the enhanced level of electrostatic waves as given by eq. (17) will affect both the electron-ion (e-i)and the electron-electron (e-e) interactions. A detailed derivation of the emission can be found in Dawson (1968). However, some simplified formulae and their physical interpretation will be given in the next section.

4. <u>E-m radiation from non-thermal and weakly turbulent plasmas</u>:

In the above section we found that a non-thermal plasma has an enhanced level of e-s waves near ω_e. Another very common situation is the case of a plasma with an established electrostatic spectrum of turbulence. Such a spectrum can be, for example, the result of an instability. We proceed below to determine the e-m radiation from such a plasma. We shall assume that, as a result of certain causes, (1) turbulence develops in the given plasma at different types of plasma waves and (2) the energy density and its distribution over the spectrum are specified. For the case $\omega_e \gg \Omega_e$, we consider only electron plasma waves ($\omega \approx \omega_e$) and ion waves ($\omega < \omega_i$). In addition, we assume that the turbulence is weak, in the sense that it is homogeneously distributed, rather than localized as in the case of plasma solitons and collapse (see section 5 below)

There are, in general, two types of conversion of e-s to e-m waves;

regular conversion in a weakly inhomogeneous medium and non-linear conversion due to the interaction of the turbulent fluctuations with each other or with free and shielded plasma particles. In the case of propagation in a weakly inhomogeneous plasma, the conversion coefficient is in general proportional to the ratio of the wave-length λ to the characteristic dimension L of the inhomogeneity. If the geometrical optics condition is violated it becomes of the order $(\frac{\lambda}{L})^{\frac{2}{3}}$. However under most conditions in space plasmas $\frac{\lambda}{L}$ is very small and the regular conversion negligible (Kaplan and Tsytovich, 1969; 1973).

The non-linear conversion mechanisms correspond to the interaction of at least one high frequency wave (ω_e) with the polarization clouds of thermal ions (Rayleigh-like scattering), ion acoustic turbulence, other thermal or non-thermal high frequency (ω_e) waves (Raman-like scattering) or suprathermal particles (Compton-like scattering). The frequency of the resulting e-m wave is near ω_e in the first two cases, $2\,\omega_e$ in the second and can be much larger than ω_e in the third case. The processes are illustrated in fig. 9. The detailed theory of the conversion processes has been considered in various papers and can be found on the basis of eq. (11) by computing the appropriate shielded currents at the appropriate frequency. We confine the discussions, therefore, only to a brief summary of the physics and the simplified approximate formulae. We present first, for comparison, the radiation formulas for a thermal plasma (Bornatici and Engelmann, 1968).

For an optically thin slab of a Maxwellian plasma, the emission spectrum $P(\omega)$ is composed of a continuum due to binary encounters ($k < k_D$) given by (Bekefi, 1966)

$$P_c(\omega) = 2x\ 10^{-38}\ \frac{n_e n_i Z^2}{T^{\frac{1}{2}}}\ \left[19.6 + \ell n\left(\frac{T^{3/2}}{\omega Z}\right)\right] \frac{erg}{cm^3\text{-Hz-sec}} \qquad (18)$$

and two peaks superimposed at ω_e and $2\omega_e$, with negligible area under them, due to collective effects given by

$$P_{th}(\omega_e) = 6 \times 10^{-25}\ n_o^{5/2}\ T^{-3/2} \left(\frac{V_e}{c}\right)^2 \frac{erg}{cm^3 sec} \qquad (19a)$$

$$P_{th}(2\omega_e) = 10^{-24} n_o^{5/2}\ T^{-3/2} \left(\frac{V_e}{c}\right)^4 \frac{erg}{cm^3 sec} \qquad (19b)$$

The factors $\left(\frac{V_e}{c}\right)^2$ and $\left(\frac{V_e}{c}\right)^4$ indicate the dipole and quadrupole nature of the collective ω_e and $2\omega_e$ radiation respectively.

We proceed next to discuss the e-s to e-m conversion processes in order of increasing frequency. We assume below that a spectrum of turbu- of the form

$$W^{\ell}(\underline{k},\omega) = W^{\ell}(\underline{k})\ \delta(\omega-\omega_{ek})$$

$$W^{s}(\underline{k},\omega) = W^{s}(\underline{k})\ \delta(\omega-\omega_s(k)) \qquad (20)$$

has been established with $\omega_s(\underline{k})$ the ion sound frequency.

a. Emission near ω_e (Sturrock, 1961; Sturrock et al., 1965)

The interaction of electron plasma waves (ℓ) with ion sound wave (s) produces e-m radiation near ω_e since it requires that both energy and momentum be conserved ($\omega_{em} = \omega_{ek} + \omega_s(k)$, $\underline{k}_\ell + \underline{k}_s = \underline{k}_{em}$). This process, usually represented by $\ell + s \rightarrow t$, generates waves in the frequency range

$$\omega_e \leq \omega \leq \omega_e\ \left[1 + \frac{3}{2}\ \frac{V_e^2}{V_p^2} + \left(\frac{m}{M}\right)^{\frac{1}{3}}\right] \qquad (21)$$

where V_p is the average phase velocity of the e.p.o.'s. The power emitted by this process is given by (Tsytovich, 1977)

$$P(\omega_e) = \omega_e W^{\ell} \frac{W^s}{nmV_e^2} \left(\frac{V_p}{c}\right)^2 \qquad (22)$$

In the absence of ion sound waves the e.p.o's can be converted to e-m waves by scattering off the polarization clouds of thermal ions. It is essentially equivalent to scattering by the low frequency thermal noise. This process is usually represented by $\ell + i \rightarrow t + i'$ and its frequency bandwidth is determined by the inequality

$$\omega_e \leq \omega \leq \omega_e \left(1 + \frac{3}{2} \frac{V_e^2}{V_p^2}\right) . \qquad (23)$$

The power emitted by this process will be given by (Smith, 1974; Melrose, 1970)

$$P(\omega_e) = \omega_e W^{\ell} \left(\frac{V_p}{c}\right)^2 \left(\frac{V_e}{V_p}\right)^3 \left(\frac{V_e}{c}\right) \frac{1}{n\lambda_D^3} . \qquad (24)$$

Finally in the case of a non-thermal stable plasma, in which $W^{\ell}(k)$ will be given in terms of the electron distribution function as in eqs. (15-17), we find (Tidman and Dupree, 1965; Papadopoulos, 1970)

$$P(\omega_e) = \frac{e^2 \omega_e^2 \sqrt{3} V_e}{3\pi^2 c^3} \int_0^{k_D} dk\, k^2 \frac{Fe\left(\frac{\omega_e}{k}\right)}{\left|F_e'\left(\frac{\omega_e}{k}\right)\right|} \qquad (25)$$

which for the distribution of eq. (16) gives

$$P(\omega_e) = 6 \times 10^{-25} n^{5/2} T^{-3/2} \left(\frac{V_E}{c}\right)^2 \alpha^{-4} \frac{\text{erg}}{\text{cm}^3 \text{sec}} . \qquad (26)$$

The thermal equilibrium result is recovered by replacing $\alpha = 1$ and $V_E - V_e$. This process corresponds to conversion of the enhanced e.p.o's by scattering off thermal ions. Notice that in all of the above processes the emission bandwidth is very narrow, typically $\frac{\Delta\omega}{\omega_e} \leq \frac{1}{3}$. In addition care should be exercised in computing the ω_e radiation to verify that reabsorption is neglible.

b. Emission near $2\omega_e$: (Aamodt and Drummond, 1964)

Coupling of two electron plasma oscillations (ω_e) can give a transverse wave at $2\omega_e$ in a similar fashion as in the previous section ($\ell + \ell \rightarrow t$). The momentum conservation imposes some limitations on the wave number of the interacting waves. The wave number of the transverse waves at $2\omega_e$ is given by $k_o = \sqrt{3}\,\frac{\omega_e}{c}$. If the wave-number of one of the interacting waves $\underline{k}_1$ has $|\underline{k}_1| \gg k_o$, then the wave-number of the other wave must be almost antiparallel so that their sum can give a small wave-number ($\underline{k}_1 \approx -\underline{k}_2$). In this case the e-m wave propagates in the direction perpendicular to the interacting waves. If however $|\underline{k}_1| \ll k_o$, then $k_2 \approx k_o \approx \sqrt{3}\,\frac{\omega_e}{c}$, in which case the e-m wave propagates in the direction of $\underline{k}_2$. The power emitted near $2\omega_e$ will be given by

$$P(2\omega_e) = \frac{\pi\sqrt{3}}{3}\,\frac{\omega_e^2}{nmc^3}\left[W^{\ell}(k_o)\int_0^{k_o} W^{\ell}(k_1)\,dk_1 + \frac{12}{5}\int_{k_o}^{k_D}\left[W^{\ell}(k_1)\right]^2\frac{\omega_e^2}{k_1^2c^2}\,dk_1\right]. \tag{27}$$

The maximum emission occurs for $k_1 \approx k_2 \approx k_o$. For the case that $k_1 \gg k_o$ eq. (27) gives an approximate value

$$P(2\omega_e) = 10W^{\ell}\omega_e\,\frac{W^{\ell}}{nmV_e^2}\left(\frac{V_p}{c}\right)^3\left(\frac{V_e}{c}\right)^2. \tag{28}$$

Notice that the validity of the weak turbulence approximation restricts the value of $\frac{W^{\ell}}{nmV_e^2} < \left(\frac{V_e}{c}\right)^2$, so that typically the maximum conversion efficiency is proportional to $\left(\frac{V_e}{c}\right)^4$ (i.e.,quadrupole). The bandwidth of the emission is

$$\frac{\Delta\omega}{2\omega_e} \approx 3\frac{k_1^2 V_e^2}{\omega_e^2} \approx 9\frac{V_e^2}{c^2} \quad . \tag{29}$$

The case of a stable non-thermal plasma can be treated in a similar fashion as above if we replace W^{ℓ} in eq. (28) by the values given by eqs. (15-17). Namely,for an isotropic plasma the oppositely directed enhanced e.p.o's collide to produce e-m radiation at $2\omega_e$. The emission formula is given by (Tidman and Dupree, 1965 ; Papadopoulos, 1970)

$$P(2\omega_e) = \frac{2e^2\omega_e^{4/3}}{5\pi^2c^3}\int_0^{k_D} dk \; \frac{F_e^2\left(\frac{\omega_e}{k}\right)}{\left|F_e'\left(\frac{\omega_e}{k}\right)\right|^2} \tag{30}$$

or for the distribution of equ. (16),

$$P(2\omega_e) = 10^{-24}\, n^{5/2} T^{-3/2} \left(\frac{V_E}{c}\right)^4 \alpha^{-3} \; \frac{erg}{cm^3 sec} \quad . \tag{31}$$

The relativistic generalizations of the above can be found in Papadopoulos (1969). Notice that for $\frac{V_e}{c} \to 1$, the ω_e and $2\omega_e$ emissions become comparable. Finally we should note that reabsorption for the $2\omega_e$ emission is usually negligible (i.e.,collisional).

c. Emission at frequencies much higher than ω_e:

If the conversion occurs by scattering of waves from non-thermal particles, whose velocity $\underline{v}$ exceeds the phase velocity of the plasma

waves, the radiation generated has a frequency close to

$$\omega = \omega_e + \underline{k} \cdot \underline{v} \lesssim \omega_e \left(1 + \frac{v}{V_p}\right) . \tag{32}$$

Therefore, high frequencies can be emitted by this process if $v > V_p$. This process becomes even more interesting in the case of relativistic particles, for which the frequency upshifting becomes

$$\omega = \frac{\omega_e + \underline{k}_1 \cdot \underline{v}}{1 - \frac{v}{c}\cos\theta} \lesssim 2\omega_e \left(1 + \frac{c}{V_p}\right) \left(\frac{\varepsilon}{mc^2}\right)^2 \tag{33}$$

The emitted frequency in this case can be extremely high. A typical distribution function that can produce important results is one with a long energetic tail. For the case of relativistic electrons this is nothing more than Compton scattering. A calculation of the emission is mathematically complicated and we refer the reader to Kaplan and Tsytovich (1973). However, in order to find some estimate we consider for the relativistic electrons a distribution of the form

$$f(\varepsilon) = \frac{\alpha(\alpha^2-1)\, n_o\, \varepsilon_o^{\alpha-1} \varepsilon^2}{2(\varepsilon_o + \varepsilon)^{\alpha+2}} . \tag{34}$$

This function behaves like $f(\varepsilon) \propto \varepsilon^{-\alpha}$ for $\varepsilon \gg \varepsilon_o$ while for $\varepsilon \ll \varepsilon_o$ we have $f \propto \varepsilon^2$. In this case

$$P(\omega) \approx \frac{\alpha(\alpha-1)}{4\pi\omega_e} \frac{n_o}{n} \frac{1}{n\lambda_D^3} \left(\frac{V_e}{c}\right)^3 \left(\frac{mc^2}{\varepsilon_o}\right)^2 \left[\ln\left(\frac{2\varepsilon_o}{mc^2}\right) - 1\right] \omega_e W^{\ell} . \tag{35}$$

The total emission can be found by multiplying (35) by the bandwidth of eq. (32) so that

$$P = \frac{\alpha(\alpha-1)}{2\pi}\left(1+\frac{c}{V_p}\right)\frac{n_o}{n}\ \frac{1}{n\lambda_D^3}\left(\frac{V_e}{c}\right)^3 x\left[\ell n\left(\frac{2\epsilon_o}{mc^2}\right)-1\right]\omega_e W^\ell . \qquad (36)$$

5. Radiation from strongly turbulent plasmas

One of the most exciting developments of the recent years, was the realization that our concept of electrostatic turbulence uniformly distributed in space is invalidated even for rather low wave energy levels, $\left(\text{i.e., } \frac{W^\ell}{nT} \leq (k\lambda_D)^2 \text{ where k is the typical wave-number of the e.p.o. spectrum}\right)$. The physical reason for this can be seen by noting that the presence of high frequency (ω_e) waves exerts a low frequency ponderomotive force (i.e. radiation pressure) on the plasma, which results in a modification of the local density n, in which the change in pressure $p = nT + \frac{1}{2}\frac{E^2}{8\pi} = nT + \frac{1}{2}W$ is zero ($\delta p = 0$). Therefore $\frac{\delta n}{n} \approx -\frac{1}{2}\frac{W}{nT}$. The dispersion relation for e.p.o.'s thus becomes (Abdulloev et al., 1975)

$$\omega_{ek} = \omega_e\left(1+\tfrac{3}{2}(k\lambda_D)^2+\tfrac{1}{2}\frac{\delta n}{n}\right) \approx \omega_e\left(1+\tfrac{3}{2}(k\lambda_D)^2-\tfrac{1}{4}\frac{W}{nT}\right) . \qquad (37)$$

Eq. (37) has a simple physical interpretation if the e.p.o.'s are viewed are quasi-particles subject to attractive and repulsive forces and capable of emitting sound waves. For non-relativistic velocities, eq. (37) can be viewed as the definition of energy of the quasiparticle (with $\hbar = 1$), with an effective mass of $m_{eff} = \frac{\omega_e}{3V_e^2}$, a momentum of k, and the quantity corresponding to the velocity of light is $c^2 \equiv 3V_e^2$. The last term corresponds to the potential energy of the quasiparticle in the field of others. Since its sign is negative it implies attraction. As long as the kinetic energy $\left(\text{i.e., } \frac{3}{2}\frac{k^2V_e^2}{\omega_e}\right)$ is

larger than the attractive potential $\left(\text{i.e., } \frac{1}{4}\,\omega_e \frac{W^\ell}{nT}\right)$, the plasma waves behave in the usual sense described by the weak turbulence theory. However, when $\frac{W^\ell}{nT} > 6(k\lambda_D)^2$ they start collapsing to smaller and smaller sizes, and form localized clumps of wave energy which have been given the name of solitons, spikons, or cavitons. As shownby Manheimer and Papadopoulos (1975) this process is equivalent to the oscillating two stream instability (O.T.S.) known from parametric interactions. The inequality

$$\frac{W^\ell}{nT} > (k\lambda_D)^2 \tag{38}$$

is usually considered as the condition for invalidation of weak turbulent theory, and has two consequences. The first is that the dispersive term in eq. (37) becomes negligible, thereby radically modifying the real part of $\epsilon_L(\underline{k},\omega)$. The second is that instead of uniformly distributed turbulence we end up with a series of highly intense and localized wave packet-like structures (fig. 10).

It was noted for the first time by Papadopoulos (1973) that since beam plasma instabilities have very small $(k\lambda_D)^2 \approx \left(\frac{V_e}{V_b}\right)^2$, where V_b is the beam velocity, these effects can play a controlling role in beam plasma interactions and an analysis of the type III bursts, auroral beams and of relativistic beam heating was presented (Papadopoulos,1972, 1975; Papadopoulos and Coffey,1974a, b; Papadopoulos et al.,1974). It was shown that the presence of the localized clumps decouples the beam from the plasma and allows it to propagate over substantially larger distances than expected on the basis of quansilinear-theory. Literally hundreds of papers followed on the subject which resulted in the resolution of many experimental mysteries both in space and laboratory plasmas. Since

most space plasmas are penetrated by beams we expect that often their radiation properties will be a reflection of the strong turbulence theory. While the complete theory of the radiation in the strong turbulence regime is still under development, some results have recently appeared in the literature. The only complete analysis has been the radiation at $2\omega_e$ from a cylindrically symmetric soliton. Assuming the electric field is of the form

$$E(r,z) = E_o\, e^{-r/L}\, \mathrm{sech}(kz) \tag{39}$$

with $\frac{E_o^2}{8\pi nT} = 12(k\lambda_D)^2$, Papadopoulos and Freund (1978) found that the power emitted per soliton is given by

$$P_s(2\omega_e) = \omega_e \frac{E_o^2}{8\pi} \frac{\sqrt{3}\pi}{4} \frac{V_e}{c} \lambda_D^3 \tag{40}$$

per soliton if $\frac{1}{2} k_o L \gg 1$ (note that $k_o = \sqrt{3}\omega_e/c$), and

$$P_s(2\omega_e) = \omega_e \frac{E_o^2}{8\pi} \frac{9\sqrt{3}\pi}{4} \left(\frac{L\omega_e}{c}\right) L^3 \tag{41}$$

per soliton if $\frac{1}{2} k_o L \ll 1$.

The most common situation is expected to be $k_o L \ll 1$, because the presence of the magnetic field and the beam direction force them to behave in a one dimensional manner (i.e., $L_\perp \gg L_{||}$). In this interesting case we notice from eq. (40) that P_s is independent of L, and is proportional to W^ℓ. This is in contrast to the $(W^4)^2$ depedence found in the case of weak turbulence. This important fact has helped explain a major scaling puzzle associated with type III bursts. The total emission per unit volume can be found by multiplying by the number N of solitons

per unit volume which will depend on the problem under consideration. For case of very energetic beams an upper bound on $2\omega_e$ radiation can be found by making the rather unrealistic assumption that N is given by closely packing the solitons. Some frontier work connected with strong turbulence theory and soliton radiation has been performed for the type III radio busts. We refer the interested reader to Smith et al. (1976, 1978), Nicholson et al.(1978), Nicholson and Smith (1978), Goldstein et al.(1978a, b), and Papadopoulos (1978).

IV. Radiation in the presence of a magnetic field:

The presence of a magnetic field has important consequences for radiation processes in plasmas. In addition to the bremsstrahlung mechanism, radiation can also result from the gyration of electrons about the magnetic field and is referred to as either cyclotron or synchrotron radiation. While the terminology varies, cyclotron radiation typically refers to induced radiation processes and synchrotron radiation is used, more often, to denote spontaneous emission. Alternately, cyclotron radiation may be used to denote radiation (either induced or spontaneous) with frequencies in the vicinity of the electron gyrofrequency, Ω_e, while synchrotron is applied to emission at the higher harmonics of Ω_e. In this work, we adopt the former usage and treat the case of the spontaneous synchrotron mechanism in the next section. Induces cyclotron emission will be considered in Chapter VI. The magnetic field also couples longitudinal and transverse oscillations in the plasma. Thus, as discussed in Chapter II, wave modes occur with mixed polarization and phase velocities less than the speed of light; specifically, the electron whistler and slow extraordinary modes. This property, in contrast to the case of a field-free plasma, permits Cerenkov emission of predominantly transverse modes via resonance with energetic electrons. Finally, bremsstrahlung processes are also affected by the magnetic field due to (1) the change in the dielectric properties of the propagating electromagnetic modes, (2) the introduction of new low and high frequency electrostatic modes, and (3) the gyro-motion of the particles which introduces wave-particle resonances of the form $\omega \cong n\Omega_e + k_{||}v$ (n is an integer). The entire subject of the bremsstrahlung

spectrum from a magnetized plasma has not been treated in the literature; however, we present in this chapter several order of magnitude estimates which follow from analogies with the field-free limit (III 2-4).

1. Synchrotron emission:

Great advances have been made in the understanding of the synchrotron radiation spectrum in the last decade. On the one hand, the synchrotron spectrum from ultrarelativistic electrons has been studied in the limit in which plasma collective effects are unimportant (Ginsburg and Syrovatskii 1965, 1967). On the other hand, the influence of the dielectric properties of the plasma on the synchrotron spectrum of weakly relativistic electrons has also received a great deal of attention in the literature (Hirshfield et al.,1961; Pakhomov et al.,1962; Liemohn,1965; Birmingham,1966; Melrose,1968; Audenaerde, 1977; Freund and Wu,1977; Freund et al.,1978a, b, c). It is beyond the scope of this review to discuss all aspects of these phenomena, and we chose to focus on the modifications in the synchrotron spectrum from individual electrons due to the collective interactions between electrons.

As in Chapter III, the average power radiated per unit frequency is determined by averaging over the microcopic instantaneous power to obtain

$$P_s(\omega) = -\frac{1}{(2\pi)^4} \lim_{T\to\infty} \frac{1}{T} \mathrm{Re} \int d\underline{k}\, \underline{E}(\underline{k},\omega)\cdot \underline{j}_s^*(\underline{k},\omega). \qquad (1)$$

In a magnetized plasma, the source current is of the form

$$\underline{j}_s(\underline{k},\omega) = - e \lim_{T\to\infty} \int_{-T/2}^{T/2} dt \sum_{\ell=1}^{N_e} \underline{v}_\ell(t) e^{i(\omega t - \underline{k}\cdot\underline{x}_\ell(t))}, \qquad (2)$$

where N_e denotes the number of electrons, and the trajectories are of the form

$$\underline{v}_\ell(t) = v_{\perp\ell} [\cos(\varphi_\ell - \Omega_e t)\hat{\underline{e}}_x + \sin(\varphi_\ell - \Omega_e t)\hat{\underline{e}}_y] \qquad (3)$$

$$\underline{k}\cdot\underline{x}_\ell(t) = \underline{k}\cdot\underline{x}_\ell(t=0) + b_\ell[\sin(\varphi_\ell - \Omega_e t) - \sin\varphi_\ell] + k_{||} x_{||\ell} t, \qquad (4)$$

φ_ℓ denotes the aximuthal angle, $\underline{k} = k_\perp \hat{\underline{e}}_x + k_{||}\hat{\underline{e}}_z$, and $b_\ell = k_\perp v_{\perp\ell}/\Omega_e$. The self-consistent radiation field is given by

$$\underline{\underline{\Lambda}}(\underline{k},\omega)\cdot\underline{E}(\underline{k},\omega) = - \frac{4\pi i}{\omega} \underline{j}_s(\underline{k},\omega), \qquad (5)$$

where $\underline{\underline{\Lambda}}(\underline{k},\omega)$ denotes the dispersion tensor and is given by

$$\underline{\underline{\Lambda}}(k,\omega) = \frac{c^2}{\omega^2}(\underline{k}\,\underline{k} - k^2\,\underline{\underline{I}}) + \underline{\underline{\varepsilon}}(\underline{k},\omega), \qquad (6)$$

where $\underline{\underline{I}}$ is the unit dyadic, and $\underline{\underline{\varepsilon}}(\underline{k},\omega)$ is the plasma dielectric tensor. It should be noted that eqs. (1)-(6) describe, in principle, the emission of self-consistent waves in the plasma (i.e., electrostatic, electromagnetic, and mixed polarization modes).

As a consequence, the power emitted per unit volume per unit frequency per unit per unit solid angle subtended by $\underline{k}$ can be shown to be (Melrose, 1968; Freund and Wu, 1977b)

$$P_s^{(\pm)}(\omega,\theta) = \frac{e^2 n_e}{4\pi}\frac{\omega^2\eta_\pm}{c}\frac{\rho\pm\sin^2\theta}{\rho}\int d\underline{u}\, F_e(\underline{u})\sum_{n=-\infty}^{\infty}\left[V_\pm J_n(b)+\frac{v_\perp}{c}J_n'(b)\right]$$

$$\times\ \delta\left[\omega\left(1-\frac{v_\parallel}{c}\eta_\pm\cos\theta\right)-n\Omega_e/\gamma\right], \tag{7}$$

where the plus (minus) sign refers to the ordinary (extraordinary) mode, $\underline{u}(\equiv p/m)$ is the relativistic velocity, $\gamma = (1 - v^2/c^2)^{-\frac{1}{2}} = (1+ u^2/c^2)^{\frac{1}{2}}$, n_e is the electron density, $F_e(\underline{u})$ is the electron distribution function, and J_n and J_n' are the usual Bessel function and its first derivative of order n. In addition, $\rho^2 = \sin^4\theta + 4(\omega^2/\Omega_e^2)(1-\omega_e^2/\omega^2)^2\cos^2\theta$,

$$V_\pm = 2\frac{\omega}{\Omega_e}\frac{\left[(1-\omega_e^2/\omega^2)\left(1-\frac{v_\parallel}{c}\eta_\pm\cos\theta\right)-\eta_\pm^2\sin^2\theta\right]}{\eta_\pm\sin\theta\,(\sin^2\theta\mp\rho)} \tag{8}$$

and

$$b = \frac{n\eta_\pm\sin\theta}{1-\frac{v_\parallel}{c}\cos\theta}\frac{v_\parallel}{c}\ . \tag{9}$$

It should be noted that the random phase approximation has been implicitly imposed in the derivation of (7). It can be formally shown (Freund and Wu 1977b) that this is valid only when the electron pair correlation function is independent of φ (i.e., the azimuthal coordinate). This corresponds, physically, to the requirement that no phase bunching of electrons occurs and, as a consequence, (7) is not strictly applicable in the presence of strong cyclotron instabilities (see Chapter VI). In addition, Eq. (7) reduces to the classical Schott-Trubnikov formula (Bekefi, 1966) in the limit in which $\omega_e \ll \omega \sim \Omega_e$, and plasma effects on the

emission can be neglected. Examination of the effect of the dielectric polarization of the plasma on the strength of the emission indicates that the radiated power tends to decrease as the plasma density increases, (Freund and Wu, 1977b) and is attributable to collective current shielding by electrons in the plasma. Finally, we remark that the plasma dielectric properties have been described in terms of the cold plasma approximation, and eq. (7) breaks down for frequencies in the vicinity of the fundamental gyroharmonic.

The synchrotron spectrum from a thermal plasma has been studied in detail by numerous authors, (Hirshfield et al., 1961; Pakhomav et al., 1962; Liemohn, 1965; Birmingham, 1966; Melrose, 1968; Audenaerde, 1977; Fruend and Wu, 1977) and will not be repeated here. Instead, we consider the synchrotron spectrum produced by a small population of suprathermal electrons streaming parallel to $\underline{B}_o$ in an otherwise thermal plasma. We assume that, since the energy of the suprathermal electrons is directed along $\underline{B}_o$, $\gamma^2 \cong 1 + u_{||}^2/c^2$, and that the electron distribution function is of the form

$$F_s(u_\perp, u_{||}) = (\pi u_p^2)^{-1} e^{-u_\perp^2/u_p^2} F_{||}(u_{||}), \qquad (10)$$

where the subscript "s" is used to describe the suprathermal electrons, u_p characterizes the perpendicular thermal spread, and $F_{||}(u_{||})$ is used to describe the streaming of the suprathermal species. As a result, the suprathermal emissivity is of the form (Freund et al., 1978a, b)

$$P_s^{(\pm)}(\omega,\theta) \cong \frac{\omega\eta_\pm}{\rho} \sum_{n=o}^{\infty} \frac{cF_{||}(u_{||} = u_n)}{|u_n - c\gamma_n\eta_\pm\cos\theta|} H[n^2\Omega_e^2 - \omega^2(1-\eta_\pm^2\cos^2\theta)]$$

$$\frac{1}{2^n n!}\left(\frac{\omega^2}{\Omega_e^2}\eta_\pm^2\sin^2\theta\right)^{n-1}\left(\frac{\omega_p^2}{c^2}\right)^n \Psi_n^{(\pm)}(\omega,\theta) \tag{11}$$

for $\theta < \pi/2$ and $u_p^2/c^2 \ll 1$. In (11), H is the Heaviside function,

$$\frac{u_n}{c} = \frac{n\Omega_e\eta_\pm\cos\theta + [n^2\Omega_e^2 + \omega^2(\eta_\pm^2\cos^2\theta - 1)]^{\frac{1}{2}}}{\omega|\eta_\pm^2\cos^2\theta - 1|}, \tag{12}$$

is the resonant momentum parallel to $\underline{B}_o$, n_s is the suprathermal density, $\gamma_n = (1 + u_n^2/c^2)^{\frac{1}{2}}$,

$$\Psi_n^{(\pm)}(\omega,\theta) = \tfrac{1}{2}\left(n^2 + \frac{X_n^2}{(1-\omega_e^2/\omega^2)^2\cos^2\theta}\right)\rho \mp \tfrac{1}{2}\left(n^2 - \frac{X_n^2}{(1-\omega_e^2/\omega^2)^2\cos^2\theta}\right)\sin^2\theta$$

$$\mp 2n\frac{\omega}{\Omega_e}X_n, \tag{13}$$

and $X_n = n(1-\omega_e^2/\omega^2) - \gamma_n(\omega/\Omega_e)\eta_\pm^2\sin^2\theta$. We observe that eq. (11) breaks down for frequencies and angles of propagation in which $u_n \lesssim u_p$, because in this limit, the relativistic γ-factor cannot be considered to be independent of $u_\perp$.

It is evident from (11) that the power level for frequencies $\omega \sim n\Omega_e$ falls off as $(u_p^2/c^2)^n$, and that substatital emission at the higher gyroharmonics is expected only when the perpendicular energy is large. Further, since $P_s^{(\pm)} \sim (\eta_\pm^2\sin^2\theta)^{n-1}$, the power spectrum is expected to become increasingly peaked in the direction perpendicular

to $\underline{B}_o$ at the higher harmonics of Ω_e.

2. Enhanced Cerenkov emission:

The principle difference in the Cerenkov radiation spectrum between a magnetized and a field-free plasma arises due to the mode structure found in the magnetized case. Since the Cerenkov resonance condition (i.e., $\omega = k_{||} v_{||}$) requires the resonance velocity $v_{res} = c/\eta\cos\theta$, the only modes which can be excited by this process are those for which $\eta\cos\theta > 1$. In an unmagnetized plasma, this condition is satisfied only by purely longitudinal Langmuir oscillations for which $\omega \cong \omega_e$. In a magnetized plasma, however, the resonance condition can be satisfied by waves in either the electron whistler or slow extraordinary modes, and a greatly expanded wave spectrum can result.

In most astrophysical or laboratory plasmas, Cerenkov emission from thermal electrons ($T_e \sim$ keV) can occur only for frequencies in the vicinity of the cold plasma resonances (see Chapter II), where $v_{res} \sim V_e$ and the wave polarization is predominantly electrostatic. In such cases, the excited frequencies are $\omega \sim \omega_e \cos\theta$ when $\omega_e < \Omega_e$ (or $\omega \sim \Omega_e \cos\theta$, for $\Omega_e < \omega_e$) for waves in the electron whistler mode, and $\omega \sim \frac{1}{2}\Omega_e + \frac{1}{2}\sqrt{\Omega_e^2 + 4\omega_e\Omega_e\sin^2\theta}$ for waves in the slow extraordinary mode. Excitation of predominantly transverse waves can occur only if a population of suprathermal electrons streaming parallel to the ambient magnetic field is present. In such a case, the power spectrum of the emission is given by eq. (11) for $n = 0$, and we write (Freund et al., 1978b, c)

$$P_s^{(\pm)}(\omega,\theta) \cong \frac{e^2 n_s}{4\pi}\left(\frac{u_o}{c}\right)^3 \frac{\omega\eta_\pm^5 \sin^2\theta(\rho\pm\sin^2\theta)}{\rho(1-\omega_e^2/\omega^2)^2} F_{||}(u_{||}=u_o)H(\eta_\pm^2\cos^2\theta - 1), \tag{14}$$

where $u_o = c(\eta_\pm^2\cos^2\theta - 1)^{-\frac{1}{2}}$, and the plus (minus) sign refers to the electron whistler (slow extraordinary) mode.

It is evident that (14) vanishes in the limit of parallel propagation. This corresponds, physically, to the fact (1) that for parallel propagation these modes are purely transverse (with right and left hand circular polarizations) with $\underline{E}_1 \cdot \underline{B}_o = 0$, and (2) that the Cerenkov process couples the parallel electron energy with the component of the wave electric field which is also parallel to $\underline{B}_o$. In addition, it should be remarked that the index of refraction approaches unity as $\omega \to \omega_e$ for oblique angles of propagation. For this reason, $\eta\cos\theta < 1$ at the plasma frequency, and the apparent singularity contained in (14) is excluded.

While the power radiated at frequencies in the vicinity of the n^{th} gyroharmonic (11) varies approximately as $(u_p^2/c^2)^n$, the power emitted via the Cerenkov interaction is of order unity in this parameter. Thus, it is expected that spontaneous Cerenkov emission from streaming suprathermal electrons dominates over the synchrotron radiation. In particular, if the streaming energy is of the order of several hundred keV, then strong emission of predominantly transverse, slow extraordinary mode waves with $\omega \sim \omega_e$ can result (Freund et al.,1978a, b, c). However, it must be borne in mind that neither the electron whistler or the slow extraordinary can freely escape from a typical plasma. This results

because, as these waves propagate out of the plasma, they traverse regions of decreasing plasma density and magnetic field strength. As a result, the cold plasma-resonances decrease along the ray path of the radiation, and strong absorption occurs when the wave frequency coincides with the resonance frequency. Thus, in order to escape the plasma, the excited waves must either (1) "tunnel" through the stop bands (see Chapter II), or (2) scatter off low frequency fluctuations in the plasma (i.e., ion acoustic oscillations, ion cyclotron waves, or magnetosonic waves). Since both of these processes have, typically, low conversion efficiencies, such radiation mechanisms are not expected to be of importance in the study of the spectra from astrophysical plasmas.

3. E-m radiation from weakly turbulent plasmas

In a plasma immersed in a strong magnetic field, e-s plasma waves can be excited either spontaneously as discussed in Section 2 or by e-s instabilities which result in wave spectra with frequencies $\omega \approx \Omega_e \cos\theta$ when $\Omega_e < \omega_e$, or $\omega \approx \omega_e \cos\theta$ if $\Omega_e > \omega_e$. The mechanisms of conversion of these waves to e-m modes are similar to the ones discussed in III-4. However, the emitted frequencies can now be near Ω_e, $2\Omega_e$ and $\Omega_e + \omega_e$. Detailed theories of these processes have yet to appear in the literature. However, some general estimates can be found on the basis of the results of III-4.

a. Emission near Ω_e:

Conversion of e-s to e-m waves near Ω_e can be either due to scattering off enhanced low frequency wave (i.e., ion acoustic, ion

cyclotron, magnetosonic,etc.) or off thermal ions. In general, the emitted radiation can be computed from eqs. (III-22, 24, 25) by replacing ω_e by Ω_e, substituting W^l by the wave energy level of the cyclotron waves W^s and using instead of W^s the appropriate wave energy level of the low frequency turbulence. These results are correct to within a factor $\frac{\Omega_e}{\omega_e}$. It should be noted however that the expressions which describe the scattering off thermal ions have been derived under the assumption of straight-line orbits and, as a result, are valid only if $V_p \ll (M/m)^{\frac{1}{2}} V_e$. Otherwise, the gyro-motion of the ions must be included the analysis.

It is worth noting that the bandwidth of the spectra excited in this manner can be rather large. In particular, since $\omega_{\underline{k}} \cong \Omega_e \times [1 + (\omega_e^2/2\Omega_e^2) \sin^2\theta]$ one may have that $\Delta\omega \sim \Omega_e$ for $\Omega_e < \omega_e$. In addition, there are no difficulties involved in the escape of the resulting electromagnetic radiation from the plasma since the index of refraction is of the order unity. Finally, when $\omega_e \sim \Omega_e$, the radiation can be continuous over a frequency range comparable to both ω_e and Ω_e.

b. Emission at frequencies near $2\Omega_e$ and $\omega_e \pm \Omega_e$:

Coupling of electrostatic waves with frequencies $\omega \sim \Omega_e$ with each other or with electrostatic waves of frequency $\omega = \omega_e$ can lead to emission of electromagnetic radiation having frequencies $2\Omega_e$ or $\omega_e + \Omega_e$. The mechanism, and all relevant conversation laws, is similar to the $2\omega_e$ case considered earlier. The emission formula for the case of interaction between two electrostatic cyclotron waves is

$$P(2\Omega_e) = 100 \frac{\omega_e}{\Omega_e} \left(\frac{V_e}{c}\right)^3 \left(\frac{V_p}{V_e}\right) \frac{W^c}{n_e T_e} \omega_e W^c , \qquad (15)$$

where W^c is the spectral energy density of the cyclotron waves, and $V_p \leq c$.

c. Emission at frequencies exceeding Ω_e:

The situation in this case is identical with the Compton scattering results discussed in III. 4c. The only changes necessary are replacement of ω_e by Ω_e and W^ℓ by W^c in eqs. (32)-(36).

V. Stimulated scattering processes:

1. General considerations:

There are two underlying notions involved in the amplification processes that will be described below. The first is the role of a relativistic scatterer, and the second the role of the ponderomotive force. These type of mechanisms represent a class which is in the forefront of microwave production in laboratory plasmas. The basic requirement is the existence of an electromagnetic signal or a large amplitude e-s or magneto static disturbance, and a fast moving mirror-like medium. Such a medium is most often a relativistic beam, but can also be any other reflecting interface such as a moving ionization front.

(a) In order to appreciate the role of a relativistic scatterer in converting microwaves to submillimeter radiation let us first consider the simple gedanken experiment sketched in Fig. 11. A plane wave with frequency ω_o and wavenumber k_o is normally incident on a perfectly reflecting mirror moving with velocity v_o. The wave scattered off the moving mirror is denoted by frequency ω_s and wavenumber k_s. If we make Lorentz transformations from the laboratory frame to the frame in which the mirror is at rest, then the frequency of the incident and scattered waves are respectively (Sprangle and Granatstein, 1974)

$$\omega_o' = \gamma(\omega_o + k_o v_o) = \gamma(1 + \beta)\omega_o \quad , \tag{1}$$

$$\omega_s' = \gamma(\omega_s + k_o v_o) = \gamma(1 - \beta)\omega_s \quad , \tag{2}$$

where $\beta = \frac{v_o}{c}$ and $\gamma = (1-\beta^2)^{-\frac{1}{2}}$. Now, in the mirror rest frame, the frequency of the two waves must be equal if the boundary conditions are to be satisfied at all times, i.e. $\omega_o' = \omega_s'$. Thus, from eqs. (1) and (2)

$$\omega_s = (1 + \beta)^2 \gamma^2 \omega_o \tag{3}$$

Furthermore, the energy of the scattered wave W_s, may be related to the energy of the incident wave by invoking conservation of action; viz., $\frac{W_o}{\omega_o} = \frac{W_s}{\omega_s}$. Thus

$$W_s = (1 + \beta)^2 \gamma^2 W_o \tag{4}$$

The implications of eq. (3) and eq. (4) are intriguing. If one had a perfect mirror moving relativistically with $\beta = .99$ ($\gamma \approx 6$), then $\omega_s = 143\ \omega_o$ and the power of the scattered signal will exceed the energy of the incident by a factor of 143. The trick is to find suitable relativistic mirrors. Two possible candidates (i.e., a relativistic e-beam and an ionizing front or shock) will be discussed later.

(b) While the above notions were completely linear, nonlinear processes are also of extreme importance. The character of the nonlinear forces can be clearly illustrated by using the concept of the ponderomotive force, i.e. the averaged high frequency force acting on a charged particle in an alternating e-m field. It is well known that in a field of two travelling waves (Litvak and Trakhtengerts, 1971) $\underline{E} = \underline{E}_1 e^{i(\omega_1 t - \underline{k}_1 \cdot \underline{r})} + \underline{E}_2 e^{i(\omega_2 t - \underline{k}_2 \cdot \underline{r})}$ with close frequencies $|\omega_1 - \omega_2| \ll \omega_1$ or ω_2, the force averaged over the periods of the partial oscillations acting on a single charged particle, is given by

$$\underline{F} = \nabla \Phi, \tag{5a}$$

where

$$\Phi = \frac{e^2 (E_1 E_2^*)}{2m\omega_1 \omega_2} e^{i(\omega t - \underline{k} \cdot \underline{r})} \tag{5b}$$

and

$$\omega = \omega_1 - \omega_2, \quad \underline{k} = \underline{k}_1 - \underline{k}_2$$

This force produces, stimulated longitudinal wave motions in the plasma. If ω and $\underline{k}$ satisfy the dispersion equation of the natural plasma oscillations (i.e.,if the condition of synchronization is satisfied between the driving force and one of the eigenfrequencies of the plasma) then resonant excitation of the oscillations occurs at the frequency difference. If the phase velocity $V_p = \frac{\omega}{|k|}$ falls outside the velocity range of the electrons (i.e.,$V_p \gg V_e$), then a hydro-dynamic interaction can occur between the three waves. If $V_p < V_e$, than a kinetic interaction (Landau type) can occur between the waves and the particles ($\omega_1 - \omega_2 = (k_1 - k_2) \cdot \underline{V}$).

2. Stimulated scattering from electron beams:

A typical situation where both of the above notions combine to amplify a signal is coherent scattering of an electromagnetic wave from a counterstreaming relativistic electron beam. In this case the interaction of the electrons with an e-m wave ($\omega_o, \underline{k}_o$) and the scattered wave ($\omega_s, \underline{k}_s$) is unstable, leading to exponential growth of both the scattered wave and the electron density modulation (Granatstein and Sprangle,1977).

The details of the process can be better understood by refering to the beam frame (fig. 12). The incident wave ($\omega_o', \underline{k}_o'$) has a transverse electric field E_{oy}' which excites a zero order transverse oscillation of the electrons with velocity

$$\underline{v}_o' = \hat{\underline{e}}_y \frac{|e|}{m} \frac{E_{oy}'}{\gamma' \omega_o'} \tag{6}$$

with $\gamma' = \left[1 - \left(\frac{v_o'}{c}\right)^2\right]^{-\frac{1}{2}}$ (Note that primed quantities refer to the beam frame).

In the presence of an incipient backscattered wave $(\omega_s', \underline{k}_s')$ with magnetic field $B_s'\hat{\underline{e}}_z$, an axial force is exerted on the electrons. The coupling between the two waves produces a ponderomotive force as described above, which leads to a low frequency modulation of the electrons $(\omega', \underline{k}')$ and a grouping of the electrons into bunches along the z axis $(\underline{F}_p = -e(\underline{v}_o' \times \underline{B}_s' + \underline{v}_s' \times \underline{B}_o'))$. The e-beam modulation occurs at

$$\omega' = \omega_o' - \omega_s', \quad \underline{k}' = \underline{k}_o' + \underline{k}_s' \tag{7}$$

(typically, $\omega' \ll \omega_o'$ and $k' \simeq 2\, k_o'$). The growth of the density modulation increases the coherence of the scattering process, resulting in further growth. We have, therefore, a feedback mechanism that can result in an instability and exponential growth.

The growth rate as well as the nonlinear saturation depend on a number of factors, viz. the strength of the incoming wave, the wavelengths of the incident and scattered waves, the electron density and the electron temperature. Two physical regions can be distinguished in analogy with the hydrodynamic and kinetic beam plasma instability. Fig. 13 shows the physical difference between the two regimes. In the first regime (Fig. 13a), usually called <u>stimulated Raman scattering</u>, $\frac{\omega'}{k'} \gg v_t$. This is like a hydrodynamic instability, in which case the entire beam participates in the density wave which takes the form of a collective plasma oscillation, i.e. $\omega' \approx \omega_e$. In this case, if $k_D \equiv \frac{\omega_e}{v_t}$, we find

$$k_D \gg k_o' + k_s'$$

and $\lambda_D = \frac{1}{k_D}$ must be much smaller than either wave-length. The growth rate, in this case, is given by

$$\Gamma_R = \frac{v_o'}{c} (\omega_s' \omega_e)^{\frac{1}{2}} \tag{8}$$

with v_o' given by eq. (6). The conditions of applicability are $\omega_e \ll \omega_s'$ and $\Gamma_R \ll k'v_t$. Notice that the growth rate is proportional to the amplitude of the incoming wave.

The second regime corresponds to the kinetic (warm) beam plasma instability (fig. 13b). For a warm beam, the phase velocity of the beam distrubance falls inside the electron velocity and only resonant electrons can participate in the scattering. This process is called stimulated Compton scattering and requires $\lambda_D \gg \lambda$. The growth rate is given by

$$\Gamma_c = \frac{\omega_e^2}{\omega_s'} \frac{v_o'^2}{v_t^2} \tag{9}$$

[Note that $\Gamma_c \approx \Gamma_R^2/k'v_t$ if $k' \approx k_D$]. Unlike the Raman growth rate, the Compton growth depends strongly on v_t.

The efficiency of the above depends on the non-linear effects or the available convective growth lengths. These topics are presently under study by use of computer simulations. Some general guidelines suggest that stimulated Raman scattering can result in thermalization of the beam by trapping the electrons; thus, it places an upper limit on the efficiency. Resonance broadening or quasi-linear flattening will affect the Compton scattering. Finally, pump depletion will also place an upper limit on the amplitude of the scattered wave. It

should be noted that stimulated scattering has been successful in producing large amounts of microwaves in laboratory experiments (Elias et al., 1976).

3. Magnetoresonant stimulated scattering:

The situation is similar to the one examined in section 2 above, with the addition of a constant external magnetic field $\underline{B} = B_o \hat{\underline{e}}_z$. In this case the transverse electron velocity in the beam frame, and for an incoming wave $(\omega_o, \underline{k}_o)$, will be given by

$$\underline{v}'_o = \hat{\underline{e}}_y \frac{|e|}{m} \frac{E'_{oy}}{\gamma' \omega'_o} \frac{\omega'_o}{\omega'_o - \Omega_e} \tag{9}$$

where $\Omega_e = \frac{|e|B_o}{mc}$. Notice that if ω'_o approaches Ω_o rather large transverse velocities can be induced. However ω'_o cannot be arbitrary but must satisfy the dispersion relation in the beam frame, i.e.

$$\omega'^2_o - k'^2_o c^2 - \frac{\omega_e^2 \omega'_o}{\omega'_o - \Omega_e} = 0 , \tag{10}$$

so that $\omega'_o - \Omega_o$ cannot be made arbitrarily small. The temporal growth rate in the beam frame will be given by

$$\Gamma'_m \approx \frac{v'_o}{c} \omega'_s \left(\frac{\omega_e}{\omega'_s + \frac{\Omega_e}{2}} \right)^{\frac{1}{2}} . \tag{11}$$

This can easily be transformed back in the laboratory frame. Such processes can be important in low density, high magnetic field plasmas penetrated by e-beams (Granatstein and Sprangle, 1977; Sprangle et al., 1975).

4. Free electron lasers

The principle of such devices is similar to the stimulated scattering processes discussed above. The major difference is that instead of amplifying an incoming wave, we pass a relativistic electron beam through a magnetic field which is periodically rippled along the flow axis. Such a field can be considered as a quasi-wave represented in the form $\underline{E}_o = 0$, $B_\perp = B_o \cos k_o z$, $\omega_o = 0$, $k_o = 2\pi/\lambda_o$. The magnetic field parallel to the beam direction does not enter the problem, and can be chosen arbitrarily to satisfy the divergence conditions. In the beam frame, the quasi-wave will have an electric field

$$E'_{oy} = \frac{\gamma V_b B_o}{c} \quad , \tag{12}$$

and a frequency

$$\omega'_o = \gamma \frac{2\pi}{\lambda_o} V_b \quad , \tag{13}$$

where V_b is the parallel beam velocity. Now the problem reduces <u>exactly</u> to the one considered before for stimulated scattering. The mechanism is similar to either the Raman or Compton scattering but with the rippled field playing the role of the incoming plasma. For a relativistic beam the amplified wavelength will be

$$\lambda = \lambda_o \frac{1}{2\gamma^2} \quad . \tag{14}$$

Extensive computer simulations performed for this case indicated that the saturation mechanism was trapping of the beam electrons by the unstable wave with a conversion efficiency of 30% (Kwan et al., 1977). An excellent review of the subject can be found in Sprangle et al.(1978) and Sprangle and Drobot (1978).

An interesting extension of the above work with application to space plasmas will be to reexamine the above process in the presence of magnetic turbulence. A simple way to do that will be by considering, instead of a single wave k_o, a spectrum of waves $k_o \pm \Delta k$, with a Gaussian amplitude distribution. There has not yet been any such calculation in the literature.

5. Plasma lasers:

An interesting variation on the above scheme, which is far from being well known or explored, is the case of a plasma containing large amplitude density fluctuations and electrons drifting through them. Again, by going to the reference frame of the drifting electrons, the ion wave can be viewed as the incoming wave coupled with a scattered wave to produce amplification in a similar fashion as above. The role of the rippled magnetic field, will be played by the density fluctuations. The process can also be viewed as a negative a.c. resistivity similar to the one discussed by Dawson and Oberman (1962) due to the presence of enhanced ion waves. The energy is supplied by the drifting electrons. Since the analysis of such processes has not appeared in any journal, we present below a brief derivation.

The process can be seen from fig. 14. Consider a plasma with finite-amplitude short-wavelength ion density fluctuations with wave number k_i and frequency $\omega_i = 0$. These fluctuations lead to a strong coupling of high-phase velocity waves (either electrostatic or electromagnetic) of wave number k_o and frequency $\omega = \omega_o \pm \omega_i \approx w_o$. Suppose, now, that the plasma electrons are streaming with respect to the ions.

Then, the interaction can be such as to couple a high-phase velocity positive energy wave to a slow negative energy plasma oscillation (wave moving slower than the streaming of the electrons). In this case both disturbances can grow while conserving energy. A second possibility is for the phase velocity of the beat disturbances to fall at such a place that it absorbs energy from them. The last process is essentially nonlinear Landau damping.

It is well known that in the limit of long wavelengths ($k_o \approx 0$, i.e., the so-called dipole approximation), the electrostatic and electromagnetic wave fields are indistinguishable. We, therefore, present the theory for long-wavelength electrostatic waves; the results should be directly applicable to long-wavelength electromagnetic waves. We shall use a fluid model with a phenomenological damping, this could be Landau damping for the electrons. We treat the ions as fixed; their dynamics is not important provided the amplitude of the ion fluctuations is large enough.

The analysis is most simply handled in a reference frame moving with the electrons. However, we shall use both the rest frame of the electrons and ions in the discussion. The reader is cautioned that such things as wave energy are frame dependent (Lin et al., 1976).

We take the ion density to be given by

$$n_i = n_o[1 + \epsilon \cos k_i(x + v_o t)], \tag{15}$$

where v_o is the mean velocity of the electrons relative to the ions. We employ Lagrangian coordinates for the electrons, and let X (x_o) be

the displacement of an electron from its equilibrium position x_o (x_o is to be the equilibrium position if the ions stream by with a uniform density and velocity, and we assume that the current leads to no charge accumulation at $\pm \infty$, the system is a torus or the circuit is closed at ∞). The equation of motion for an electron is

$$\ddot{X}(x_o) = -\frac{e}{m} E(x_o) \tag{16}$$

By Gauss' law, $E(x_o)$ is 4π times the excess charge (excess over that due to the mean ion current) which passes from the right of electron x_o to its left. Thus,

$$E(x_o) = 4\pi e\, n_o[1 + \epsilon \cos k_i(x_o + v_o t)] + \frac{4\pi e n_o \epsilon}{k_i} \sin k_i(x_o + v_o t) \tag{17}$$

The equation of motion thus becomes

$$\ddot{X}(x_o) = -\omega_e[1 + \epsilon \cos k_i(x_o + v_o t)]\, X(x_o) + \frac{e\omega_e^2}{k_i} \sin k_i(x_o + v_o t) \tag{18}$$

The last term gives the steady driving of the electrons due to the passing ion fluctuations, but does not give rise to instability and so it may be ignored in the linear theory. Introducing the variable y as $2y = k_i(x_o + v_o t)$

$$\frac{\partial^2 X}{\partial y^2} + \frac{4\omega_e^2}{k_i^2 v_o^2}(1 - \epsilon \cos 2y)\, X = 0 \tag{19}$$

This is the standard Mathieu equation which describes parametrically

driven oscillations. For $\epsilon \ll 1$, it exhibits instabilities when the coefficient $\frac{2\omega_e}{k_i v_o} = p$ is an integer. The instability is strongest for $p = 1$, and in that region the growth rate is given by

$$\frac{\Gamma}{\omega_e} = \tfrac{1}{2}\left[\frac{\epsilon^2}{4} - (p-1)^2\right]^{\frac{1}{2}} \tag{20}$$

For large ϵ, one can obviously have strong off-resonant growth also. For $p = 2,3$ etc., the growth rates are smaller.

Physically, the above analysis shows that for a cold plasma (where plasma oscillations of all wavelengths have the same frequency) all modes are unstable. Equation (19) does not involve the wavelength of the plasma oscillation if $pk_i v_o = 2\omega_e$. The ion density oscillates at frequency $k_i v_D$ in the rest frame for the electrons. Waves of wave number k_o and $k_o + pk_i$ are coupled by p successive interactions with the ion wave, the condition for frequency matching being

$$\omega_1 + \omega_2 = 2\omega_e = pk_i v_o \,. \tag{21}$$

The driving energy comes from the ion oscillations. As mentioned, the energy is a frame dependent quantity. In the rest frame of the ions, the short wavelength mode with wave number $k_o + pk_i$ has phase velocity slower than the electrons and is a negative energy wave, while the long wavelength mode, wave number k_o, has phase velocity faster than the electrons and has positive energy. The pair can grow while conserving energy. In both cases, momentum is transferred to the ions.

The above analysis can be extended to the case of warm electrons. The instability criterion in this case is that the frequency mismatch does not exceed the variation in the plasma frequency associated with the ions, i.e.

$$|k_i v_o - \omega_o - \omega_1| < \tfrac{1}{2} \epsilon \omega_e \tag{22}$$

with $\omega_n^2 \equiv \omega_e^2 + 3(k_o + nk_i)^2 v_e^2$. The growth rate is $\frac{1}{4} \epsilon\omega_e$.

Even when an exact frequency matching is not possible, an instability can be excited for the high-phase velocity disturbance if the slow side-band falls in a region of negative absorption. (Note that this does not mean that plasma waves in this region are unstable since these are negative energy waves; this discussion applies to the rest frame of the ions). To investigate this we introduce a phenomenological damping term $-\nu_{\pm 1} X$ for the side band $k_o \pm k_i$ into the righthand side of eq. (11). In general, $\nu_{\pm 1}$ is associated with Landau damping and is given by

$$\frac{\nu_{\pm 1}}{\omega_e} = - \frac{2\pi\omega_e}{|k_i|} \left(u \frac{\partial F_o}{\partial u} \right)_{u = (-v_o \pm \omega_o/k_i)}, \tag{23}$$

where F_o is the electron distribution function. Proceeding as above, in the limit $\epsilon \ll 1$, assuming the ν_{+1} term dominates over the ν_{-1}, we find

$$\Gamma = - \frac{\epsilon^2}{8} \frac{\omega_e^4}{\omega_o} \frac{\nu_1 (\omega_o - k_i v_o)}{[\omega_1^2 - (\omega_o - k_i v_o)^2]^2 + \nu_1^2 (\omega_o - k_i v_o)^2} \tag{24}$$

For $\nu_1 > 0$ and $\frac{\omega_o}{k_1} < v_o$ this leads to growth. One may use the formula of the a.c. Dawson-Oberman resistivity to derive virtually the same result.

Finally, one might ask how a spectrum of ion waves (in place of a monochromatic ion wave) affects our results. Clearly, the resonant case will be strongly affected, since it will be like driving a parametric oscillator with a band of frequencies. The phase relations essential for parametric resonance will be destroyed and the resonant effects will be vitiated. In actual fact, a substantial reduction of growth rate occurs for a spectrum of ion waves. On the other hand, the non-resonant laser action discussed above will be relatively unaffected and the effects due to various ion waves will be merely additive.

An extension of the above notions has been applied to the auroral kilometric radiation problem. The driving source is an electron beam streaming through a plasma with enhanced density waves in the presence of a magnetic field. A complete analysis of this situation can be found in Palmadesso et al. (1976).

6. Scattering from ionization fronts and density discontinuities:

In all previous situations the scattering medium was a moving electron beam. However an upshift in the frequency and an accompanying increase in energy in accordance with eqs. (1-4) can also be achieved even when the plasma itself is not moving by scattering of radiation from a moving ionization front, a moving discontinuity, or a relativistic shock (Fig. 14). While the frequency of the reflected wave-packet is always found to satisfy the double Doppler shift relation given by equ. (3), care should be exercised in using eq. (4). As pointed out by Lampe et al. (1977)

equ. (4) is valid only for a sharply discontinuous front, in the sense that its width $L \gg \frac{u}{\omega_o}$, so that the change in the dielectric coefficient is adiabatic. Otherwise the reflection coefficients and the physics can be substantially different. For the unmagnetized case, instead of equ. (4), it is found that

$$\frac{W_s}{W_o} = \frac{\omega_o}{\omega_s} \tag{25}$$

for an oncoming, overdense ionization front when $\omega_o < \omega_s$. In the presence of a magnetic field however the ratio $\frac{W_s}{W_o}$ can considerably exceed the value of $\frac{\omega_o}{\omega_s}$. We refer the interested reorder to Lampe et al. (1977) for a detailed analysis.

The physical reason for the radically different results given by eqs. (4) and (25) is the following. When the oscillator frequencies of the dielectric are changing adiabatically, work is done on the oscillator by a mechanism that changes the frequency. This energy is available to enhance the reflected wave. However, if the oscillator frequency changes suddenly no work is done. A physical equivalent of the two limits above is the case of an electron attached by a spring to an atom, in the presence of an electric field. In the spring is released slowly, work is done against the electric field; but, if the electron is initially tied down by a string, no work is done in cutting the string (i.e., instantaneously increasing the susceptibility).

VI. Linear electromagnetic instabilities

1. General considerations

In this section, we treat several linear instability mechanisms which result in the direct excitation of electromagnetic radiation from magnetized plasmas. The physical configuration is one in which the plasma is composed of both thermal and suprathermal electrons. It is assumed that the wavelengths of interest are much less than the scale lengths for variation of the plasma density and magnetic field, so we may treat the case of a homogeneous plasma immersed in a uniform magnetic field $\underline{B}_o = B_o \hat{\underline{e}}_z$. The frequencies under consideration are high (of the order of the electron plasma and cyclotron frequencies), so ion dynamics may be ignored. Finally, the density of the suprathermal electrons is assumed to be much less than that of the thermal plasma; thus, the dielectric properties of the plasma are determined primarily by the thermal plasma. The role of the suprathermal electrons is to provide a small imaginary component of the frequency, which results in amplification of thermal fluctuations in the plasma. Propagation of the radiation may be treated within the context of the geometrical optics approximation.

The source of free energy for the instability mechanisms is a velocity space anisotropy of the electron distribution function which stems from the presence of the suprathermal species. We confine the discussion, here, to cases in which anisotropy results either from suprathermal electrons streaming along or trapped by the magnetic field (i.e., either beam or loss cone type distributions). Such processes are sometimes referred to as "maser amplification" in the astrophysical literature,

and involves the convective amplification of thermal fluctuations in the plasma. Therefore, in traversing the ray path between points s_1 and s_2, an electromagnetic wave undergoes an amplification given by

$$W(s_2) = W(s_1) e^{2\int_{s_1}^{s_2} ds\, \gamma(s)/V_g(s)}, \tag{1}$$

where W denotes the spectral energy density of the wave, and $\gamma(s)$ and $V_g(s)$ are the growth rate and group velocity of the wave mode as a function of position. As a consequence, the overall amplification of the radiated mode from a system of scale size L is approximately

$$W_{rad} \cong W_{th} e^{2\gamma L/V_g}, \tag{2}$$

where W_{th} is the thermal fluctuation level, and significant radiation results only if $2\gamma L/V_g > 1$.

2. The physical mechanism

The physical mechanism for instability is electron bunching either in the axial or azimuthal direction, depending on whether the Doppler or cyclotron resonance is dominant. The former case is sometimes referred to as a Weibel instability (Weibel,1959; Fried,1959; Harris,1961; Sagdeev and Shafranov,1961) and the latter as an electron cyclotron maser instability (Twiss,1958; Schneider,1959; Gapanov,1959; Hirschfield et al., 1965; Gapanov et al.,1967; Friedman et al.,1973; Sprangle and Manheimer, 1975; Granatstein et al.,1975; Sprangle et al.,1977; Chu and Hirshfield, 1978). In order to clearly illustrate the process, we consider the case of an electron moving in the field of a parallel propagating, plane electromagnetic wave of frequency ω and wavevector $\underline{k} = k_z \hat{\underline{e}}_z$. The

geometrical relationships of the particle trajectory and the wave fields, in the plane perpendicular to $\underline{B}_o$ are shown in Fig. 15.

The appropriate resonant frequency is $\Omega_{res} = n\Omega_e/\gamma + k_z v_z$, where n is an integer and $\gamma \equiv (1 - v^2/c^2)^{-\frac{1}{2}}$, and we consider the evolution of Ω_{res} under the action of the induced fields. In a short time $\Delta t (= t_1 - t_o)$, the resonant frequency changes by an amount

$$\Delta\Omega_{res} = n\Omega_e \frac{\Delta\gamma}{\gamma_o(\Delta\gamma + \gamma_o)} + k_z \Delta v_z , \tag{4}$$

where Δ indicates the change in a given quantity in time Δt, and the subscript "o" refers to an initial value. Under the assumptions that $\Delta\gamma < \gamma_o$ and $v^2 < c^2$, it can be shown that (Chu and Hirshfield, 1978)

$$\Delta v_z \cong - \frac{ek_z}{\gamma_o m\omega} (\underline{v}_\perp \cdot \underline{E}_1) \Delta t, \tag{5}$$

and

$$\Delta\gamma \cong - \frac{e}{mc^2} (\underline{v}_\perp \cdot \underline{E}_1) \Delta t, \tag{6}$$

where $\delta\underline{E}$ is the induced electric field. It can be shown, after combination of eqs. (4)-(6), that

$$\Delta\Omega_{res} \cong - \frac{ek_z^2}{\gamma_o n} \left(1 - \frac{n\Omega_e\omega}{\gamma_o k_z^2 c^2}\right) (\underline{v}_\perp \cdot \underline{E}_1) \Delta t. \tag{7}$$

Several conclusions are now apparent. First, both Δv_z and $\Delta\gamma$ vary with the aximuthal position of the electrons, and have opposite sign for the electrons shown in Fig. 15. Thus, bunching occurs because while one

electron experiences a gain in axial and/or azimuthal velocity, the other electron suffers a decrease. Second, both electron bunching mechanisms are operable unless: (1) the magnetic field vanishes, (2) $k_z = 0$ (i.e., perpendicular propagation), or (3) $n = 0$ (i.e., the Cerenkov resonance is dominant). Third, the azimuthal bunching mechanism is dominant if $n\Omega_e\omega/\gamma_o k_z^2 c^2 > 1$, and the axial bunching mechanism dominates if the reverse holds. A more comprehensive description of the physics of the interaction can be found in Sprangle et al. (1977) and Chu and Hirshfield (1978).

3. The electron beam instability (cyclotron maser)

Basic research into the electron cyclotron maser instability has been motivated by attempts to develop intense sources of microwave radiation through the use of relativistic electron beams. Such sources are called either gyrotrons or electron cyclotron masers, and the power generated has ranged from 1.5 kW at 0.9 mm (Zaitsev et al., 1974) wavelengths to 1 GW at 4 cm (Granatstein et al.,1976). Applications of such research has been to electron cyclotron heating in tokamaks; however, numerous applications also occur in astrophysical plasmas.

The laboratory experiments have been conducted by injecting a relativistic beam into a tube with a uniform guide field $\underline{B}_o$. Assuming a distribution of the form

$$F_e(u_\perp, u_\parallel) = \frac{1}{2\pi u_\perp}\,\delta(u_\perp - u_p)\,\delta(u_\parallel), \tag{8}$$

and plane wave solutions, $\exp(-i\omega t + ik_z z)$, the dispersion equation is (Chu and Hirshfield,1978; Sprangle and Drobot, 1977; Ott and Manheimer,1975)

$$\omega^2 - k_z^2 c^2 = \frac{\omega_e^2}{\gamma_o} \left(\frac{\omega}{\omega - \Omega_e/\gamma_o} - \frac{\beta_{\perp o}^2 (\omega^2 - k_z^2 c^2)}{2(\omega - \Omega_e/\gamma_o)^2} \right) . \qquad (9)$$

where $\gamma_o = \left(1 + u_p^2/c^2\right)^{\frac{1}{2}}$, and $\beta_{\perp o} = u_p/\gamma_o c$. Solution of (9) may be obtained under the assumptions that $\omega = \omega_o + \delta\omega$, where $\omega_o = \Omega_e/\gamma_o$ and $|\delta\omega| \ll \omega_o$. In such a case, we find the approximate equation

$$\left(\omega_o^2 - k_z^2 c^2 - \frac{\omega_e^2}{\gamma_o}\left(1 - \tfrac{1}{2}\beta_{\perp o}^2\right)\right)\delta\omega^2 - \frac{\omega_e^2}{\gamma_o}\left(1 - \beta_{\perp o}^2\right)\omega_o \delta\omega + \tfrac{1}{2}\frac{\omega_e^2}{\gamma_o}\beta_{\perp o}^2(\omega_o^2 - k_z^2 c^2) = 0 \qquad (10)$$

which has the solutions

$$\frac{\delta\omega}{\omega_o} = \frac{(\omega_e^2/\gamma_o)(1-\beta_{\perp o}^2)}{2\left[\omega_o^2 - k_z^2 c^2 - \frac{\omega_e^2}{\gamma_o}\left(1 - \frac{1}{2}\beta_{\perp o}^2\right)\right]} \left[1 \pm \right.$$

$$\left. \pm \sqrt{1 - \frac{2\gamma_o}{\omega_e^2 \omega_o^2} \frac{\beta_{\perp o}^2}{(1-\beta_{\perp o}^2)^2} (\omega_o^2 - k_z^2 c^2)\left(\omega_o^2 - k_z^2 c^2 - \frac{\omega_e^2}{\gamma_o}\left(1 - \tfrac{1}{2}\beta_{\perp o}^2\right)\right)} \right] . \qquad (11)$$

As a result, instability occurs when

$$\frac{\beta_{\perp o}^2}{(1-\beta_{\perp o}^2)^2} (\omega_o^2 - k_z^2 c^2)\left(\omega_o^2 - k_z^2 c^2 - \frac{\omega_e^2}{\gamma_o}\left(1 - \tfrac{1}{2}\beta_{\perp o}^2\right)\right) > \frac{\omega_e^2 \omega_o^2}{2\gamma_o} . \qquad (12)$$

In the limit in which $\omega_o^2 > k_z^2 c^2, \omega_e^2$ (in which the azimuthal bunching mechanism dominates) the instability criterion becomes

$$\frac{\beta_{\perp o}^2}{(1-\beta_{\perp o}^2)^2} > \frac{\gamma_o}{2}\frac{\omega_e^2}{\Omega_e^2} \quad , \tag{13}$$

If (13) is satisfied, the solution assumes the comparatively simple form

$$\omega \cong \Omega_e/\gamma_o + i\beta_{\perp o}\omega_e(2\gamma_o)^{-\frac{1}{2}} \quad . \tag{14}$$

In the opposite limit (i.e., $k_z \to \infty$), in which the axial bunching mechanism dominates, the solution is identical, but the threshold required for instability is

$$\frac{\beta_{\perp o}^2}{(1-\beta_{\perp o}^2)^2} > \frac{1}{2\gamma_o}\frac{\omega_e^2}{c^2k_z^2}\frac{\omega_o^2}{c^2k_z^2} \quad . \tag{15}$$

The case of hollow beams has been discussed by Uhm et al. (1978).

4. Electromagnetic anisotropy and beam-plasma instabilities

In the remainder of this section, the physical configuration that we adopt is one in which instability arises from the presence of a relatively small population of suprathermal electrons in an otherwise thermal plasma. In such cases, the real frequency and polarization of the excited modes are determined, primarily, by the thermal plasma, and the effect of the suprathermal electrons is to provide a small imaginary contribution to the frequency. As a consequence, the wave frequency is of the form $\omega(\underline{k}) = \omega_r(\underline{k}) + i\,\omega_i(\underline{k})$, where $|\omega_i/\omega_r| \ll 1$. The dispersion equation, typically, is written as the sum of contributions from the thermal and suprathermal electrons (which we denote by subscripts "t" and "s" respectively)

$$\Lambda(\underline{k}, \omega) = \Lambda_t(\underline{k}, \omega) + i\sum_{\ell = t,s}\Lambda_\ell(\underline{k}, \omega) = 0 \tag{16}$$

The contribution to the imaginary part of $\Lambda(\underline{k},\omega)$ from the thermal electrons is responsible for (Landau or cyclotron) damping. However, since we employ the cold plasma approximation for simplicity, thermal damping is unimportant and will be ignored. It should be noted, before we proceed, that the cold plasma approximation is valid as long as

$$\frac{k_\perp V_e}{\Omega_e} \ll 1 \text{ and } \left|\frac{\omega - n\Omega_e}{k_{||} V_e}\right| \gg 1, \tag{17}$$

where V_e denotes the thermal speed. If eq. (16) is expanded in powers of ω_i, it can be shown that the frequency and growth rate are given by the equations

$$\Lambda_t(\underline{k},\omega_r) = 0, \tag{18}$$

and

$$\omega_i = -\frac{\Lambda_s(\underline{k},\omega_r)}{\frac{\partial}{\partial\omega_r}\Lambda_t(\underline{k},\omega)} \tag{19}$$

The characteristics of the wave modes (i.e., frequency and polarization as functions of wavelength and angle of propagation) in the cold plasma approximation have been discussed in Chapter II, and will not be repeated here. Instead, in the remainder of this section, we discuss the characteristics of the instabilities and, hence, the radiation, which arises from populations of either trapped or streaming suprathermal

electrons.

a. Loss cone instabilities:

Populations of trapped particles which are found in astrophysical plasmas occur, most often, in the presence of dipole magnetic fields (i.e., planetary magnetospheres), and provide a tool for the mapping of such fields as well as for determining the relevant physical processes in the plasma. Loss cone distributions are characterized by a depletion of particles having small pitch angles, $\alpha = \tan^{-1}(v_z/v_\perp)$, relative to the ambient magnetic field, thereby, constituting a population inversion in the perpendicular energies of the trapped species. No net parallel current arises from such a population, and the distribution function is symmetric in parallel velocity. In addition, average particle energies in the direction perpendicular to the ambient magnetic field exceed those directed parallel to the field, and the source of free energy which drives the instability is the anisotropy which exists in the perpendicular velocity distribution.

The most efficient coupling to the excited modes occurs for perpendicular propagation (i.e., $k_z = 0$), and we consider this case first. Further, the electric field vector is directed parallel to the ambient magnetic field for the ordinary mode, and primary coupling is to the parallel motion of the suprathermal electrons. As a consequence, the growth rate of the O mode can be shown to depend linearly on the parallel energy of the trapped species (Freund and Wu, 1976). However, since this is, typically, small for trapped particles, it is the extraordinary mode which is more strongly radiated, and we limit discussion to the X mode here. Relativistic effects are included throughout.

The suprathermal distribution function we consider is of the form $F_s(u_\perp^2, u_\parallel^2) = F_\parallel(u_\parallel^2)F_\perp(u_\perp^2)$, where $F_\parallel(u_\parallel^2)$ is an arbitrary, even function of $u_\parallel$,

$$F_\perp(u_\perp^2) = (\pi\alpha_{\perp 1}^2)^{-1}\left(1 + \frac{\alpha_{\perp 2}^2}{\alpha_{\perp 1}^2}\right)e^{-u_\perp^2/\alpha_{\perp 1}^2}\left(1 - e^{-u_\perp^2/\alpha_{\perp 2}^2}\right), \tag{20}$$

and $\underline{u}$ ($\equiv p/m$) is a relativistic velocity. The resonant condition in this limit is $\omega_r = n\Omega_e/\gamma$ where , under the assumption that the average perpendicular energy of the suprathermals is much greater than the average parallel energy, we have that $\gamma \cong (1 + u_\perp^2/c^2)^{\frac{1}{2}}$. Thus,the resonant $u_\perp$ is given by

$$u_n^2 = \left(\frac{n^2\Omega_e^2}{\omega_r^2} - 1\right) c^2 , \tag{21}$$

and the growth rate becomes (Freund and Wu,1977a)

$$\frac{\omega_i}{\omega_r} \cong \pi^2 \frac{\omega_s^2}{\omega_r^2}\Psi(k_\perp,\omega_r)\sum_{n=1}^{\infty} H(u_n^2)\frac{n\Omega_e}{\omega_r}\left[\frac{1}{(n-1)!}\left(\frac{k_\perp u_n}{2\Omega_e}\right)\right]^2 c^4 \frac{\partial}{\partial u_\perp^2}F_\perp(u_\perp^2 = u_n^2) \tag{22}$$

In (22), ω_s is the plasma frequency of the suprathermal electrons, H is the heaviside function,

$$\Psi(k_\perp,\omega_r) = 2\frac{\omega_r^2}{c^2k_\perp^2}\left(\frac{\omega_r^2}{\Omega_e^2} - 1\right)\left[\frac{3}{2}\frac{(\omega_r^2-\Omega_u^2)}{\Omega_e^2} - \frac{c^2k_\perp^2}{\omega_r^2}\left(1-\frac{\omega_r^2}{\Omega_e^2}\right) - 2\frac{\Omega_e}{\omega_r}\frac{\omega_e^2}{\Omega_e^2}\right]$$

$$\times\left[\left(\frac{c^2k_\perp^2+2\omega_e^2}{\Omega_e^2}\right)\frac{\omega_r^4}{\Omega_e^4} + \left(\frac{\Omega_u^2c^2k_\perp^2+\omega_e^4}{\Omega_e^4}\right)\left(1-2\frac{\omega_r^2}{\Omega_e^2}\right)\right]^{-1} \tag{23}$$

includes the effect of the dielectric polarization of the plasma, and ω_r satisfies the X mode dispersion relation

$$\omega_{r\pm}^2 = \tfrac{1}{2}\left\{(c^2k_\perp^2 + \Omega_e^2 + 2\omega_e^2) \pm [(c^2k_\perp^2-\Omega_e^2)^2 + 4\omega_e^2\Omega_e^2]^{\frac{1}{2}}\right\}, \qquad (24)$$

where the plus (minus) sign refers to the fast (slow) extraordinary mode. We note that in the limit of $\omega_e^2/\Omega_e^2 \ll 1$, in which plasma dielectric effects are expected to be negligible, $\Psi(k_\perp,\omega_r)$ approaches unity.

Several conclusions follow readily from analysis of eq. (22) First, the growth rate vanishes at the cyclotron harmonics themselves, and excitation occurs for frequencies $\omega_r \lesssim n\Omega_e$ in accord with the inclusion of relativistic effects in the gyroresonance. Second, for suprathermal energies as high as several hundred keV, $k_\perp^2u_n^2/\Omega_e^2 \ll 1$ and the growth rate falls off rapidly with an increase in the gyroharmonic under consideration. Third, growth is possible only when $\partial F_\perp(u_\perp^2 = u_n^2)/\partial u_\perp^2 > 0$, so the range of frequencies in the vicinity of each harmonic which leads to instability varies as

$$n^2\Omega_e^2\left[1 - \frac{\alpha_{\perp 2}^2}{c^2}\ell n\left(1 + \frac{\alpha_{\perp 1}^2}{\alpha_{\perp 2}^2}\right)\right] \lesssim \omega_r^2 \lesssim n^2\Omega_e^2 \quad . \qquad (25)$$

Finally, it should be noted that a stop band (see Chapter II) exists for $\Omega_u < \omega_r < \omega_R$. Thus, while maximum excitation is expected to occur in the vicinity of the fundamental gyroharmonic (i.e., on the slow X mode), these waves cannot readily escape from the plasma.

In order to excite fast extraordinary mode waves (i.e., $\omega_r > \omega_R$) directly via the fundamental gyroresonance, a Doppler shift of the wave frequency above the stop band is required. Consider, for simplicity, a parallel distribution function of the form

$$F_{||}(u_{||}) = \tfrac{1}{2}[\delta(u_{||} - U) + \delta(u_{||} + U)], \tag{26}$$

and finite $k_z^2 \ll k_\perp^2$. We assume that $U^2 \ll \int d^3u\, u_\perp^2\, F_s(u_\perp^2, u_{||})$, that k_z is sufficiently small that the dielectric properties of the plasma can be adequately described in terms of the limit of perpendicular propagation, and ω_r is given by eq. (24). Under such conditions, the sole effect of finite k_z is on the resonance condition, which now becomes $\omega_r - n\Omega_e/\gamma \pm k_z U = 0$. As a result, instead of (23), the resonant $u_\perp$ takes the form ($\gamma_{||}^2 \equiv 1 + U^2/c^2$)(Freund and Wu, 1977a), for $\gamma_{||}^2 \equiv 1 + U^2/c^2$,

$$u_n^2 = \left[\frac{(n\Omega_e \pm k_z U)^2}{\omega_r^2} - \gamma_{||}^2\right] c^2 , \tag{27}$$

in which the Doppler contribution may be viewed as providing an effective shift of the gyrofrequency. It is clear from (27) that (1) waves can be excited by means of the fundamental gyroresonance as long as $\omega_r^2 < \gamma_{||}^{-2}(\Omega_e + |k_z U|)^2$, and (2) that such waves can be excited for k_z directed both parallel and antiparallel to the ambient magnetic field. In order for waves on the fast X mode to be excited in this fashion, we require that $\gamma_{||}^{-2}(\Omega_e + |k_z U|)^2 < \omega_R^2 < \omega_r^2$ which implies that $U_- < U < U_+$, where

$$\frac{U_{\pm}^2}{c^2} = \frac{k_{||}c}{\Omega_e} \pm \left[\frac{k_{||}^2c^2}{\Omega_e^2} - 2\frac{\omega_e^2}{\Omega_e^2}\right]^{\frac{1}{2}} \quad . \tag{28}$$

It is clear, therefore, that $\omega_e^2 < k_{||}^2c^2/2$ is required. Since $ck_{\perp} \sim \Omega_e$ for the electromagnetic waves which are excited, an extremely narrow stop band (i.e., $\omega_e^2 < \Omega_e^2$) is necessary for excitation of waves which can escape from the plasma.

While conditions in which $\omega_e < \Omega_e$ are not uncommon in the laboratory, they are relatively rare among astrophysical plasmas. Within the solar system, such conditions hold only at low altitudes ($< 1\ R_j$) in the Jovian magnetosphere and in the auroral zone within the terrestrial magnetosphere. However, since these regions have been identified as the source regions of the Jovian decametric radiation and the terrestrial kilometric radiation, such a mechanism has been proposed as an explanation of the source mechanism in each case (Wu and Freund,1977; Wu and Lee,1978; Melrose,1975; Smith, 1976).

Finally, we remark that while a small Doppler shift is required in order to obtain excitation of the escape mode via the fundamental gyroresonance, the primary mechanism of this instability is the phase (i.e., azimuthal) bunching of the suprathermal electrons.

b. Streaming instabilities:

In the case in which a population of suprathermal electrons is streaming along the ambient magnetic field, a restriction of the analysis to predominantly perpendicular propagation is not possible. This occurs because particle energy is predominantly directed parallel

to $\underline{B}_o$, and the particle energy couples strongly to the parallel component of the induced electric field. Thus, radiation occurs over a relatively broad angular range. In addition, substantial emission of the ordinary mode is possible, and the analysis cannot be restricted solely to the X mode. Relativistic effects can be neglected when

$$\eta\cos\theta > \tfrac{1}{2}\,\frac{n\Omega_e}{\omega}\,\frac{v_{||}}{c}\,, \tag{29}$$

for which the relativistic contribution to the resonance condition can be neglected in comparison with the Doppler effect. For $\omega \sim n\Omega_e$, $\eta \sim 1$, and a 10 keV streaming energy, the Doppler effect dominates for angles of propagation $0° < \theta \leq 80°$ and it is this regime which will be discussed here. In this limit, the resonance condition is of the form $\omega_r - n\Omega_e - k_{||}v_{||} = 0$, and it is evident, in contrast to the loss cone instability discussed previously, that instability is due to the axial bunching of the suprathermal electrons. As before, we employ the cold plasma approximation for the thermal plasma which yields the well-known Appleton-Hortree dispersion relation (Stix,1962) for the ordinary and extraordinary modes (which we denote with "+" and "-" signs respectively)

$$\eta_\pm^2 = 1 - \frac{2\alpha^2(1-\alpha^2)}{2(1-\alpha^2)-\beta^2(\sin^2\theta \mp \rho)} \tag{30}$$

where $\alpha^2 \equiv \omega_e^{\,2}/\omega_r^{\,2}$, $\beta^2 \equiv \Omega_e^{\,2}/\omega_r^{\,2}$, and $\rho^2 \equiv \sin^4\theta + 4(1-\alpha^2)\cos^2\theta/\beta^2$.

The suprathermal distribution is, again, assumed to be a separable function of parallel and perpendicular velocity, and we write $F_s(v_\perp^{\,2}, v_{||}) = F_{||}(v_{||})F_\perp(v_\perp^{\,2})$ where

$$F_{\perp}(v_{\perp}^2) = (\pi\alpha_{\perp}^2)^{-1} e^{-v_{\perp}^2/\alpha_{\perp}^2}, \tag{31}$$

and

$$F_{||}(v_{||}) = (\pi\alpha_{||}^2)^{-\frac{1}{2}} e^{-(v_{||}-\alpha_s)^2/\alpha_{||}^2} \tag{32}$$

In (31) and (32), $\alpha_{||}$ and $\alpha_{\perp}$ characterize the random velocities in the parallel and perpendicular directions, and α_s is the streaming velocity. The resonant parallel velocity, in this case, is given by

$$v_n = \frac{\omega_r - n\Omega_e}{\omega_r \eta |\cos\theta|}\, c, \tag{33}$$

and the growth rates of the O and X modes is given by (Melrose 1973)

$$\frac{\omega_i^{(\pm)}}{\omega_r} \cong 2\pi \frac{\omega_s^2}{\omega_r^2} \frac{c}{\eta_{\pm}^2 |\cos\theta|\, \partial(\omega_r \eta_{\pm})/\partial\omega_r} \sum_{n=0}^{\infty} A_n^{(\pm)} \left[\frac{\alpha_{\perp}^2}{\alpha_{||}^2}\left(\frac{\alpha_s - v_n}{c}\right)\eta_{\pm}\cos\theta - \frac{n\Omega_e}{\omega_v}\right]$$

$$\times F_{||}(v_{||} = v_n). \tag{34}$$

Under the assumption that $k_{\perp}^2\alpha_{\perp}^2/\Omega_e^2 \ll 1$

$$A_n^{(\pm)} = \frac{1}{2n!}\left(\frac{k_{\perp}\alpha_{\perp}}{2\Omega_e}\right)^{|n|-1} \frac{1}{1+T_{\pm}^2}\left[\frac{\omega_r}{\Omega_e}(K_{\pm}\cos\theta - T_{\pm}\sin\theta)\tan\theta + nT_{\pm}\sec\theta + |n|\right]^2, \tag{35}$$

where

$$T_{\pm} = 2\frac{\omega_r}{\Omega_e}\frac{(1-\alpha^2)\cos\theta}{\sin^2\theta \mp \rho}, \text{ and } K_{\pm} = 2\frac{\beta\alpha^2\sin\theta}{2(1-\alpha^2) - \beta^2(\sin\theta \mp \rho)} \tag{36}$$

Examination of eqs. (34)-(36) shows that growth is possible (i.e.,

$\omega_i^{(\pm)} > 0$) only if

$$\frac{\alpha_\perp^2}{\alpha_\parallel^2}\left(\frac{\alpha_s - v_n}{c}\right)\eta_\pm \cos\theta - \frac{n\Omega_e}{\omega_r} > 0. \tag{37}$$

The additional requirement that the growth rate not be exponentially small (i.e., that $|v_n - \alpha_s| < \alpha_\parallel$), then, implies (1) that for instability

$$\frac{\alpha_\perp^2}{c\alpha_\parallel} > \frac{n\Omega_e}{\omega_r}\ \frac{1}{\eta\cos\theta}\ \sim 1, \tag{38}$$

and (2) that the bandwidth in the vicinity of each gyroharmonic is

$$1 + \left(\frac{\alpha_s - \alpha_\parallel}{c}\right)\eta_\pm \cos\theta \leq \frac{\omega_r}{n\Omega_e} \leq \left(1 - \frac{\alpha_\parallel^2}{\alpha_\perp^2}\right)\left(1 + \frac{\alpha_s}{c}\ \eta_\pm \cos\theta\right). \tag{39}$$

It should be noted, however, that relativistic electrons play an increasingly important role at the higher gyroharmonics, and modifications to the results given,herein, may be required.

A detailed analysis of (34) is beyond the scope of this review, and we shall only present a summary of the principle conclusions with regard to the radiation properties of the medium. The interested reader is referred to Melrose (1973) for more details. First, Cerenkov emission (i.e., n = 0)is not possible on either the O mode or the fast X mode (i.e., the escape mode). This follows because $\eta_\pm < 1$ for these waves and the resonance velocity $v_o = c/\eta_\pm\cos\theta$ exceeds the speed of light. Second, emission of the X mode is favored over that of the O mode at each gyroharmonic for this case, as well as, for

the loss cone instability. Third, emission of fast extraordinary waves via the fundamental gyroresonance is possible only when the extraordinary mode stop band is sufficiently narrow that

$$\frac{\omega_e^2}{\Omega_e^2} \leq \frac{\alpha_s}{c} \eta \cos\theta + \frac{\alpha_{\parallel}^2}{\alpha_{\perp}^2} \tag{40}$$

We note that the physical mechanism for such excitation of the fast extraordinary mode is the same as that in the case of the loss cone instability discussed previously; specifically, a Doppler shift of the wave frequency between the electron rest frame and the observer.

Finally, it should be noted that substantial reabsorption of this obliquely propagating radiation is possible when the wave frequency is sufficiently close to the local values of the various gyroharmonics. At these frequencies the cold plasma approximation breaks down, and cyclotron damping by the thermal plasma is possible.

VII. An example-type III solar radio bursts:

In the previous chapters we reviewed the various isolated mechanisms that produce coherent emission in plasmas. Our aim here is to present an example of an entire problem that includes not only the properties of the observed radioemission, but also the details of the particle distribution functions and of the electrostatic turbulence.

For reasons that will become obvious we have chosen the problem of the type III solar radio bursts. Observationally by type III bursts we mean solar, radio-emission having a drift frequency with time, from high to low frequencies. The starting frequency is in the range of 50-300 MHz which corresponds to plasma frequencies in the lower corona, while ending frequencies could be measured down to 10 MHz at the earth's surface due to the ionospheric cut-off with advent of satellites. Frequencies down to several tens of kHz were measured and it was confirmed that the excitor is an energetic electron beam (10-100 keV) streaming from the sun down to 1AU.

The persistent interest in this phenomenon has been due to the theoretical difficulties encountered in constructing a convincing interpretation of many of the most striking properties of the bursts. Several basic questions were posed by Sturrock fifteen years ago, and are only now beginning to be answered. Among the issues raised by Sturrock (1964) are the following three. First, why is the electron beam that excited the bursts not significantly decelerated. Second, why is the radiation predominately emitted at the second harmonic of the local plasma frequency, ω_e. Finally, why does the beam have such a well defined velocity, typically between 0.2 and 0.3c.

In 1976 yet another curious observation was reported by Fitzenreiter, et al. (1976). In looking at simultaneous observations of both the electron and radio fluxes of type III bursts that had traveled out to 1 AU, they found that for electron fluxes less than about 100 $(cm^2 sec\, ster)^{-1}$, the radio intensity, I, and the electron flux, J_E, were approximately linearly proportional. For larger electron fluxes $I \propto J_E^{2.4}$.

It was first shown (Papadopoulos et al., 1974) that effects of strong plasma turbulence (see III-5) can readily account for the observed fact that the electron streams associated with the bursts are able to travel large distances without significant deceleration. In contrast, conventional weak turbulence plasma theory predicts that all the streaming energy should be dissipated within a few kilometers of the injection site.

The strong turbulence theory also suggested an explanation for the dominance of second harmonic radiation. During the last several years, that theory has been expanded in a series of papers (Smith et al., 1976, 1978; Goldstein et al., 1978; Nicholson et al., 1978). In its present version, the theory not only accounts for the minimal energy losses suffered by the electrons, but also is able to account for the observed intensities of electromagnetic radiation (at $2\omega_e$), the correlation between the radio and electron fluxes, and for the observed decay times of the radiation. The full impact of the theory, was however, due to the results of the numerical modeling. Rate equations including strong turbulence mode coupling effects, reabsorption and collisionless

damping were utilized to model actual observations. The complete set of equations can be found in Smith et al. (1976, 1978) and will not be repeated here. The input to the code was a beam distribution based on in situ particle observations at 1AU. The numerical computations can be performed at any point in space at which the density and temperature of the ambient solar wind can be estimated. Typically, distances between 0.1 and 1.0 AU were chosen, and it was assumed that the ambient density varied as r^{-2}. At a given location the calculation began ($t = 0$) with the arrival of energetic electrons with velocities of about 0.7c. The exact velocity distribution being given by the beam evolution model. As an example, consider the burst on May 16, 1971. The local plasma frequency at 1 AU on that date was about 30 kHz and electrons with energies above 100 keV were first observed at 1305 UT when the radiometer on IMP-6 first detected radio noise at 55 kHz ($\simeq 2\omega_e/2\pi$). The radio noise increased in intensity until 1335 UT, and little further evolution was observed in the electron spectrum after that time. From Fig. 16 we can see that the distribution function had a positive slope below the peak energy. The other parameters needed for the numerical model were the path length traversed by the electron beam, taken to be 1.5 AU; the ratio of the beam to solar wind density, η, estimated to be 5×10^{-6}. The result of the modeling are shown in Fig. 17 as a function of time, where the logarithm of the electron distribution function $f_T(\underline{v})$, the electron plasma wave energy level W^{ℓ} (normalized to nT) and the amplitude of the density fluctuations $(\frac{\delta n}{n})$ are plotted as a function of $V_p = \frac{\omega_e}{k}$.

Initially, the linearly unstable beam produces resonant plasma waves (indicated by cross hatching in(Fig. 16a) that grow until the the modulational threshold is reached (Fig. 17a). Axperiodic ion waves are then excited (gray shading) as are shorter wavelength "daughter" Langmuir waves (Fig. 17b-d). The combined effects of nonlinear changes in the Bohm-Gross disperion relation and anomalous resistivity then complete the decoupling of the electron beam from the Langmuir turbulence (Fig. 17d-f). In the calculations the collapse to short wavelengths ceases when Landau damping by the thermal solar wind electrons balances the spectral transfer. No further energy exchange will then take place. Gradually the ion fluctuations and Langmuir waves will simultaneously decay back to thermal levels whereupon the linear instability will again be excited, and the process will cyclically repeat until the electron beam has merged with the ambient solar wind distribution and no positive slope exists to $f_T(\underline{v})$.

It is important to note that the total elapsed time between the onset of the OTSI and its final stabilization was little more than 0.1sec, during which the electron distribution is essentially constant. Therefore, neither reabsorption nor quasilinear relaxation can be important.

Similar calculations were performed at 0.5 and 0.1 AU and for the type III bursts observed on May 25, 1972 and February 28, 1972; the results are similar to those described here and are reported in Goldstein et al.(1978). In all cases stabilization and decoupling of the electron beam from the Langmuir turbulence is due to excitation of the periodic modulational instability (i.e., oscillating two stream).

Initially, the linearly unstable beam produces resonant plasma waves (indicated by cross hatching in(Fig. 16a) that grow until the the modulational threshold is reached (Fig. 17a). Axperiodic ion waves are then excited (gray shading) as are shorter wavelength "daughter" Langmuir waves (Fig. 17b-d). The combined effects of nonlinear changes in the Bohm-Gross disperion relation and anomalous resistivity then complete the decoupling of the electron beam from the Langmuir turbulence (Fig. 17d-f). In the calculations the collapse to short wavelengths ceases when Landau damping by the thermal solar wind electrons balances the spectral transfer. No further energy exchange will then take place. Gradually the ion fluctuations and Langmuir waves will simultaneously decay back to thermal levels whereupon the linear instability will again be excited, and the process will cyclically repeat until the electron beam has merged with the ambient solar wind distribution and no positive slope exists to $f_T(\underline{v})$.

It is important to note that the total elapsed time between the onset of the OTSI and its final stabilization was little more than 0.1sec, during which the electron distribution is essentially constant. Therefore, neither reabsorption nor quasilinear relaxation can be important.

Similar calculations were performed at 0.5 and 0.1 AU and for the type III bursts observed on May 25, 1972 and February 28, 1972; the results are similar to those described here and are reported in Goldstein et al.(1978). In all cases stabilization and decoupling of the electron beam from the Langmuir turbulence is due to excitation of the periodic modulational instability (i.e., oscillating two stream).

We now turn to the question of why type III bursts are preferentially observed at the second harmonic of the local plasma frequency. Much of this discussion is based on a recent paper by Papadopoulos and Freund (1978).

From a comparison of Fig. 17a and f, one sees that the long wavelength pump waves have collapsed into shorter wavelength daughter waves. In configuration space these short wavelength structures are solitons (Papadopoulos and Manheimer, 1975), whose spatial extent in the direction parallel to the magnetic field can be estimated to be about $50\lambda_D$, with an energy density, $\frac{W}{nT}$, of nearly 10^{-2}. Such structures are very difficult to observe with present spacecraft instrumentation. In a 400 km/s solar wind, a 350 m ($50\lambda_D$) soliton is convected past a 30m dipole antenna in little more than a millisecond. This must be compared to the electronic response times of plasma wave experiments typically no faster than 20 ms (Gurnett, private communication).

Papadopoulos and Freund (1978) found that the total volume emissivity of a soliton, integrated over solid angle is

$$J(2\omega_e) = \frac{3\sqrt{3}}{8}\left(\frac{V_e}{c}\right)^4 \frac{cE_o^2}{8\pi\Delta Z}\left(\frac{1}{k_o L}\right)^2 \qquad (1)$$

where Δz is the parallel dimension of the linearly unstable wave-packet, $k_o = \sqrt{3}\omega_e/c$ is the wavelength of the electromagnetic wave at $2\omega_e$, E_o is the electric field in the soliton, and L is the dimension of the soliton transverse to the magnetic field. Eq. (1) is valid for $k_o^2 L^2 \gg 4$, a good approximation throughout the interplanetary medium. The intensity of emission outside a spherical shell of radius R and

thickness ΔR centered on the sun is (Gurnett and Frank, 1976) $I = JR(2\omega_e/2\pi)$. For the May 16 burst at the time of soliton formation (Fig. 17f), $I(2\omega_e) \cong 1 \times 10^{-17}$ W m^{-2} sec^{-1}, close to the peak intensity observed at 55 kHz. Finally we should note that using the results of computations such as shown in Fig. 17 and eq. (1), excellent detailed agreement was found concerning the exponent α of the $I \sim J_E^{\alpha}$ dependence between the radio intensity and electron flux (Fig. 18).

Thus far it was tacitly assumed that because the electron beam becomes decoupled from the radiation field, no significant energy loss will occur. Smith et al. (1978) have investigated this in some detail; we only summarize that discussion here.

If the beam is injected near the solar surface, the total energy lost by the beam in propagating to the point R is given by

$$\Delta E = \int_{R_o}^{R} dr A(r) \int_{t_1(r)}^{t_2(r)} dt \, \frac{d\tilde{W}(r,t)}{dt} \qquad (2)$$

where $A(r)$ is the source area at r, and $t_1(r)$, and $t_2(r)$ are the times at which the instabilities at r begin and end. Because all the beam energy loss occurs in the resonant region until the onset of the collapse one can assume that it takes place at the steady rate $dW/dt = W_T/\tau_o$, where W_T is taken to be $W_o \exp(\gamma_L \tau_o)$.

When eq. (2) was evaluated, Smith et al. (1978) found that ~ 90% of the energy loss occured in the inner corona, and that $\Delta E = 10^{30}$ W(ergs). With $W \cong 10^{-4}$, the exciter loses some 10^{26} ergs in leaving the corona. The total energy in the type III exciter will typically

thickness ΔR centered on the sun is (Gurnett and Frank, 1976) $I = JR(2\omega_e/2\pi)$. For the May 16 burst at the time of soliton formation (Fig. 17f), $I(2\omega_e) \cong 1 \times 10^{-17}$ W m^{-2} sec^{-1}, close to the peak intensity observed at 55 kHz. Finally we should note that using the results of computations such as shown in Fig. 17 and eq. (1), excellent detailed agreement was found concerning the exponent α of the $I \sim J_E^{\alpha}$ dependence between the radio intensity and electron flux (Fig. 18).

Thus far it was tacitly assumed that because the electron beam becomes decoupled from the radiation field, no significant energy loss will occur. Smith et al. (1978) have investigated this in some detail; we only summarize that discussion here.

If the beam is injected near the solar surface, the total energy lost by the beam in propagating to the point R is given by

$$\Delta E = \int_{R_o}^{R} dr A(r) \int_{t_1(r)}^{t_2(r)} dt \, \frac{d\tilde{W}(r,t)}{dt} \qquad (2)$$

where $A(r)$ is the source area at r, and $t_1(r)$, and $t_2(r)$ are the times at which the instabilities at r begin and end. Because all the beam energy loss occurs in the resonant region until the onset of the collapse one can assume that it takes place at the steady rate $dW/dt = W_T/\tau_o$, where W_T is taken to be $W_o \exp(\gamma_L \tau_o)$.

When eq. (2) was evaluated, Smith et al. (1978) found that ~ 90% of the energy loss occured in the inner corona, and that $\Delta E = 10^{30}$ W(ergs). With $W \cong 10^{-4}$, the exciter loses some 10^{26} ergs in leaving the corona. The total energy in the type III exciter will typically

lose only a few percent of its energy.

One additional consequence of this energy-loss calculation was that it provided an explanation for why the electron streams appear to have such well-defined velocities, of order c/3 at high frequencies, decreasing to c/2 or less at low frequencies.

The peak intensity at any frequency is reached just before the linear beam-plasma instability stops at that frequency, for at that time the density in the energetic electron beam is maximum. It is this peak velocity which is directly deduced from the observed frequency drift rates as being the nominal velocity of the beam.

Smith et al. (1978) found that in the inner corona the peak velocity when the linear instability stopped was $v_p = 0.3c$, while near 1 AU, because the ambient solar wind is cooler, v_p was about 0.2c. This suggests that the nominal velocity (c/3) is not characteristic of electron acceleration, but rather reflects the evolution of the particle spectrum. In addition, the observations do not necessarily imply that the exciter is decelerated between 0.005 AU - 1 AU, bur rather reflects the decrease in the temperature of the solar wind with increasing heliocentric distance.

In concluding this section we should note that the most important lesson from the above, is the fact that plasma theory supported by computation has reached the level of sophistication where detailed predictions can be derived even in complex systems.

VIII. Summary and conclusions:

The present review dealt with radiation processes occurring in plasmas, with an emphasis on astrophysical applications. Enhanced radiation from stable non-equilibrium plasmas, having suprathermal particles, occurs mainly near the eigenfrequencies of the plasma (ω_e, Ω_e, Ω_u) or their multiples ($2\omega_e$, $2\Omega_e$, $2\Omega_u$, $\omega_e + \Omega_e$, $n\Omega_e$) and is due to synchrotron, Cerenkov, or the Cerenkov emission of e-s waves followed by the conversion to e-m waves by means of scattering on low frequency fluctuations. Typical enhancements over the thermal level vary between a factor of $10\text{-}10^4$. Plasmas with enhanced levels of e-s turbulence in high frequency modes (ω_e, Ω_e, Ω_u) can also radiate in the above frequency ranges, but the emitted radiation can be much stronger than in stable plasmas. In the absence of relativistic particles, amplification processes such as e-m instabilities also produce radiation in the above frequency range of a few times the plasma eigenfrequencies. The presence of relativistic particles, however offers the possibility of emission at frequencies much larger than the plasma frequencies, either by spontaneous or stimulated Compton scattering or by e-m instabilities. The upper limit on the emitted frequency is given by the usual double Doppler shift, i.e., $\omega < (1+\beta^2)\gamma^2\Omega_u$. A summary table of the radiation processes by frequency and of the section or formula that applies to them can be found in our appendix.

It should be emphasized that our discussion of the radiation processes, their efficiency and constraints represents only one block of the ones necessary to build our understanding of astrophysical

plasmas. This can be understood from our type III burst example of the last chapter. The energy flows from the electron stream to e-s waves to the observed e-m radiation. In order to build comprehensive models it was necessary to examine and understand (using computer simulations, theory and laboratory experiments) the individual processes controlling the interplay of the energy flow. Only after this was achieved was it possible to reach the almost complete and highly sophisticated understanding of the type III bursts. A similar linkage of the processes controlling astrophysical plasmas will be required, whose ultimate test will be the prediction of the levels and scalings of the observed radioemissions. We believe that such an effort will be extremely beneficial both for astrophysics and plasma physics.

Acknowledgements: The present review would have never been written, except for the encouragement and stimulating discussions of the participants of the Snowmass Workshop on Astrophysical Plasmas in Aug. 1978, and its chairman, Prof. C. F. Kennel. Many people contributed in shaping the ideas presented above. A short list includes Drs. M. Lampe, P. Sprangle, K. R. Chu, R. Smith, D. Tidman, and M. Goldstein. The work of one of us (H.P.F.) was supported by ONR and NASA.

Frequently used symbols:

Latin symbols:

$\underline{B}_o$	ambient magnetic field
$\underline{B}_1$	perturbed magnetic field
c	speed of light
$\underline{E}_1$	perturbed electric
H	Heaviside function
$\underline{\underline{I}}$	unit dyadic
$\underline{k}$	wavevector of radiation fields
k_D	inverse Debye length
m,M	electron and ion mass
T_e,T_i	electron and ion temperature
$\underline{u}$	relativistic velocity
V_e,V_i	electron and ion thermal speeds
$V_p,\underline{V}_g$	wave phase and group velocities
W	wave spectral energy density

Greek symbols:

γ	relativistic factor $(=1/\sqrt{1-v^2/c^2} = \sqrt{1+u^2/c^2})$
$\underline{\underline{\epsilon}}$	plasma dielectric tensor
ϵ_L, ϵ_T	longitudinal and transverse components of $\underline{\underline{\epsilon}}$ in isotropic media (i.e., $\underline{\underline{\epsilon}} = \underline{k}\,\underline{k}\,\epsilon_L/k^2 + (\underline{\underline{I}} - \underline{k}\,\underline{k}/k^2)\epsilon_T$)
η	index of refraction
θ	angle between $\underline{k}$ and $\underline{B}_o$
$\underline{\underline{\Lambda}}$	plasma dispersion tensor (i.e. $\underline{\underline{\Lambda}} = \frac{c^2}{\omega^2}(\underline{\underline{kk}} - k^2\underline{\underline{I}}) + \underline{\underline{\epsilon}}$)
Λ	determinant of $\underline{\underline{\Lambda}}$
λ_D	Debye length

Ω_e	electron cyclotron frequency
Ω_u	upper hybrid frequency
ω	wave frequency
ω_e	electron plasma frequency

Appendix:

Radiation near ω_e:	Section	Equation
Thermal	III	19a
Stable (non-thermal)	III (field-free)	25,26
" " "	IV (magnetized)	14
Weakly turbulent plasma	III	22,23
Radiation near $2\omega_e$		
Thermal	III	196
Stable (non-thermal)	III	30,31
Weakly turbulent plasma	III	27,28
Strongly turbulent plasma	III	41
Stimulated scattering	V	5
Radiation near $n\Omega_e$:		
Thermal	IV	7
Electromagnetic instabilities	VI	11,22,34
Radiation at $\omega \gg \omega_e, \Omega_e$:		
Compton scattering	III	35
Stimulated emission by laser	V	

References

Aamodt, R. E., and Drummond, W. E.: 1964, J. Nucl. En. (Pt.C) 6, 147.

Abdulloev, K. E., Bogolyubskii, E. L., and Makhamov, V. G.: 1975, Nucl. Fusion 15, 21.

Audenaerde, K.: 1977, Plasma Phys. 19, 299.

Bekefi, G.: 1966, Radiation Processes in Plasmas, Wiley, New York.

Birmingham, T. J.: 1966, Ph.D. Thesis, Princeton University.

Birmingham, T. J., Dawson, J. M., and Oberman, C.: 1965, Phys. Fluids 8, 297.

Birmingham, T. J., Dawson, J. M., and Kulsrud, R. M.: 1966, Phys. Fluids 9, 2014.

Bornatici, M., and Engelman, F.: 1968, Il Nuovo Cim. LVIB, 220

Chu, K. R., and Hirshfield, J. L.: 1978, Phys. Fluids 21, 461.

Dawson, J. M.: 1968, Advances in Plasma Physics, Vol. 1, p. 1-66, Ed. A. Simon and W. B. Thompson, Interscience New York, 1968.

Dawson, J. M., and Nakayama, T.: 1966, Phys. Fluids 9, 252.

Dawson, J. M., and Oberman, C.: 1962, Phys. Fluids 5, 517.

Elias, L., Fairbank, W., Madey, J.M.J., Schwettman, H. A., and Smith, T.: 1976, Phys. Rev. Lett. 36, 717.

Fitzenreiter, R. J., Exaus, L. G., and Lin, R. P.: 1976, Solar Phys. 46 357.

Freund, H. P., and Wu, C. S.: 1976, Phys. Fluids 19, 299.

Freund, H. P., and Wu, C. S.: 1977a, Phys. Fluids 20, 619.

Freund, H. P., and Wu, C. S.: 1977b, Phys. Fluids 20, 963.

Freund, H. P., Lee, L. C., and Wu, C. S.: 1978a, Phys. Rev. Lett. 40, 1563.

Freund, H. P., Wu, C. S., Lee, L. C., and Dillenburg, D.: 1978b, Phys. Fluids 21, 1502.

Freund, H. P., Lee, L. C., and Wu, C. S.: 1978c, Inst. Phys. Sci. and Tech. - Univ. of Maryland Technical Report BN-886.

Fried, B. D.: 1959, Phys. Fluids 2, 337.

Friedman, M., Hammer, D. A., Manheimer, W. M., and Sprangle, P.: 1973, Phys. Rev. Lett. 31, 752.

Gapanov, A. V.: 1959, Izv. Vyssh. Uchebn. Zaved., Radiofizi. 2, 450.

Gapanov, A. V., Petelin, M. I., and Yulpatov, V. K.: 1967, Radio Phys. Quantum Electron. 10, 794.

Ginzburg, V. L., and Syrovatskii, S. I.: 1965, in Annual Reviews of Astronomy and Astrophysics, Vol. 3, Annual Reviews, Palo Alto, California.

Ginzburg, V. L., and Syrovatskii, S. I.: 1967, in Annual Reviews of Astronomy and Astrophysics, Vol. 5, Annual Reviews, Palo Alto, California.

Goldstein, M. L., Smith, R. A., and Papadopoulos, K.: 1978a, Waves and Instabilities in Space Plasmas, Ed. P. Palmadesso and K. Papadopoulos, D. Reidel, Holland (in press).

Goldstein, M. L., Papadopoulos, K., and Smith, R. A.: 1978b, Ap.J. (communicated).

Granatstein, V. L., and Sprangle, P.: 1977, IEEE Trans. Microwave Th. and Tech. MIT-75, 545.

Granatstein, V. L., Herndon, M., Sprangle, P., Carmel, Y., and Nation, J. A.: 1975, Plasma Phys. 17, 23.

Granatstein, V. L., Sprangle, P., Parker, R. K., Pashour, J., Herndon, M., and Shlesinger, S. P.: 1976, Phys. Rev. A. 14, 1194.

Harris, E. G.: 1961, J. Nucl. Energy C, 2, 138.

Hirshfield, J. L., Baldwin, D. E., and Brown, S. C.: 1961, Phys. Fluids 3, 45.

Hirshfield, J. L., Bernstein, I. B., and Wachtel, J. M.: 1965, Quantum Electron. QE-1, 237.

Kaplan, S. A., and Tsytovich, V. N.: 1969, Sov. Phys. Uspekhi. 12, 42.

Kaplan, S. A., and Tsytovich, V. N.: 1973, Plasma Astrophysics, Perganon Press.

Kwan, T., Dawson, J. M., and Lin, A. T.: 1977, Phys. Fl. 20, 581.

Lampe, M., Ott, E., and Walker, J. H.: 1978, Phys. Fluids 21, 42.

Liemohn, H. B.: 1965, Radio Sci. 69D, 741.

Litvak, A. G., and Trahktengerts, V. Yu.: 1971, Sov. Phys. JETP 33, 921.

Lin, A. T., Kaw, P. K. and Dawson, J. M.: 1976, Princeton Univ. MATT Report (unpublished).

Manheimer, W., and Ott, E.: 1975, Trans. IEEE PS-3,5.

Manheimer, W., and Papadopoulos, K.: 1975, Phys. Fluids 18, 1397.

Melrose, D. B.: 1970, Australian J. of Phys. 23, 871, 875.

Melrose, D. B.: 1968, Astrophys. Space Sci. 2, 171.

Melrose, D. B.: 1976, Astrophys. J. 207, 651.

Montgomery, D., and Tidman, D.: 1964, Plasma Kinetic Theory, McGraw-Hill, New York.

Nicholson, D., Goldman, M. V., Hoyng, P., and Weatherall, J.: 1978, Ap. J. (in press).

Nicholson, D., and Smith, D. F.: 1978, Waves and Instabilities in Space Plasmas, Ed. P. Palmadesso and K. Papadopoulos, D. Reidel, Holland (in press).

Pakhomov, V. I., Aleksin, V. F., and Stepanov, K. N.: 1962, Sov. Phys. - Tech. Phys. 6, 856.

Palmadesso, P., Coffey, T. P., Ossakow, S. L., and Papadopoulos, K.: 1976, J. Geophys. Res. 81, 1762.

Papadopoulos, K.: 1969, Phys. Fluids 12, 2185.

Papadopoulos, K.: 1970, Am. Journ. of Phys. 38, 87.

Papadopoulos, K.: 1973, Bull. of Am. Phys. Soc. 18, 1306 (NRL Memo 2749).

Papadopoulos, K., and Coffey, T.: 1974a, J. Geophys. Res. 79, 674.

Papadopoulos, K., and Coffey, T.: 1974b, J. Geophys. Res. 79, 1558.

Papadopoulos, K., Goldstein, M. L., and Smith, R. A.: 1974, Ap. J., 190, 175.

Papadopoulos, K.: 1975, Phys. Fluids 18, 1769.

Papadopoulos, K.: 1978, Proceed. of Varenna School (in press).

Papadopoulos, K., and Freund, H. P.: 1978, Geophys. Res. Lett. 5,881.

Rostoker, N.: 1961, Nucl. Fusion 1, 101.

Sagdeev, R. F., and Shafranov, V. D.: 1961, Sov. Phys. - JETP 12, 130.

Schneider, J.: 1959, Phys. Rev. Lett. 2, 504.

Smith, D. F.: 1979, Sp. Sci. Rev. 16, 91.

Smith, R. A.: 1976, Jupiter, Ed. T. Gehrels, Univ. of Arizona Press.

Smith, R. A., Goldstein, M. L., and Papadopoulos, K.: 1976, Solar Physics 46, 515.

Smith, R. A., Goldstein, M. L., and Papadopoulos, K.: 1978, Ap. J. (communicated) NASA Tech. Memo 78079.

Sprangle, P., and Drobot, A.T.: 1977, IEEE Trans. MTT-25, 6, 528.

Sprangle, P., and Drobot, A.T.: 1978, NRL Memo Rept. 3587, J. Appl. Phys. (to be published).

Sprangle, P., and Granatstein, V. L.: 1974, NRL Memo 2834.

Sprangle, P., Granatstein, V. L., and Baker, L.: 1975, Phys. Rev. A 12, 1697.

Sprangle, P., Granatstein, V. L., and Drobot, A.: 1977, J. Physique 12, C6-135.

Sprangle, P., and Manheimer, W. M.: 1975, Phys. Fluids 18, 224.

Sprangle, P., Smith, R. A., and Granatstein, V. L.: 1978, NRL Memo Rept. 3388.

Stix, T.: 1962, The Theory of Plasma Waves, McGraw-Hill, New York.

Sturrock, P. A.: 1961, Journ. Nucl. En. (Pt.C) 2, 158.

Sturrock, P. A.: 1964, AAS-NAS Symposium on the Physics of Solar Flares, ed. W. N. Hess, NASA SPSO, 357.

Sturrock, P. A., Ball, R. H., and Baldwin, D. E.: 1965, Phys. Fluids 8, 295.

Tidman, D. A., and Dupree, T. H.: 1965, Phys. Fluids 8, 1860.

Tsytovich, V. N.: 1973, Non Linear Effects in Plasmas, Plenum Press, New York.

Tsytovich, V. N.: 1977, Theory of Turbulent Plasma, Consultants Bureau. New York.

Twiss, R. Q.: 1958, Australian J. Phys. 11, 564.

Weibel, E. S.: 1959, Phys. Rev. Lett. 2, 83.

Wu, C. S., and Freund, H. P.: 1977, Astrophys. J. 213, 575.

Wu, C. S., and Lee, L. C.: 1978, Astrophys. J. (commun.)

Uhm, H., Davidson, R. C., and Chu, K. R.: 1978, Phys. Fluids 21, 1866.

Zaitsev, N. I., Pankratova, T. B., Petelin, M. A. and Flyagin, M. V.: 1974, Radio Eng. Electron. Phys. 19, 103.

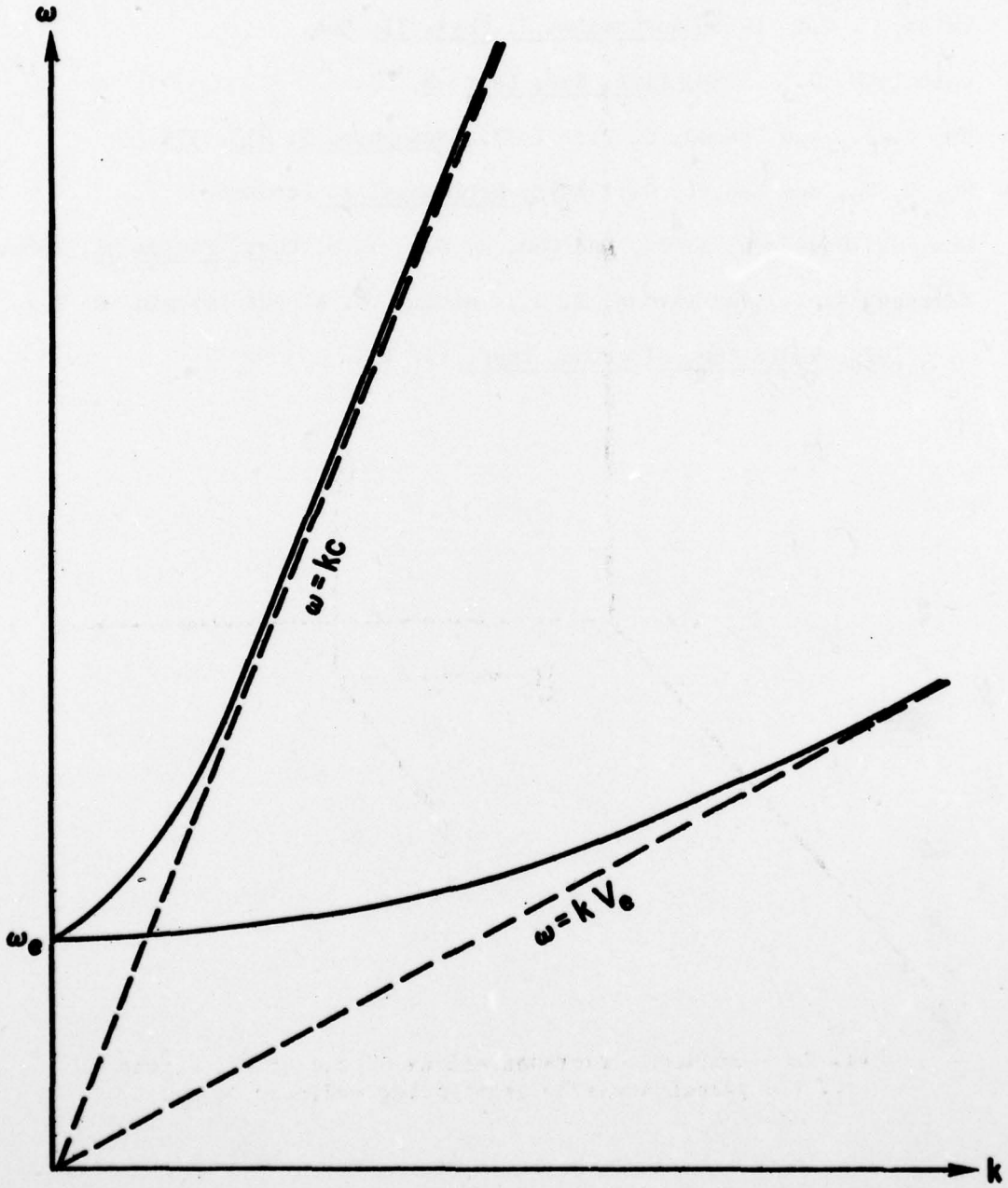

Fig. 1 - Plot of the dispersion equations of the electrostatic and electromagnetic modes in a field-free plasma.

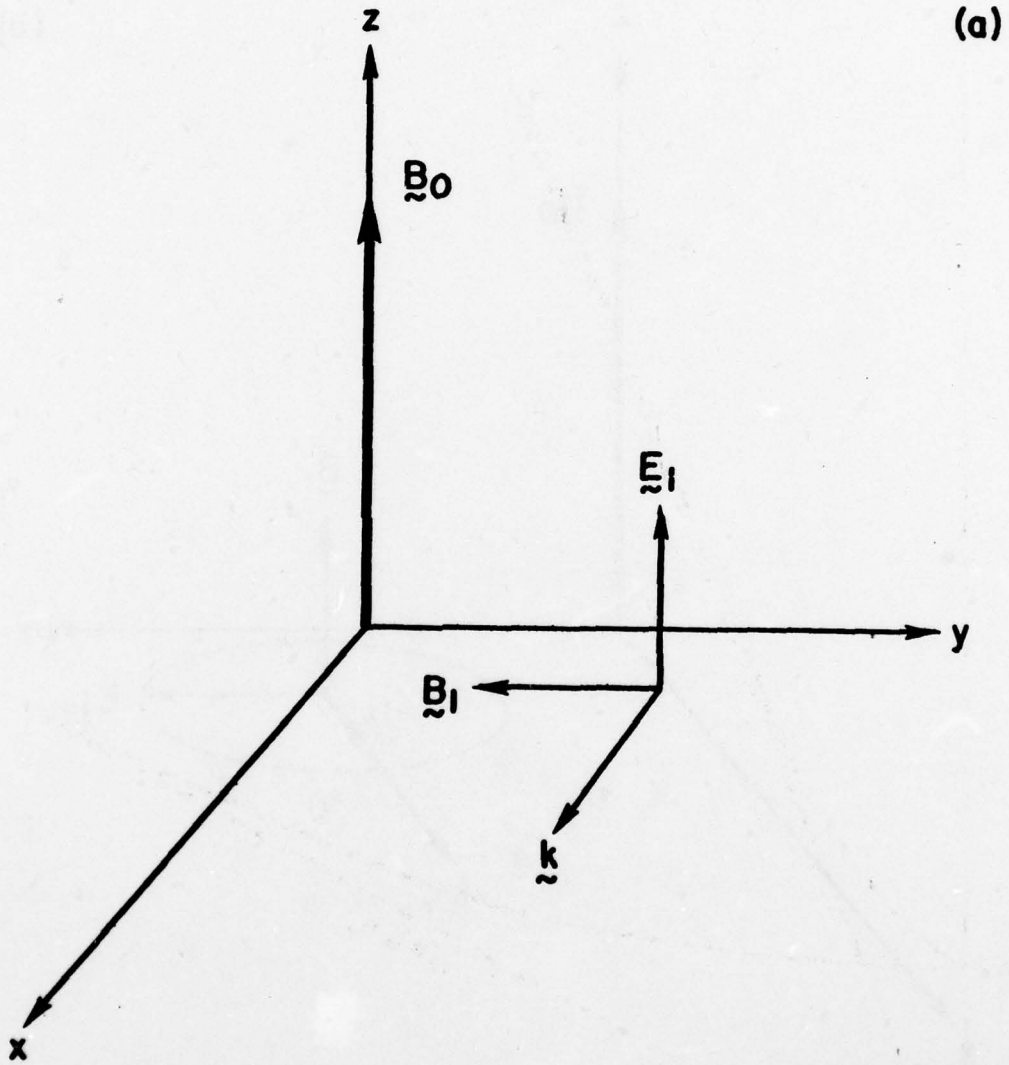

Fig. 2a - Schematic representations of the polarizations of the perpendicularly propagating ordinary modes.

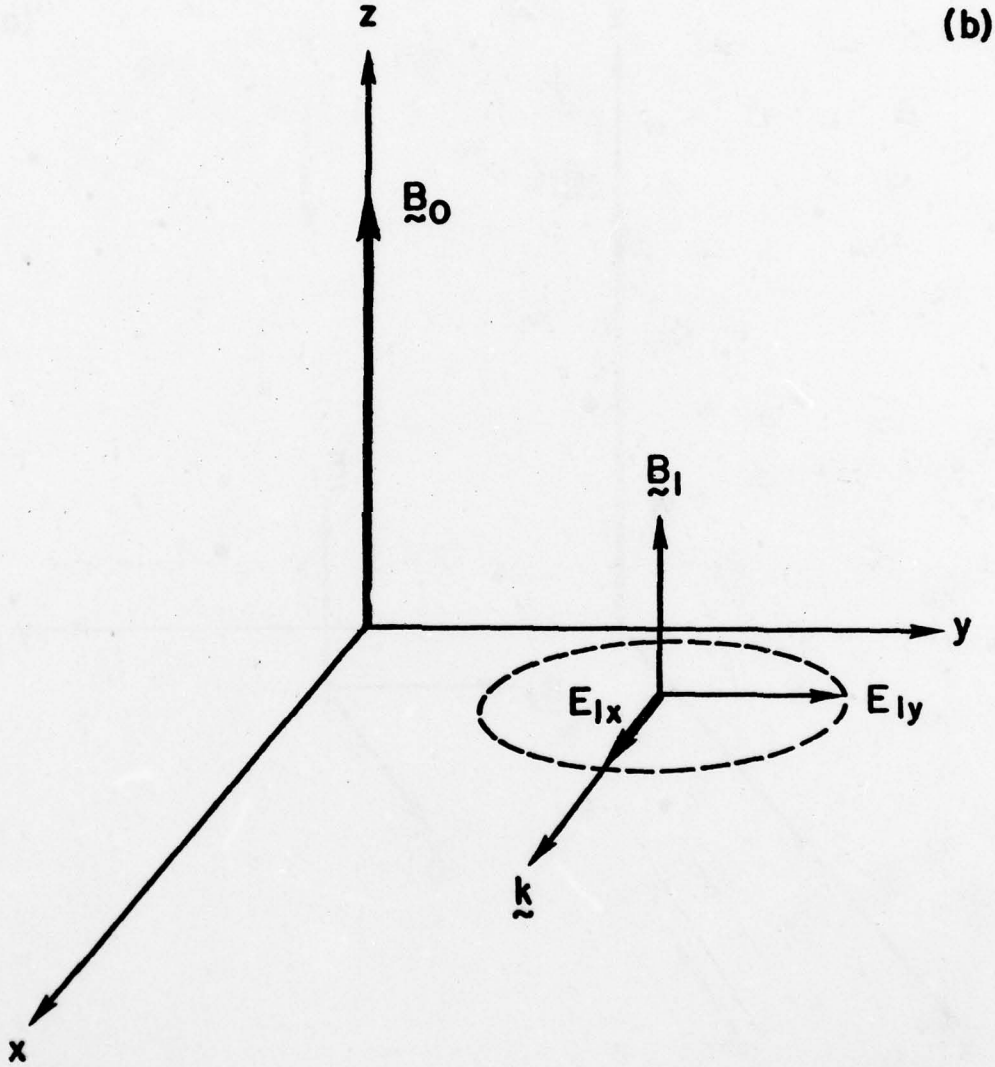

Fig. 2b - Schematic representations of the polarizations of the perpendicularly propagating extraordinary modes.

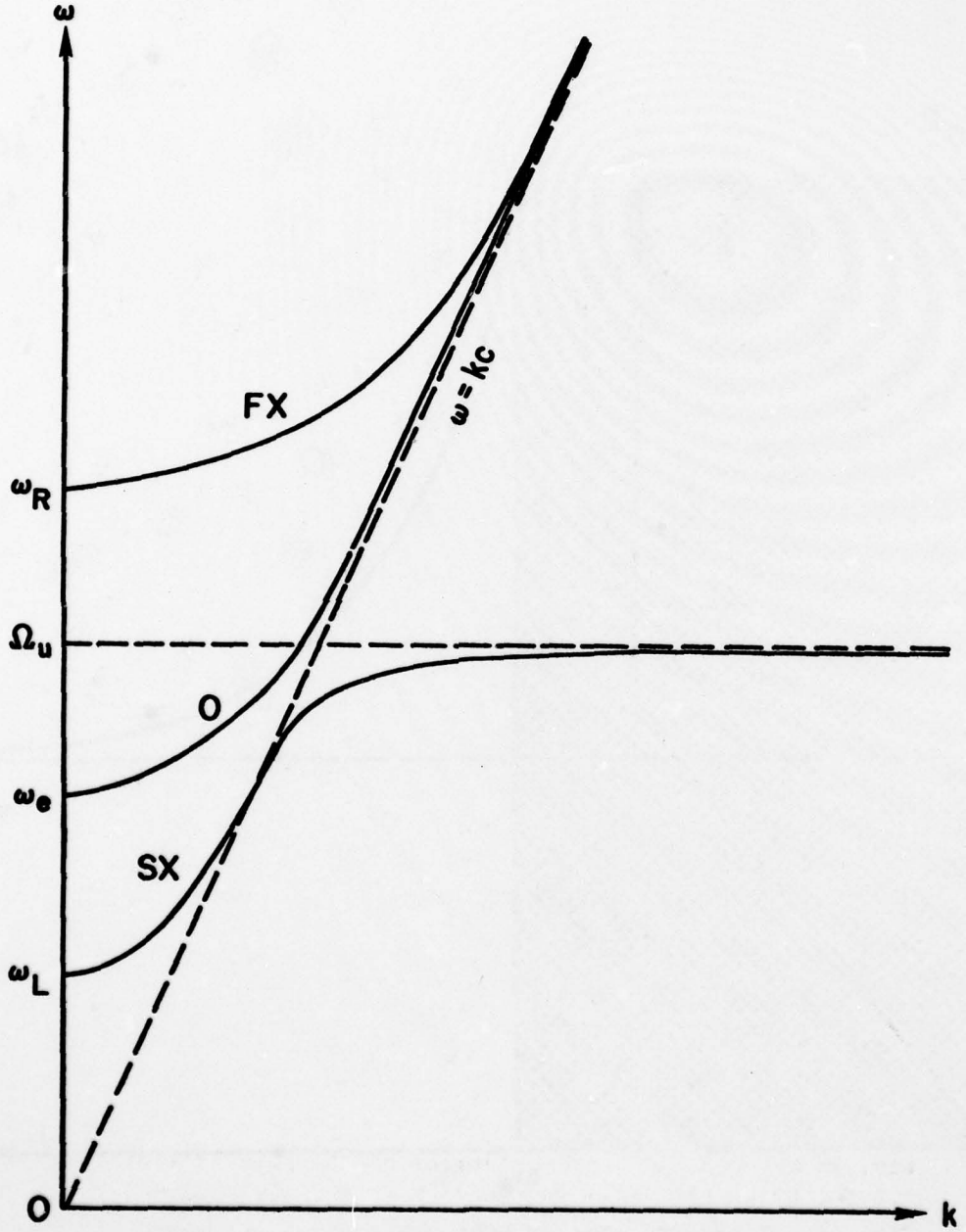

Fig. 3 - Plot of the dispersion equations for the ordinary and extraordinary modes in the limit in which $\underline{k} \cdot \underline{B}_o = 0$.

AD-A066 923 NAVAL RESEARCH LAB WASHINGTON D C F/G 20/9
COLLECTIVE RADIO-EMISSION FROM PLASMAS.(U)
FEB 79 K PAPADOPOULOS, H P FREUND
UNCLASSIFIED NRL-MR-3922 SBIE-AD-E000 277 NL

2 OF 2
AD
AD A066923

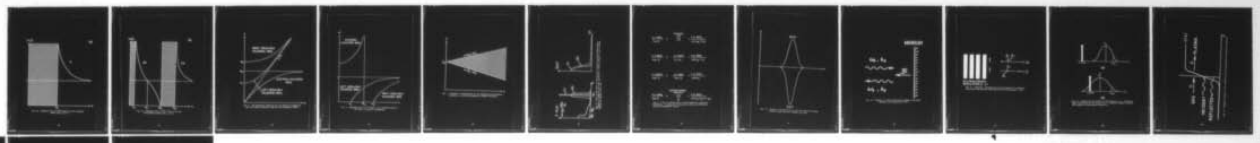

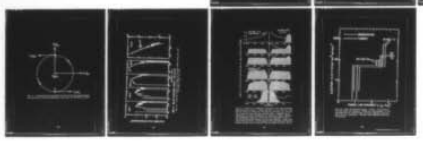

END
DATE
FILMED
6-79
DDC

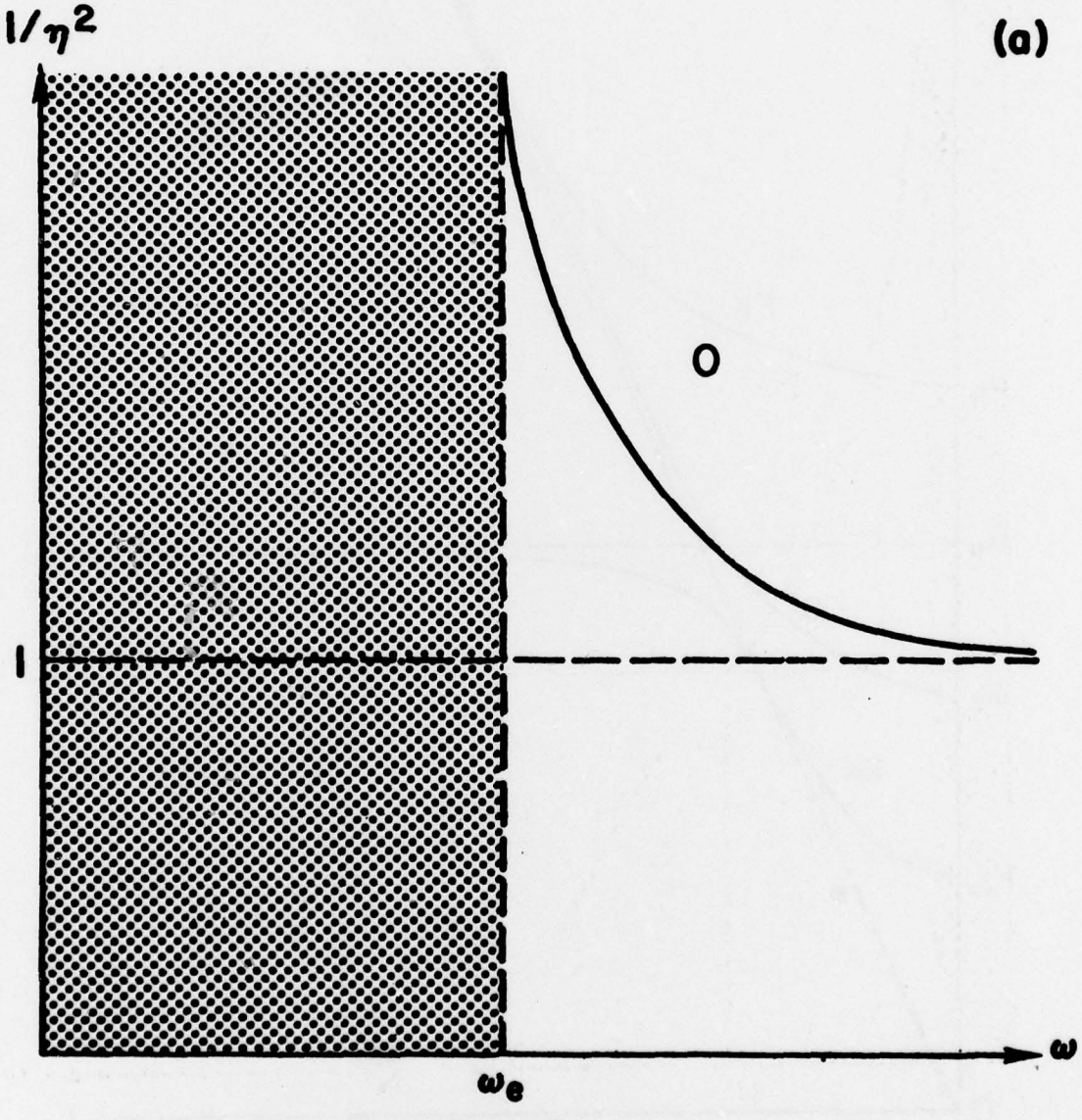

Fig. 4a - Schematic plot of $1/\eta^2$ versus ω for the ordinary modes for $\underline{k} \cdot \underline{B} = 0$.

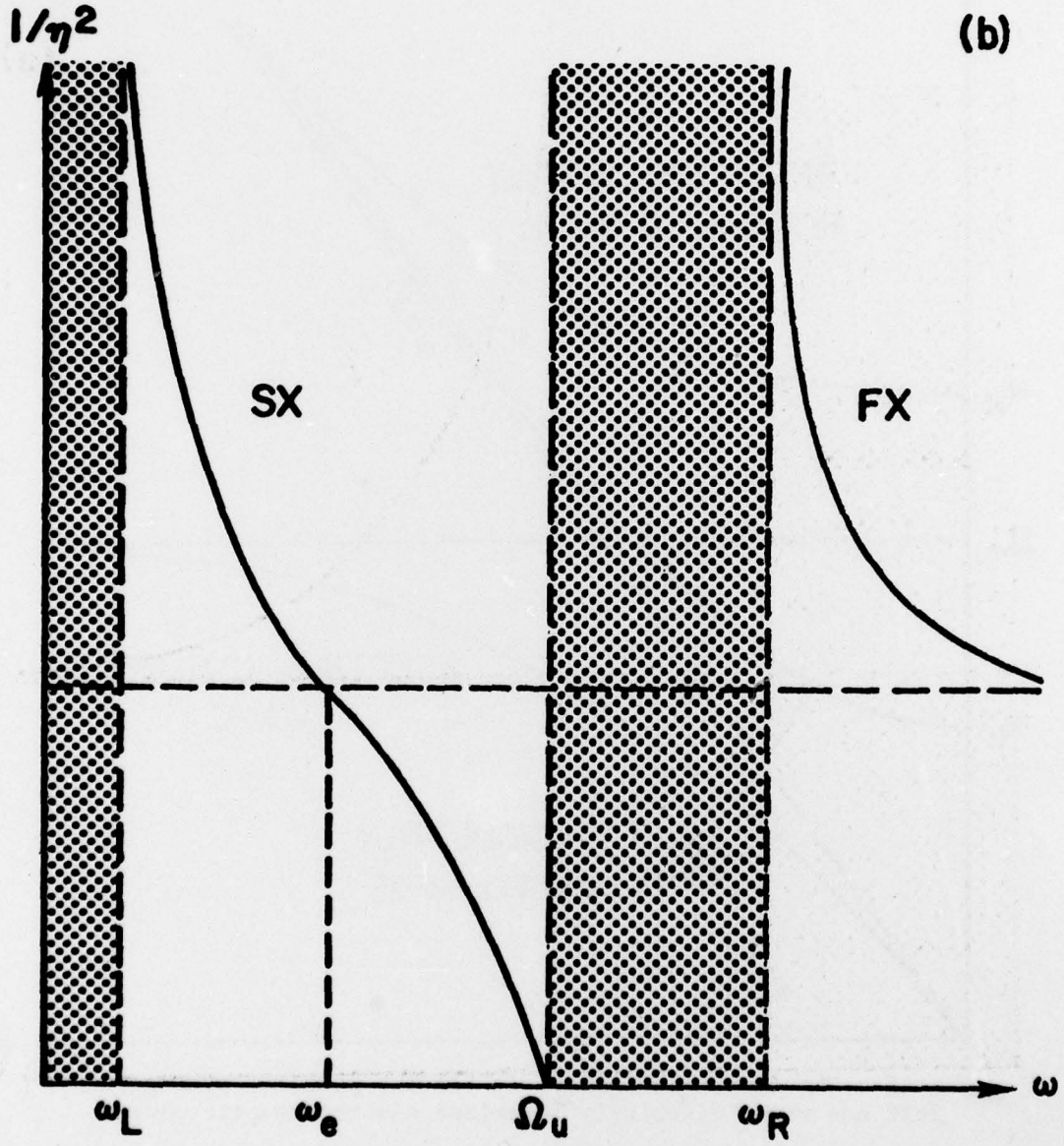

Fig. 4b - Schematic plot of $1/\eta^2$ versus ω for the extraordinary modes for $\underline{k} \cdot \underline{B} = 0$.

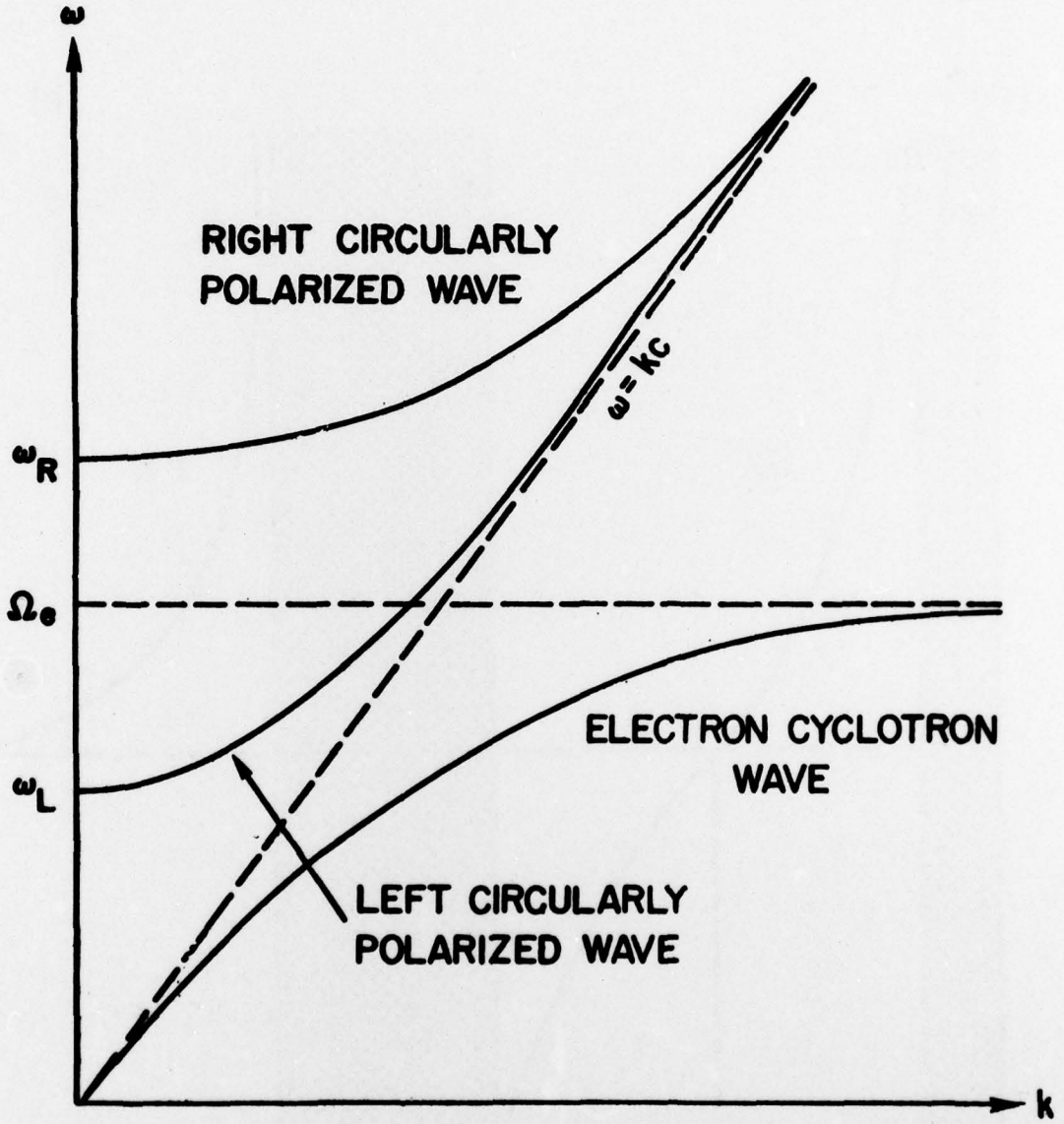

Fig. 5 - The dispersion equations for the parallel propagating left and right circularly polarized electromagnetic modes.

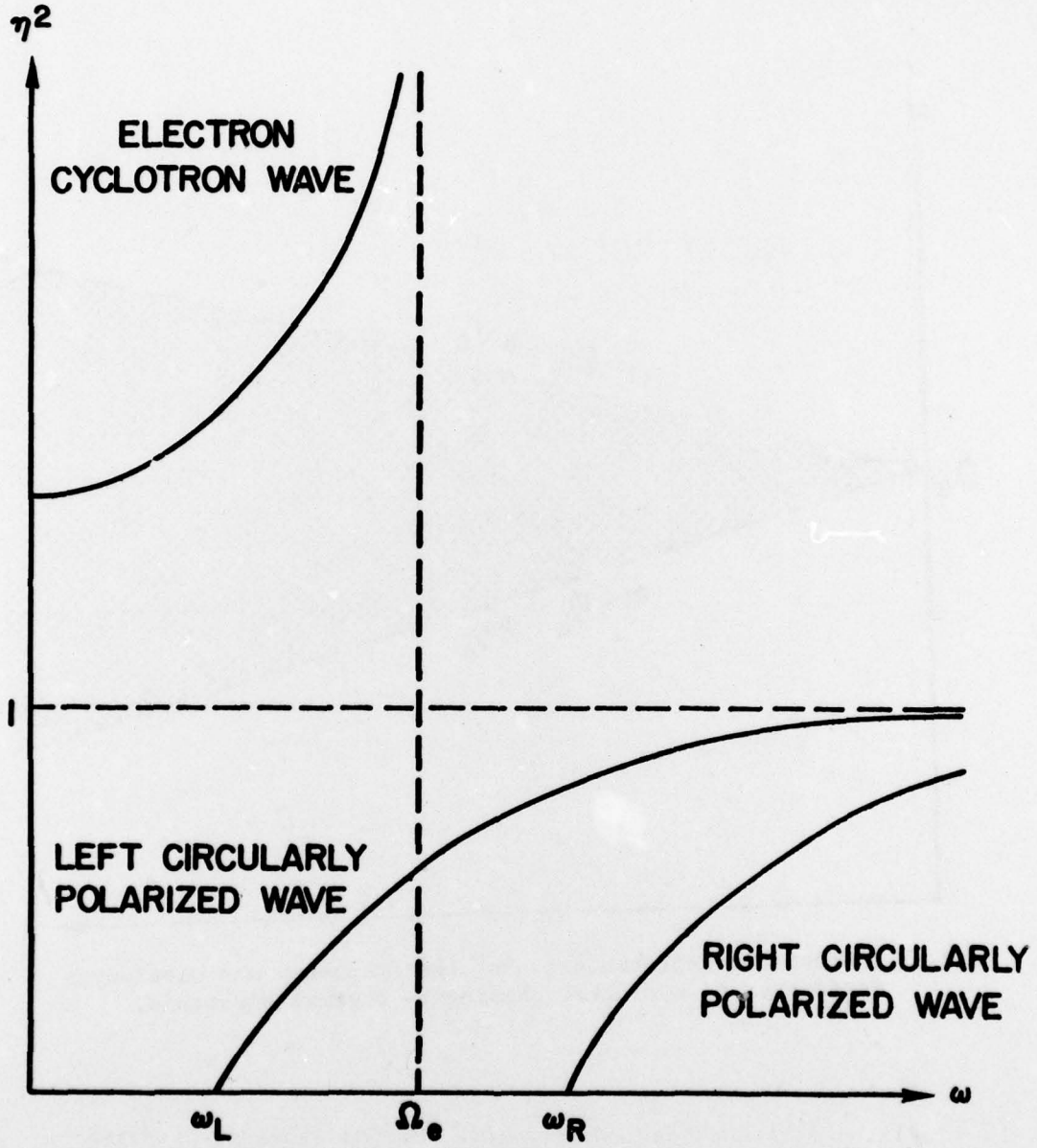

Fig. 6 - Representation of η^2 versus ω for transverse modes in the limit of parallel propagation.

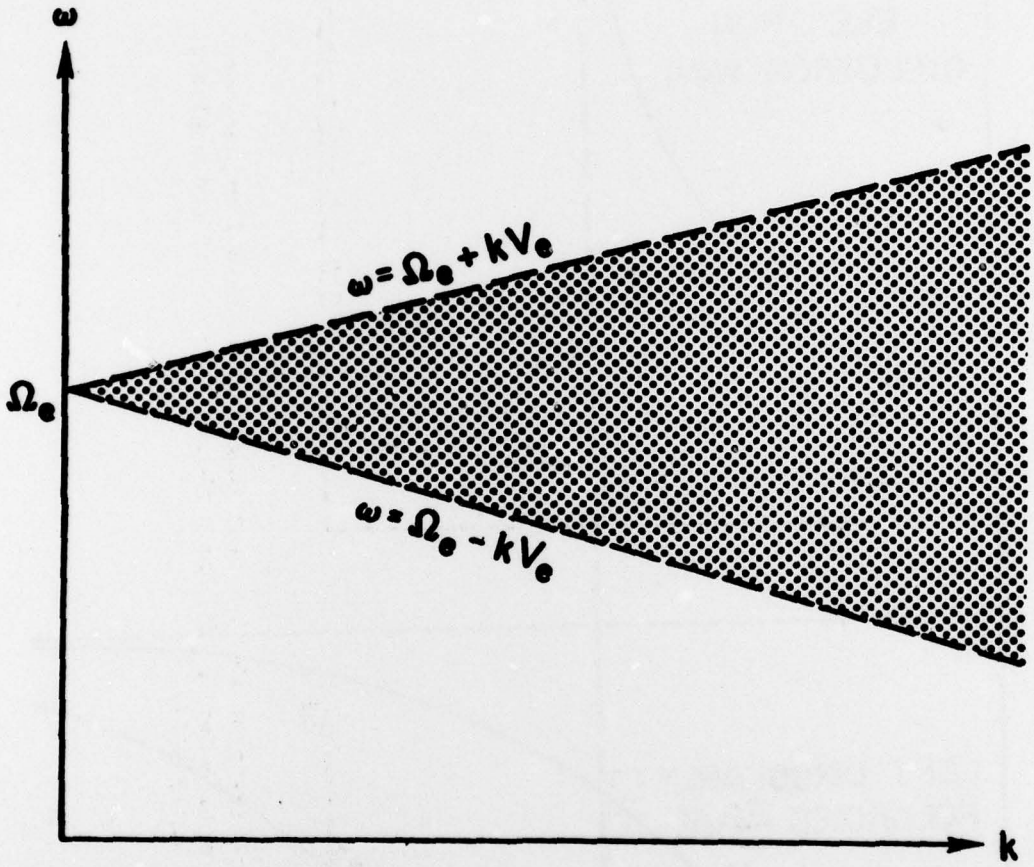

Fig. 7 - Schematic representation of the frequency and wavelength dependence of cyclotron damping by thermal electrons.

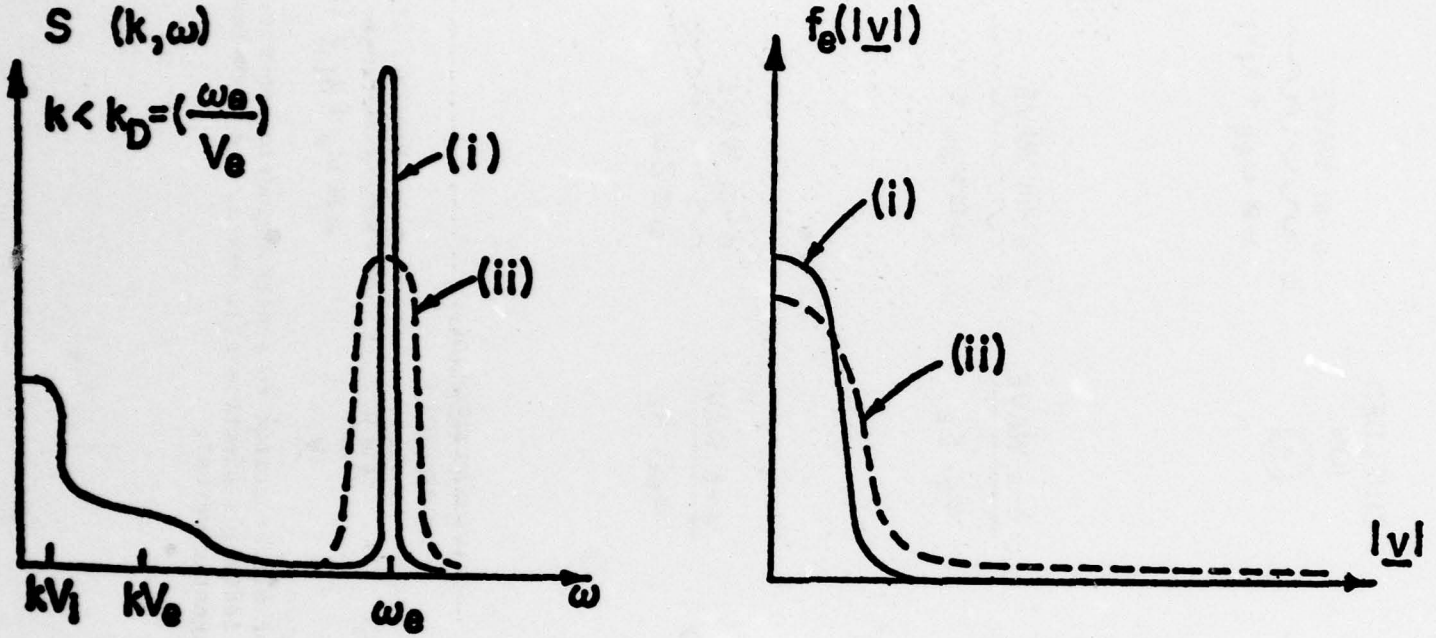

Fig. 8 - Plot of the trace of the spectral function of field fluctuations $S(\underline{k},\omega)$ as a function of ω and $f_e|\underline{v}|$ for a thermal plasma (i) and a plasma having non-thermal tails (ii).

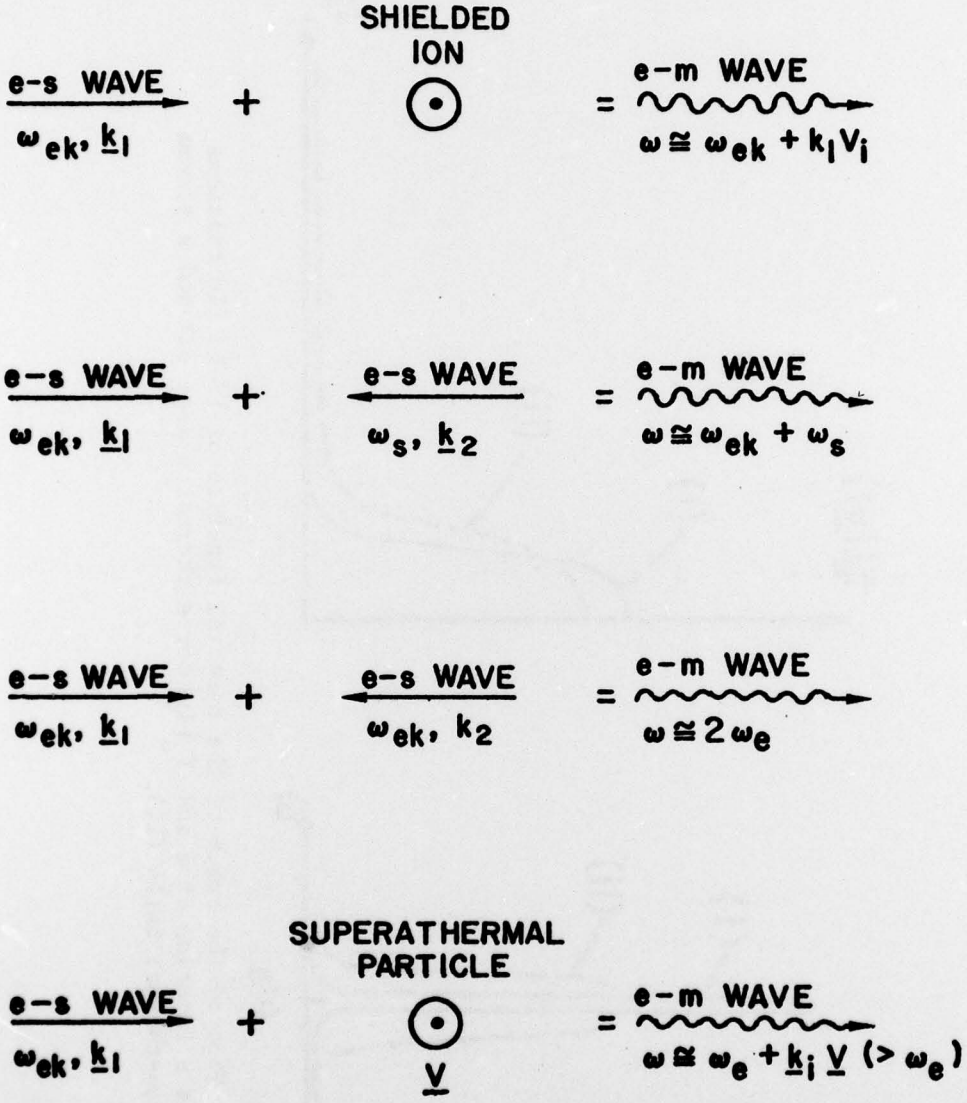

Fig. 9 - List of electrostatic to electromagnetic conversion processes. (→ indicates electrostatic waves, and ∿∿→ indicates electromagnetic waves).

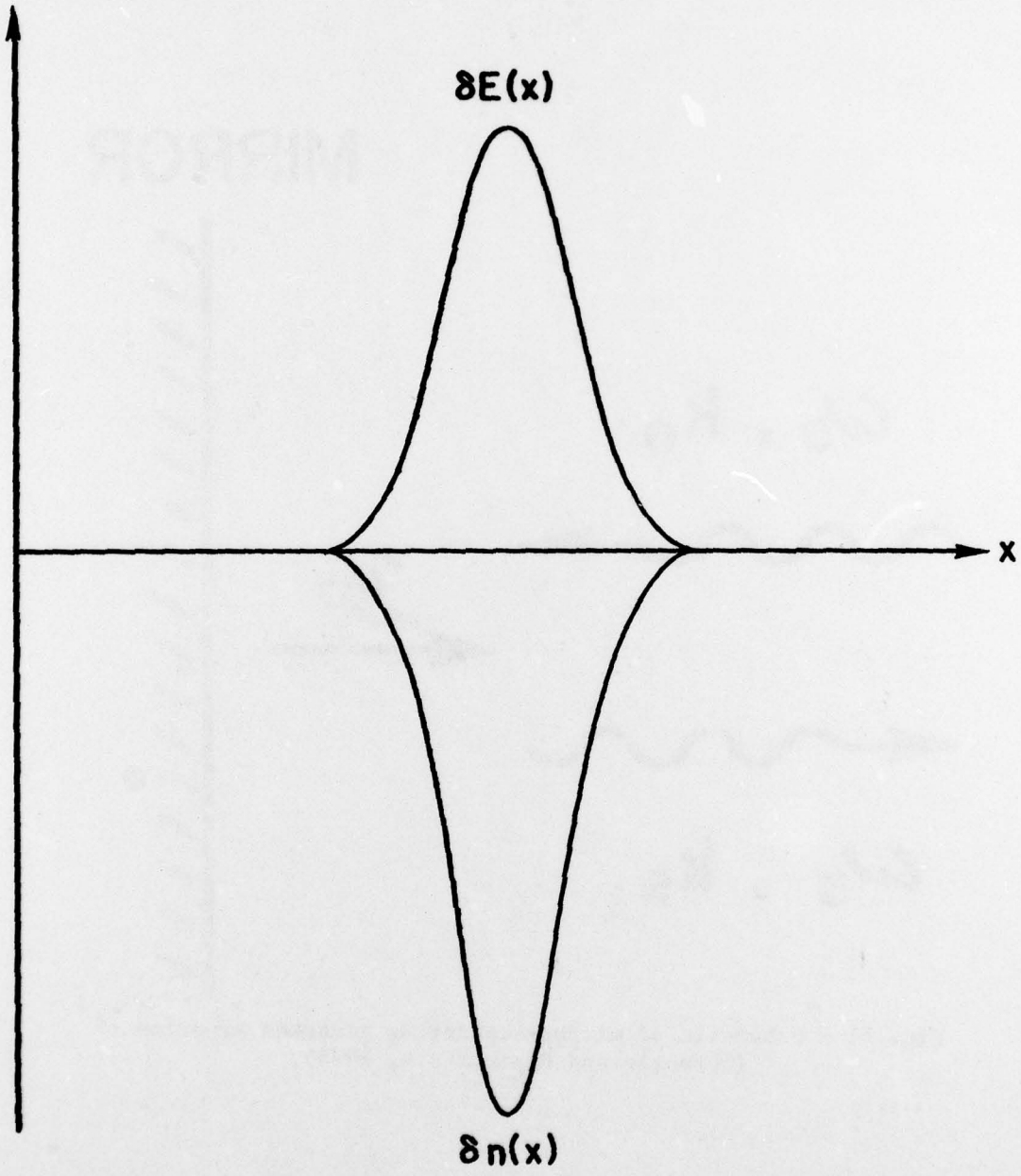

Fig. 10 - Schematic representation of electric field and plasma density associated with Langmuir solitons.

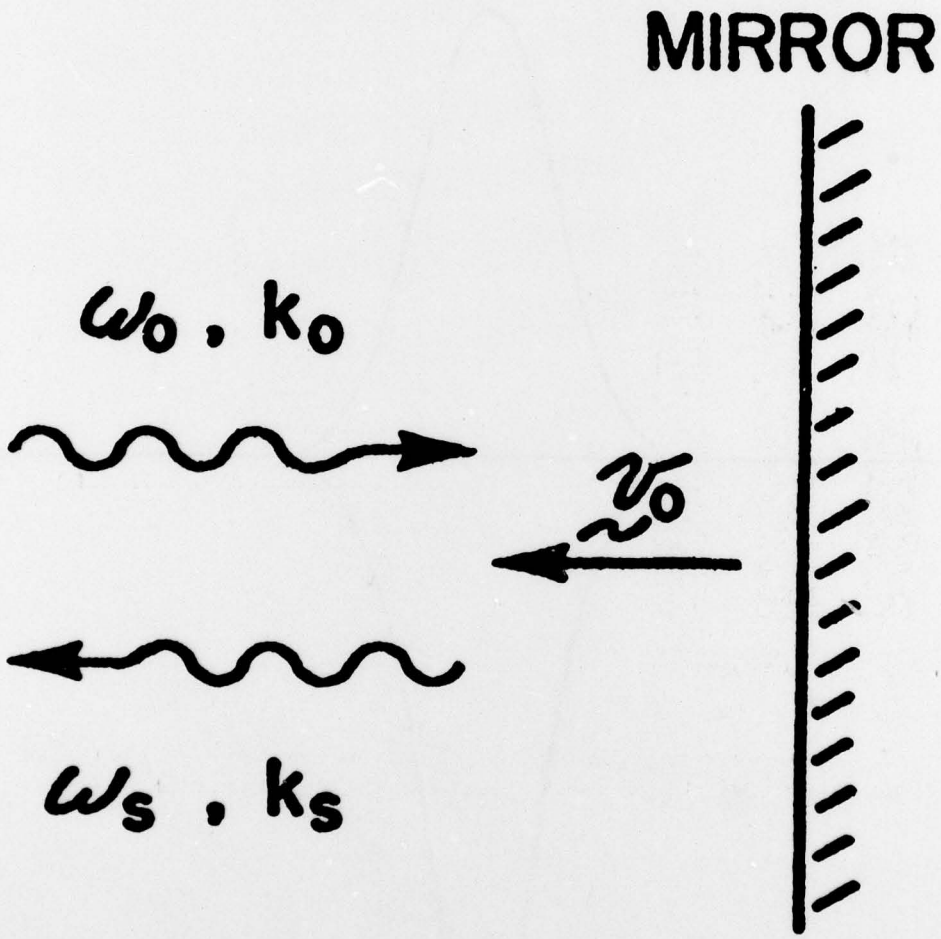

Fig. 11 - Schematic of mirror-scattering gedanken experiment (Sprangle and Granatstein, 1974).

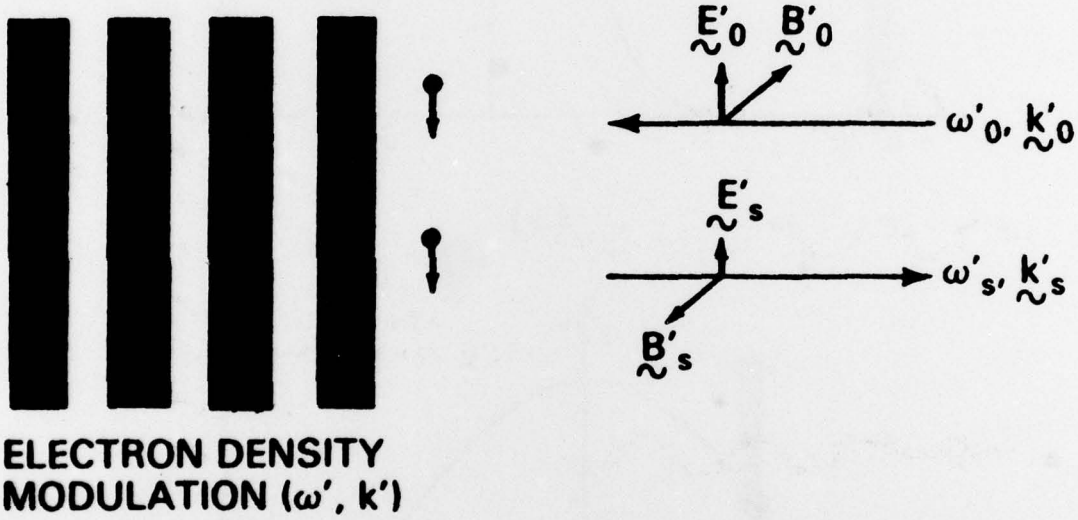

Fig. 12 - Schematic representation of the mechanism of stimulated scattering from electron beams (Granatstein and Sprangle, 1977).

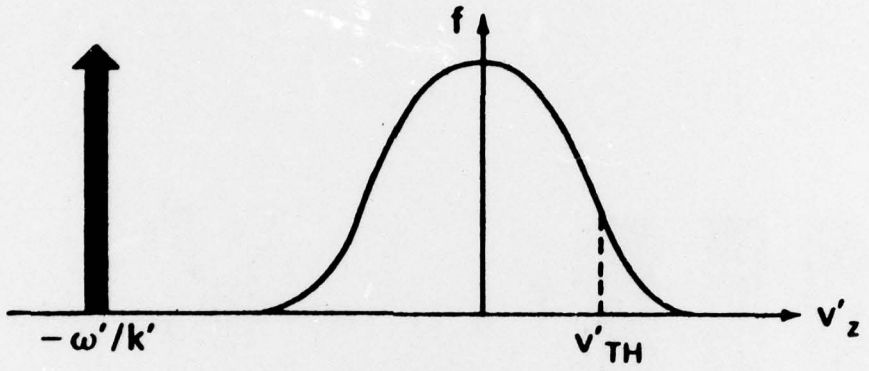

(a)

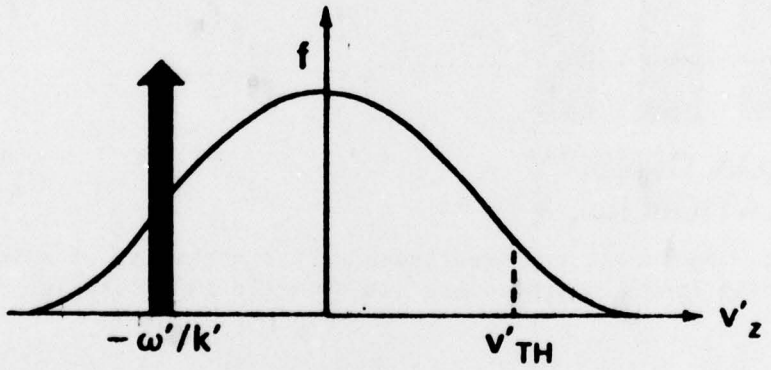

(b)

Fig. 13 - Representation showing (a) hydrodynamic (i.e., stimulated Raman scattering) and (b) kinetic (i.e., stimulated Compton scattering) regimes in beam-plasma instability.

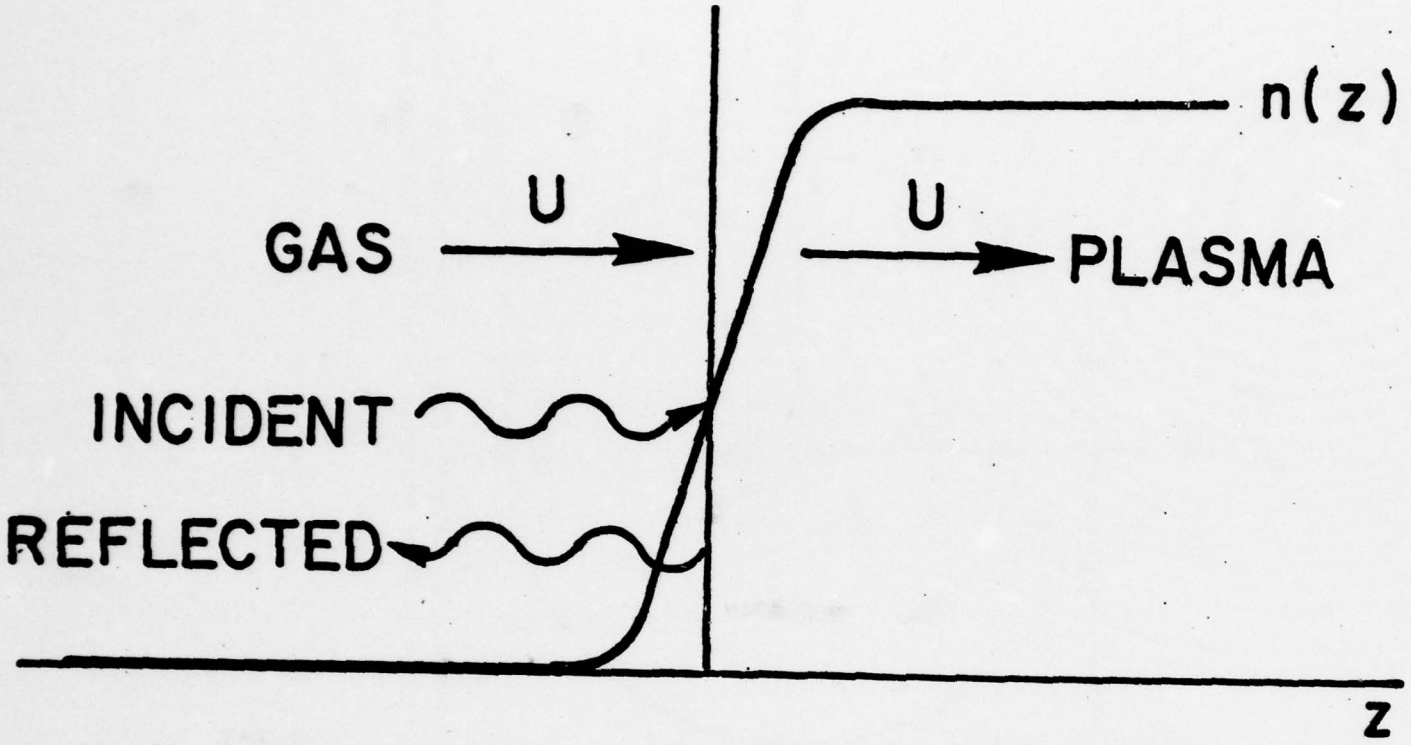

Fig. 14 - Schematic drawing of the stimulated scattering process from density gradients.

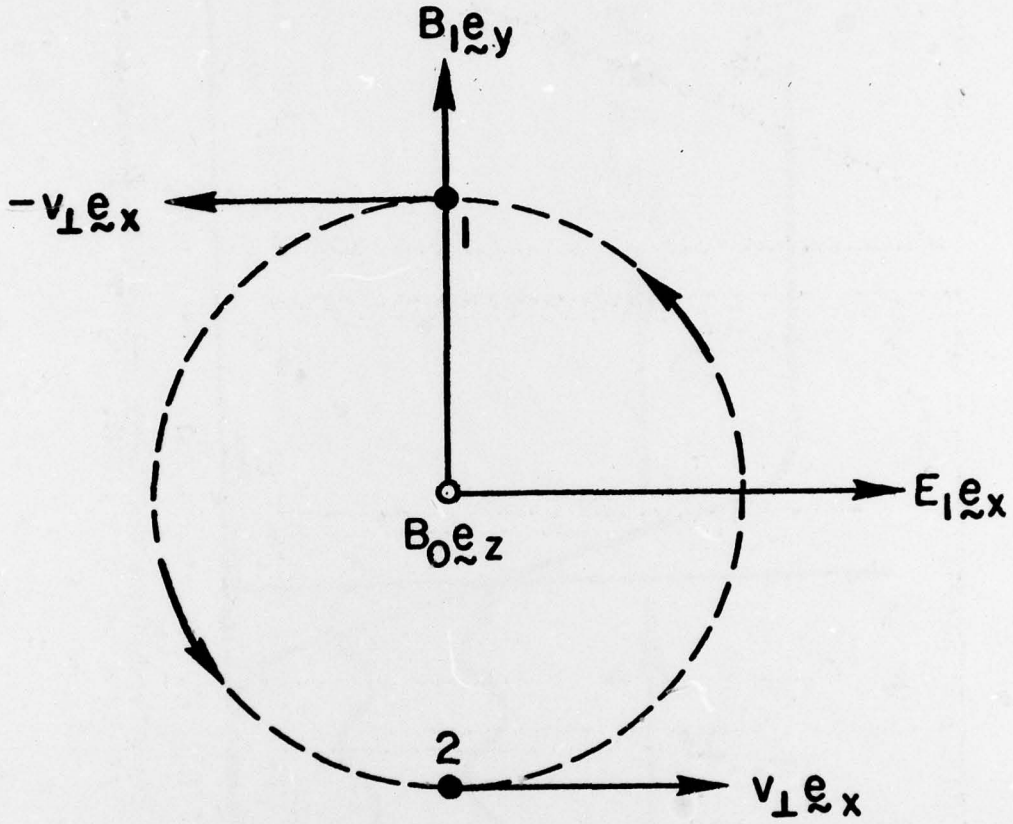

Fig. 15 - Instantaneous relationship of wave fields and perpendicular electron motion in uniform magnetic field (Chu and Hirshfield, 1978).

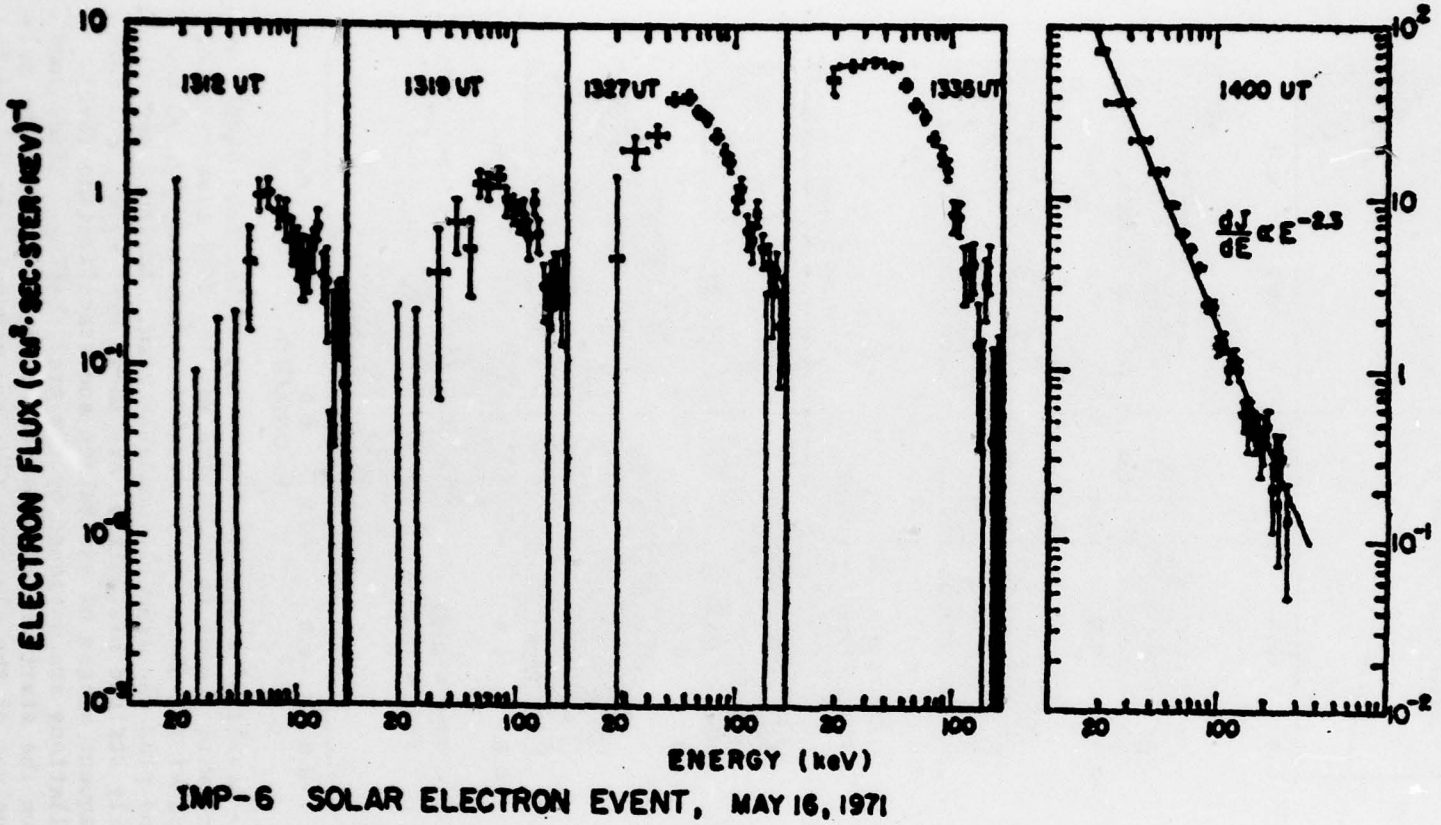

Fig. 16 - Electron spectra are shown at various times during the type III burst of May 16, 1971.

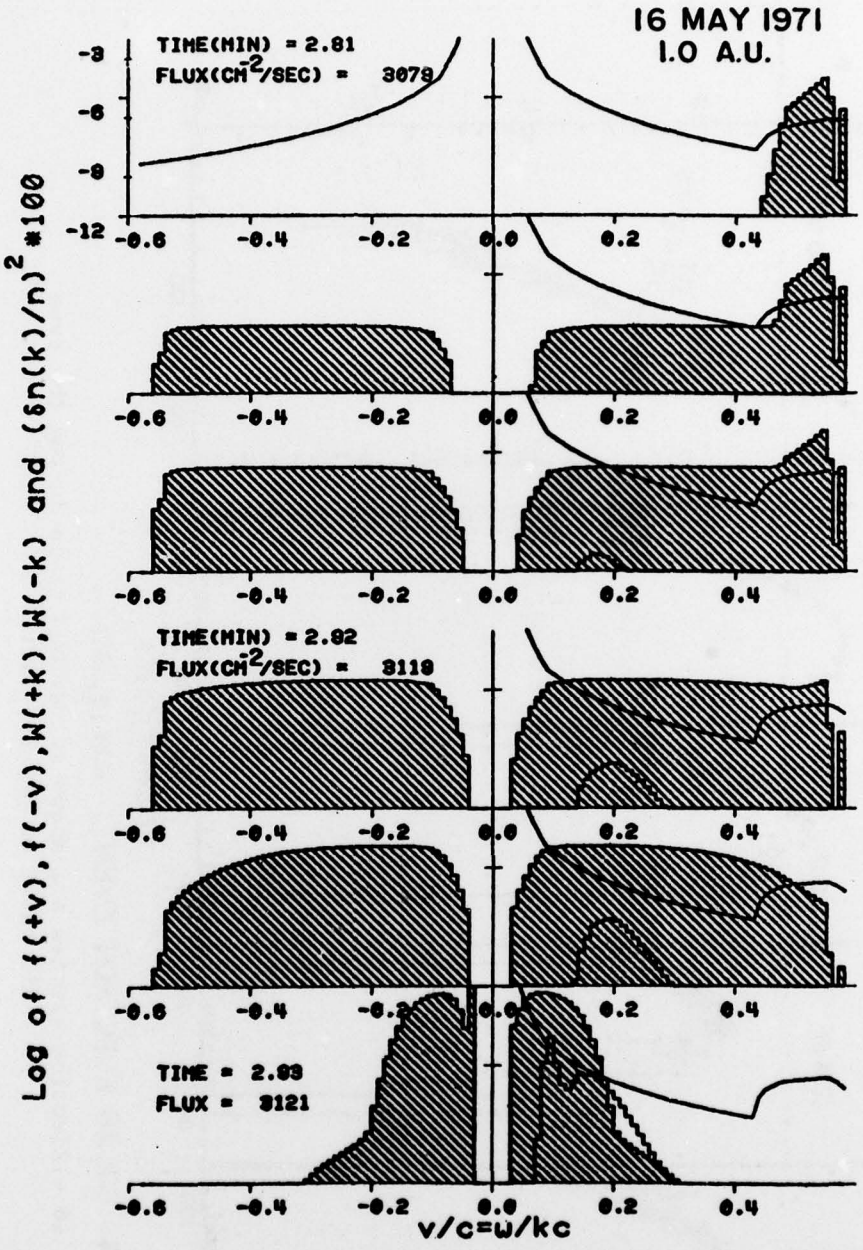

Fig. 17 - Result of a numerical solution of the rate equations Parameters were chosen to model the May 16, 1971 event at 1 AU. The top panel (a) shows the distribution function, f_r, of the solar wind plus the linearly unstable beam. Langmuir waves (diagonally striped histograms) are shown near W_T(a), and during subsequent stages of excitation and stabilization (b-f). Ion oscillations are depicted by the gray shading. Times computed from the start of the numerical calculations and the calculated values of the electron flux are given in 17a,d, and f.

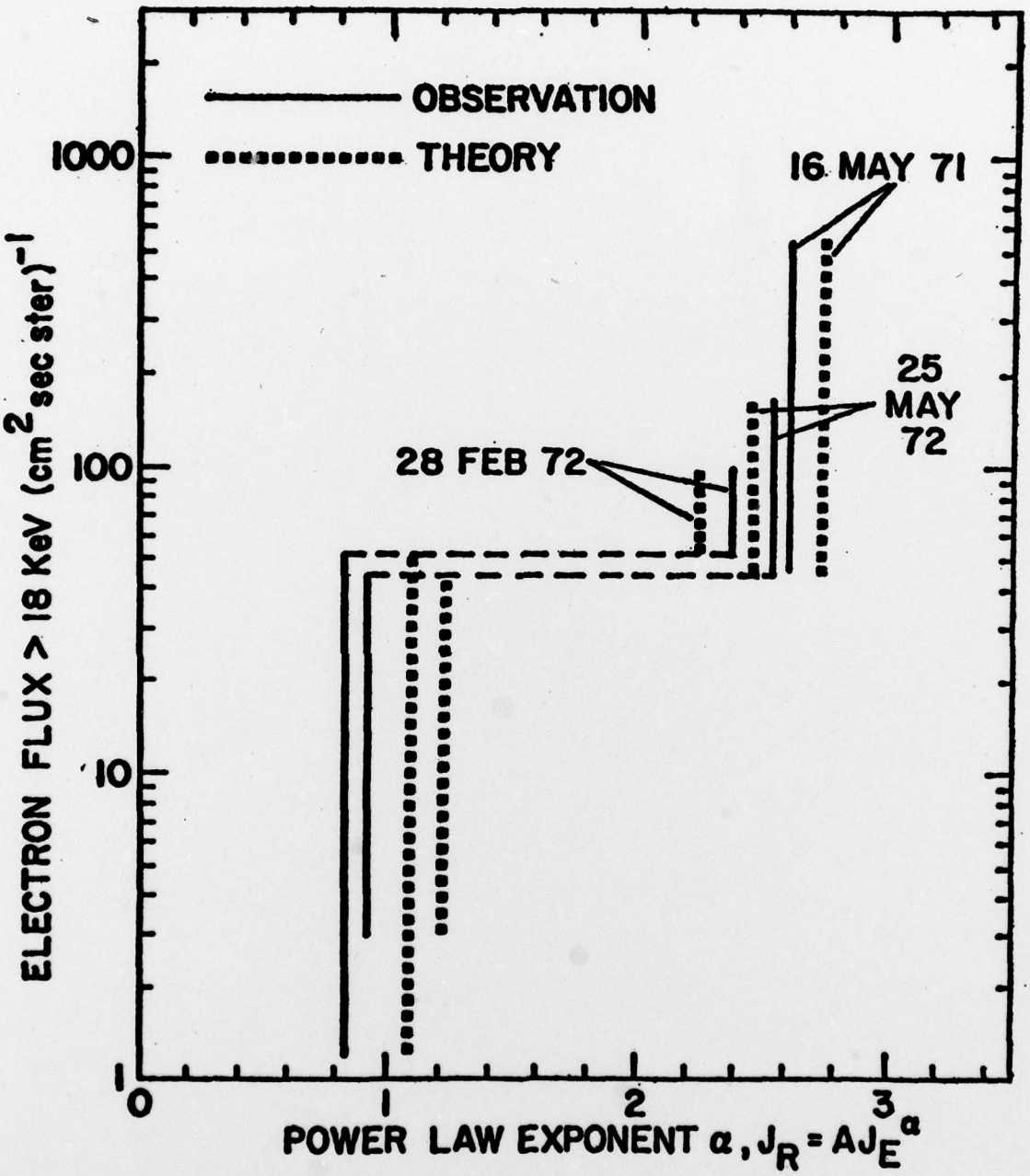

Fig. 18 - After Fitzenreiter et al. (1976). The electron flux and power law exponent, α from the relationship $I \propto J_E^{\alpha}$ are shown for the three events for which numerical calculations could be performed. Observed and computed values of α are plotted.

U.S. GOVERNMENT PRINTING OFFICE:1979 281-404/213 1-3